# SYNTHESIS OF SURFACE ACTIVE ALKANES FOR CELLULOSE MODIFICATION

**By**

**Alvira Moses**

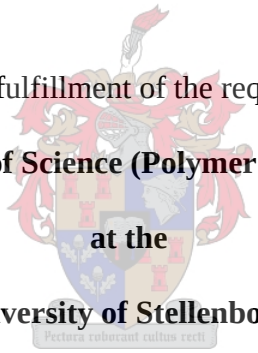

Thesis presented in partial fulfillment of the requirements for the degree of

**Master of Science (Polymer Science)**

**at the**

**University of Stellenbosch**

**Promoter:**

**Prof. R.D. Sanderson**

**Co-promoter:**

**Me V. Cloete**

**Stellenbosch**

**April 2006**

# DECLARATION

I, the undersigned, hereby declare that the work contained in this thesis is my own original work and that I have not previously in its entirety or in part submitted it at any university for a degree.

..... .....

Signature: Date:

# ABSTRACT

The properties and interactions of cellulose surfaces are of a great technical interest during papermaking and recycling. Sizing, the modification of fiber surfaces, e.g. with the purpose to reduce water penetration into the paper structure, plays an important role in obtaining paper with good printability and water resistance. Water resistance is the key end-property of paper being investigated in this study.

Firstly a comparison was made between the degree of surface modification of cellulose by means of anionic, nonionic and reactive surfactants. The amount of surfactant adsorbed by the paperboard was determined and the paper surface evaluated via scanning electron microscopy (SEM). The sizing efficiency of the three industrial surfactants was evaluated in order to establish the surfactant structure best suited for sizing recycled paperboard. This was done via the Cobb test, an industrial method to measure water uptake by paper, and contact angle measurements. The reactive surfactant was found to have the best sizing efficiency and focus shifted to synthesizing selected copolymer surfactants via free radical copolymerization.

Two copolymers were synthesized, with maleic anhydride as the polar part in both. Butyl methacrylate and lauryl methacrylate were selected as the hydrophobic parts in the respective copolymer systems. The unavailability of reactivity ratios for the respective copolymer systems led to the use of in situ proton nuclear magnetic resonance spectroscopy ($^{1}$H NMR) for the determination of the co-monomer incorporation in both copolymer systems. Quantitative $^{13}$C NMR spectroscopy was also employed in order to establish the co-monomer content of the isolated copolymers obtained during bench-scale (laboratory) experiments.

Lastly, a comparison of the degree of surface modification of cellulose was made between that which was achieved with the industrial reactive surfactant and that with the two synthesized polymeric reactive surfactants. The two synthesized polymeric

surfactants were found to have a better sizing efficiency than the industrial reactive surfactant, and the maleic anhydride-lauryl methacrylate copolymer system gave the best results.

# OPSOMMING

Die eienskappe en interaksies van sellulose-oppervlaktes is van groot tegniese belang gedurende die vervaardiging en hergebruik van papier. Oppervlakte behandeling, die modifikasie van vesel-oppervlaktes bv. met die doel om water indringing in die papierstruktuur te verminder, speel ‘n belangrike rol in die daarstel van papier met goeie drukkwaliteit en waterweerstand. Waterweerstand is die sleuteleienskap van papier wat in hierdie werkstuk ondersoek word.

Eerstens is daar ‘n vergelyking getref tussen die verandering van sellulose-oppervlaktes deur middel van anioniese, nie-ioniese en reaktiewe sepe. Die hoeveelheid seep geadsorbeer deur die papierbord is bepaal en die papier-oppervlak ondersoek deur middel van skandeer-elektronmikroskopie (SEM). Die behandelingsdoeltreffendheid van die drie industriële sepe is ondersoek om vas te stel watter seep die beste struktuur het om hergebruikte papierbord effektief te behandel. Dit is gedoen deur middel van die Cobb-toets, ‘n industriële metode om wateropname van papier te meet, asook kontakhoekmetings. Daar is gevind dat die reaktiewe seep die beste behandelingsdoeltreffendheid het en daar is vervolgens gekonsentreer op die bereiding van geselekteerde reaktiewe kopolimeersepe deur middel van vrye-radikaalkopolimerisasie.

Twee kopolimere is berei, met maleïenanhidried as die polêre gedeelte van albei. Butielmetakrilaat en laurielmetakrilaat is gekies vir die nie-polêre gedeeltes van die onderskeie kopolimeersisteme. Die onbeskikbaarheid van reaktiwiteitsverhoudings vir die onderskeie kopolimeersisteme het gelei tot die gebruik van in situ proton kern magnetiese resonansie spektroskopie ($^{1}$H KMR) vir die bepaling van die ko-monomeer insluiting in beide kopolimeersisteme. Kwantitatiewe koolstofdertienkernmagnetiese-resonansie spektroskopie ($^{13}$C KMR) is ook gebruik om die ko-monomeerinhoud van die geisoleerde kopolimere, verkry tydens laboratoriumeksperimente, te bepaal.

Laastens is ‘n vergelyking getref tussen die graad van modifikasie van sellulose-oppervlaktes deur middel van die industriële reaktiewe seep in vergelyking met die twee bereide polimeriese reaktiewe sepe. Daar is gevind dat die twee gesintetiseerde polimeriese sepe beter behandelingsdoeltreffendheid as die industriële reaktiewe seep het, met die maleïenanhidried-laurielmetakrilaat-kopolimeersisteem wat die beste resultaat lewer.

# ACKNOWLEDGEMENTS

I would like to give thanks to my heavenly Father who has led me on my current journey. Father, you have given me the strength, faith and health to work for what I want in life.

My beloved parents who has stood by me through all the good and bad times. Thank you for giving me life and walking the distance with me.

A special thank you goes to Prof. J. Dillen. I will be forever grateful to you for giving me the opportunity to further my studies.

Prof. R.D. Sanderson, my promoter, thank you for believing in my ability as a researcher and for all the motivation. You have a great spirit and it tends to rub-off on people because one starts to believe in yourself.

Me. V. Cloete, the role model I never had before. You are truly a special person and you inspire everyone you come into contact with. Thank you for all the financial help, not only for my masters but also for my karate.

Jean McKenzie and Elsa Malherbe, thank you for your patients with all my NMR experiments and analyses. Thank you Jean for coming in early in the morning to start my experiments.

Me. P. Skillington, for all the SEM analyses and little favours in times of need. Thank you for not only being a colleague but also a good friend.

The paper family, thank you for being my companions for the past few years. I love you guys and look forward to working with you for a long time.

Dr. M. Hurndall, thank you for editing my thesis. Your input helped a great deal.

# LIST OF CONTENTS

---

## Chapter 3: Pre-screening Experiment: Investigation of the Effect of Surfactant Structure on the Sizing Efficiency of Recycled Paperboard

---

## Chapter 4: Synthesis of Surface-active Alkanes

---

## Chapter 5: Cellulose modification



---

## Chapter 6: Conclusions and Recommendations

# LIST OF TABLES

## CHAPTER 3



## CHAPTER 4



## CHAPTER 5

# LIST OF FIGURES

## CHAPTER 1



## CHAPTER2

## CHAPTER 3

## CHAPTER 4



## CHAPTER 5

# LIST OF SCHEMES

## CHAPTER 4

# LIST OF ABBREVIATIONS

| | |
|---|---|
| **NMR** | **Nuclear magnetic resonance** |
| **CMC** | **Critical micelle concentration** |
| **°** | **Degrees (angle)** |
| **°C** | **Degrees Celsius** |
| **HLB** | **Hydrophilic/lipophilic balance** |
| **ASA** | **Alkenyl succinic anhydride** |
| **AKD** | **Alkyl ketene dimmer** |
| **GPC** | **Gel permeation chromatograph** |
| **MAH** | **Maleic Anhydride** |
| **BMA** | **Butyl methacrylate** |
| **LMA** | **Lauryl methacrylate** |
| **SE** | **Sucrose ester** |
| **SDS** | **Sodium lauryl sulphate** |
| **$MgSO_4$** | **Magnesium sulphate** |
| **SEM** | **Scanning electron microscopy** |
| **SEC** | **Size exclusion chromatography** |
| **HPLC** | **High performance liquid chromatography** |
| **mJ** | **Milli joule** |
| **Pa** | **Pascal** |
| **$\eta$** | **Viscosity** |
| **$\gamma$** | **Surface tension** |
| **l** | **Length** |
| **r** | **Radius** |
| **t** | **Time** |
| **UV** | **Ultraviolet** |
| **IS** | **Isodine solubilization** |
| **OH** | **Hydroxyl** |
| **THF** | **Tetrahydrofuran** |
| **DDI** | **Distilled deionized** |

| | |
|---|---|
| **nOe** | **Nuclear Overhauser enhancement** |
| **σ** | **Shielding factor** |
| **Δ** | **Difference in the shielding factor of two solvents** |
| **AIBN** | **Azobisisobutyronitrile** |
| **CPR** | **Controlled radical polymerization** |
| **RAFT** | **Reversible addition fragmentation chain transfer polymerization** |

# CHAPTER 1

# INTRODUCTION AND OBJECTIVES

## 1.1. Introduction

Surfactant molecules, defined as surface-active agents, are amphiphilic substances that consist of a hydrophobic and a hydrophilic moiety that are clearly separated in the molecular structure (*see Figure 1.1*) [1,2,3,4]. The hydrophilic part engages in electrostatic interactions (hydrogen bonding, dipolar interactions, ionic bonding etc.) with surrounding molecules, e.g. water and ions, while the hydrophobic part associates with neighbouring non-polar structures via hydrophobic and van der Waals interactions [2]. This amphiphilic nature of surfactants results in their adsorption to interfaces, dispersion and solubilization of otherwise insoluble substances and the alteration of foaming properties of aqueous solutions [5,6]. The structural characteristics and the ability of surfactants to modify interfacial properties have led to their widespread use in numerous applications in the mineral, environmental, pharmaceutical, biological, agricultural, cosmetic, textile and coating industries [7].

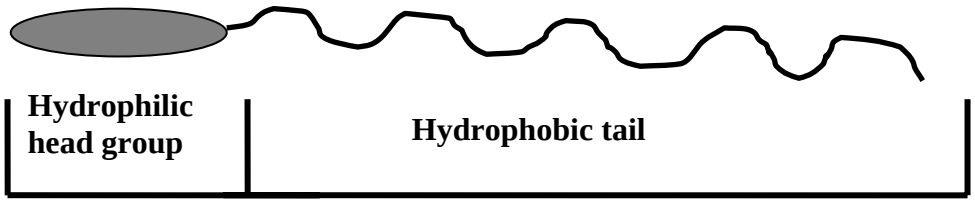


**Figure 1.1: General structure of a surfactant.**

The raw materials used in the manufacturing of surfactants are classified according to their origin as either natural or petroleum-based [3]. The surfactant industry has gone from natural to petroleum-based and, with a steady trend, back to natural again [1,8]. The use of

petroleum-based surfactants, which includes alkanolamides, alkyl phenol ethoxylates, amino oxides, betaines, fatty acid ester ethoxylates, polyacrylate dispersants, etc. began to overtake the use of natural materials mainly because of improved socio-economic conditions. The latter created an increased demand for larger volumes of personal cleansing agents and fabric detergents with consistently higher performances and ease of use [8].

Natural surfactants, including sucrose esters, sorbitol esters, alkyl polyglucosides, biosurfactants, fatty amides, fatty amines, etc. are formed from biological processes or are produced from natural renewable raw material through synthetic chemical processes [1,8]. The two most important examples of surfactant polar head groups of natural origin are sugars and amino acids. There is an increasing interest in sugar (mono- and disaccharides) and fatty acid-based surfactants mainly because of environmental concerns surrounding currently used petrochemically synthesized surfactants [9,10]. The interest in sugar surfactants is motivated by the fact that they can be made from renewable materials, are non-toxic, highly biodegradable and have favourable properties with respect to applications in various fields [11]. A better understanding of biological processes and environmental aspects, where surface-active substances are involved, can be achieved by evaluating the physico-chemical properties of natural surfactants.

Current developments in the surfactant industry are driven by new specific applications and the demand for environmentally-friendly surfactants (biodegradable, low irritant) [12]. Increased environmental awareness among consumers has led to the increasing search for biological surfactants (biosurfactants) as possible alternatives to existing products [5]. Biosurfactants are increasingly used in a number of important industrial applications due to their advantages of biodegradability, production of renewable resources and functionality under extreme conditions [6]. Considerable efforts are now being made in the research and development of starch and cellulose as the basic materials in new surfactant applications. These polymers are widely used as raw materials in the paper, paint, textile, food and pharmaceutical industries. They have a broad range of important functional properties, are non-toxic, renewable, biodegradable and modifiable [13]. Other polymeric

surfactants are also receiving considerable attention for their use in nano-structures, latex stabilizers, emulsifiers, biomedical and pharmaceutical applications [14].

The availability of petroleum will decrease in the future, which consequently will raise the price of petroleum-based products such as ethylene oxide, the precursor to the hydrophilic portion of conventional nonionic surfactants [1]. Semisynthetic substances, on the other hand, can be produced from inexpensive and reproducible starting material such as sugars and glycerol derived from oils and fats [15]. The amount of surfactants used in formulations can also be considerably reduced by enhancing the surfactant's properties [12].

## 1.2. Motivation of study

Improving the end performance of paper is a major goal for all papermakers hence the properties and interactions of cellulose surfaces are of a great technical interest during papermaking and recycling [16,17]. The paper industry recycles paper because it is both economically and ecologically sound, and serves as an example of the sustainable use of resources [18]. There are, however, a number of issues related to the use of recycled paper which include:

- variations in fiber type due to previous pulping, bleaching and papermaking techniques,
- contamination from inks, adhesives, varnishes, coatings, binders, packaging, etc.,
- contamination from recycling processes that could affect the multiple recycling of fiber,
- soluble organic and inorganic contaminants, and
- the higher level of fines* causes a higher surface area which increases the sizing demand and affects the sizing efficiency of paper [20].

Sizing occurs during the modification of fiber surfaces with the purpose of reducing water penetration into the paper structure [21]. Sizing plays a vitally important role in

* Highly refined fiber [19].

obtaining paper with good printability and water resistance, which are the two key end-paper properties. Achieving optimum sizing performance and cost efficiency remains a massive challenge for the paper industry [16,22].

This study will focus on the modification or sizing of recycled paperboard by using surfactants to improve the water resistance property of the paperboard.

## 1.3. Objective

The main objective of this research was to increase the hydrophobicity or sizing efficiency of recycled paperboard, with surfactants, in order to decrease the amount of water absorbed.

## 1.4. Methodology

1) Firstly a comparison was made between the degree of surface modification of cellulose by means of three different types of industrial surface-active agents (anionic, nonionic and reactive surfactant) according to:

- The type of bond (covalent, hydrogenic or ionic) formed with cellulose. This gave an indication of the ability of the surfactant to adsorb to the paper surface.
- The hydrophobicity of the surfactants. This gave an indication of the sizing efficiency of the surfactants.

The main aim of the above comparison was thus on finding the surfactant structure best suited for the sizing of recycled paperboard.

2) After results of the above comparison *(see Chapter 3, Section 3.3)* indicated that polymeric surfactants were best suited for the surface modification of cellulose, focus shifted to synthesizing selected copolymer surfactants via free radical copolymerization. The two copolymers that were to be synthesized were to have the following structures:

- maleic anhydride, the reactive (towards cellulose fiber surface) polar part for both copolymers, and

- butyl methacrylate and lauryl methacrylate, the hydrophobic parts of the respective copolymers.

3) The properties of a copolymer are very dependent on its monomer distribution. In free radical copolymerizations knowledge about the reactivity ratios of the co-monomers is important because it gives an understanding of the copolymerization system and thus allows for reaction conditions to be tuned in order to obtain the desired copolymer content [23]. The reactivity ratios of the co-monomers used to synthesize the two copolymers were unavailable from literature. Knowledge about the co-monomer incorporation during copolymerization for the respective copolymer systems thus had to be obtained. In situ proton nuclear magnetic resonance ($^1$H NMR) was used to determine the co-monomer incorporation in both copolymer systems. This was done by carrying out the respective copolymerization reactions in an NMR tube and monitoring the decrease in the peak intensities of the co-monomers.

3) Lastly, a comparison of the degree of surface modification of cellulose was made between the industrial polymeric surfactant and the two synthesized polymeric surfactants. This was done in order to determine whether the synthesized surfactants induced a comparative or better water resistance property to the recycled paperboard than the industrial polymeric surfactant. The main outcome was thus to establish whether the synthesized polymeric surfactants had a better sizing efficiency than the currently used industrial polymeric surfactant.

## 1.5. Thesis layout

This thesis consists of six chapters. Chapter 1 sheds light on some of the applications of surfactants and it also addresses the current changes in the surfactant industry. Brief mention is made of the problems associated with currently used petroleum-based surfactants and the increasing demand for biodegradable, non toxic surfactants. The motivation and objectives of the study are also outlined.

Chapter 2 gives a theoretical background to surfactants, paper, free radical copolymerization and in situ $^{1}H$ NMR spectroscopy.

Chapter 3 describes the analytical and industrial techniques used for the application and testing of the industrial- and the laboratory synthesized surfactants. A pre-screening experiment done on three industrial surfactants, the results of which determined the type of surface-active agents that were to be synthesized, is described.

Chapter 4 describes the syntheses of the respective copolymers via in situ proton $^{1}H$ NMR and laboratory scale reactions. The use of $^{13}C$ NMR for the quantification of the co-monomer composition of the laboratory synthesized copolymers, are also discussed.

Chapter 5 describes the modification of cellulose by the two synthesized copolymers. A comparison, in terms of sizing efficiency, was also made between the industrial polymeric surfactant, which was used for the modification of cellulose in Chapter 3, and the two laboratory synthesized polymeric surfactants.

Chapter 6 summarizes the main conclusions drawn and also gives some recommendations for future work.

## 1.6. References

(1) Holmberg, K. *Current Opinion in Colloid & Interface Science* **2001**, *6*, 148-159.

(2) Piispanen, P.S., 2002. Synthesis and Characterization of Surfactants Based on Natural Products, Kungl Tekniska Hogskolan, Stockholm, 1-60 pp.

(3) Salager, J-L. *Surfactants: Types and uses*; Laboratory of formulation, interfaces, rheology and processes: Merida-Venezuela, 2002; Vol. 2.

(4) Ganeva, D.E., 2003. Nanochemistry Through Self-assembly: Polymerisation of the Organised Phases of Polyelectrolyte-Surfactant Complexes. PhD Thesis, University of Stellenbosch, 135 pp.

(5) Sarney, D.B.; Vulfson, E.V. *Trends in Biotechnology* **1995**, *13*, 164-172.

(6) Banat, I.M. *Bioresource Technology* **1995**, *51*, 1-12.

(7) Musselman, S.W.; Chander, S. *Colloids and Surfaces A: Physicochemical and Engineering Aspects* **2002**, *206*, 497-513.

(8) Bognolo, G. In *ICI Surfactants*; Central Science Laboratory Agency: York, 1998; pp 1-9.

(9) Sadtler, V.M.; Guely, M.; Marchal, P.; Choplin, L. *Journal of Colloid and Interface Science* **2004**, *270*, 270-275.

(10) Ferrer, M.; Comelles, F.; Plou, F.J.; Cruces, M.A.; Fuentes, G.; Parra, J.L.; Ballesteros, A. *Langmuir* **2002**, *18*, 667-673.

(11) Stubenrauch, C. *Current Opinion in Colloid & Interface Science* **2001**, *6*, 160-170.

(12) Chevalier, Y. *Current Opinion in Colloid & Interface Science* **2002**, *7*, 3-11.

(13) Richardson, S.; Gorton, L. *Analytica Chimica Acta* **2003**, *497*, 27-65.

(14) Ngimhuang, J.; Furukawa, J-I.; Satoh, T.; Furuike, T.; Sakairi, N. *Polymer* **2004**, *45*, 837-841.

(15) Shinoda, K.; Carlsson, A.; Lindman, B. *Advances in Colloid and Interface Science* **1996**, *64*, 253-271.

(16) Lancaster, E.P. In *Pira*: Florida, USA, 2004.

(17) Freudenberg, U.; Zschoche, S.; Simon, F.; Janke, A.; Schmidt, K.; Behrens, S.H.; Auweter, H.; Werner, C. *Biomacromolecules* **2005**, *6*, 1628-1634.

(18) Ottenio, D.; Escabasse, J-Y.; Podd, B.; International Life Sciences: Belgium, 2004; p 48.

(19) Smook, G.A. *Handbook for Pulp & Paper Technologists*, 3rd ed.; Angus Wilde Publications Inc.: Vancouver, 2002.

(20) Jenkins, S.; Cytec Industries: U.K., 2002; p 9.

(21) Fardim, P. *Tappi* **2002**, *1*, 1-14.

(22) Mattsson, R., 2002. AKD Sizing - Dispersion Colloidal Stability, Spreading and Sizing with Pre-flocculated Dispersion. Licentiate Thesis, Lulea University of Technology, Sweden, 34 pp.

(23) Vosloo, J.J., 2005. Model comb-like poly(butyl methacrylate): Synthesis, characterization and structure-property correlations. PhD Thesis, University of Sydney, 123 pp.

# CHAPTER 2

# Theoretical Background

## 2.1. Surfactants

### 2.1.1. Introduction

Surfactants are an important class of industrial chemicals and are widely used in almost every sector of modern industry [1]. Their activity and application depend on the net effects of their polar and non-polar functional groups [2]. Surfactants fulfill several purposes, including emulsification, dispersion, foaming, wetting, cleaning or removal, de-emulsification, coagulation or coalescence, de-foaming or antifoaming, de-wetting and deposition or coating [3]. They are used for their detergency, solubilization, and surface-wetting capabilities in the mining, petroleum, chemical, and pharmaceutical industries, as well as in biochemical and medical research [2,4,5,6].

Surfactant science is a technologically important domain which aims to increase the performance of surfactant formulations and to provide new surface properties [7]. There is an increasing interest in the designing of surfactants that possess more complex structures and, thereby, exhibiting new chemical and biological functionalities [8]. New molecular architectures which have borderline structures, between the classical surfactants, hydrotropes* and polymeric surfactants, are also appearing (*see Figure 2.1*) [7]. The synthesis of tailor-made polymeric surfactants offers great opportunities in terms of flexibility, diversity and functionality [10].

* Hydrotropes are structurally similar to surfactants but possess a weaker hydrophobic character in comparison to that of a surfactant [9].

In the first half of this chapter the properties and classification of surfactants are discussed. In the second half the application of surfactants to paper, the main focus of this study, is discussed.

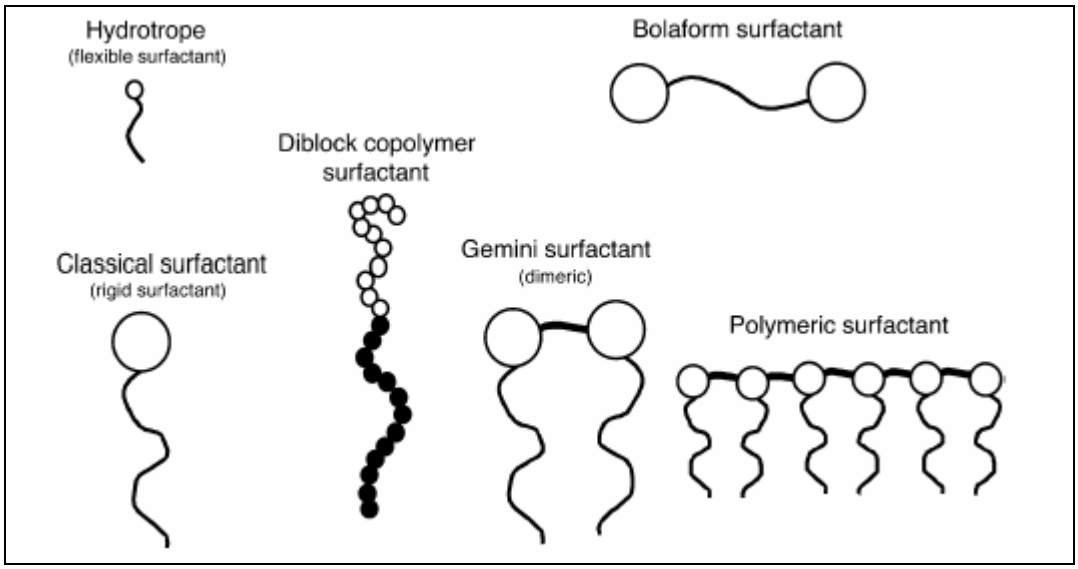


**Figure 2.1: Different molecular architectures of surfactants [7].**

## 2.1.2. Properties of surfactants

Surfactants have unique physical and chemical properties which determine their economic value and make their commercial applications important [11,12]. These physical and chemical properties are affected by parameters such as the degree of chain branching, the position of the polar headgroup and the chain length of the surfactant [13]. The effects of these parameters will become evident when the surfactant's ability to lower the surface tension, self-assembly structures and hydrophile-lipophile balance are discussed in the following three subsections.

### 2.1.2.1. Lowering of surface tension

Surfactants are characterized by their tendency to adsorb* at surfaces* and interfaces* in order to lower the surface tension* [13]. The different interfaces that exist are [15]:

- solid-gas
- solid-liquid
- solid-solid
- liquid-gas
- liquid-liquid

This ability to reduce the surface and interfacial tensions is one of a surfactant's most important properties [11]. Surfactants can adsorb to all of the interfaces listed above but only the solid-liquid and liquid-vapour interfaces are discussed in the following two paragraphs.

The adsorption of surfactants at a solid-liquid interface is influenced by factors such as the nature of the structural groups on the solid surface, the molecular structure of the surfactant and the environment of the liquid phase (pH, temperature, electrolyte content, etc.). Surfactant adsorption alters the surface free energy of the solid-liquid interface and thereby influences the wetting of solids. The surfactant molecules' orientation at the solid-liquid interface also determines the effectiveness of the surfactant to improve the wetting ability of the liquid [16].

Surfactants' decrease the surface tension when added to aqueous solutions because they minimize their energy by creating a monolayer on the liquid-vapour interface [17,18]. This occurs when the surfactant directs its hydrophobic parts toward the less polar air and the hydrophilic parts toward the polar liquid molecules [18].

---

* Adsorption occurs when particles attach themselves to a surface [14].
* A surface indicates that one of the phases is a gas [13].
* An interface denotes a boundary between any two immiscible phases [13].
* Surface tension is the amount of work required to change the surface area of a sample [14].

Surfactants ability to lower the surface tension reaches its limit when micelles start to form in the bulk solution [13]. This will be discussed in the next section.

### 2.1.2.2. Self-assembly of surfactant structures

An increase in surfactant concentration, in an aqueous solution, leads to an increase in the formation of closed structures called micelles (*see Figure 2.2*) [17-19.] Micelles are colloidal dispersions that consist of separate particles distributed within a continuous phase or dispersion medium. These colloidal dispersions are divided into three principal groups: lyophobic*, lyophilic* and association colloids. Micelles belong to the group of association or amphiphilic* colloids [21].

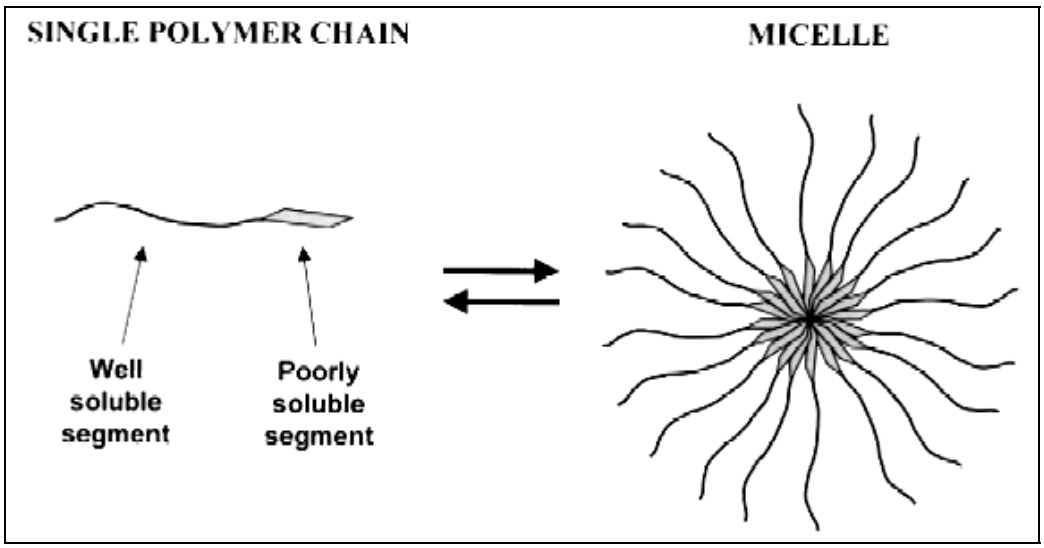


**Figure 2.2: Micelle formation from surfactant molecules [21].**

The two factors involved in the spontaneous formation of micelles are the hydrophobic effect and the interactions between the hydrophilic head groups. The hydrophobic effect causes the non-polar portion of the surfactant to be directed either toward the interior or

* Lyophobic colloids tend to accumulate at the surface [20].
* Lyophilic colloids tend to accumulate in the bulk phase [20].
* Amphiphilic colloids consist of both lyophobic and lyophilic moieties [20].

exterior of the micelle, depending on the type of media. The interactions of the hydrophilic head groups determine how closely the molecules pack in the micelle [22]. Micelles can exist in various shapes and sizes depending on the surfactant concentration, structure, pH, ionic strength, temperature etc. [18]. The particular size of a micelle is described by the aggregation number, m, which is the average number of amphiphilic molecules in a single micelle [22]. At high surfactant concentrations micelles start to self-assemble and pack into lamellar, hexagonal or cubic structures (*see Figure 2.3*) [18, 23].

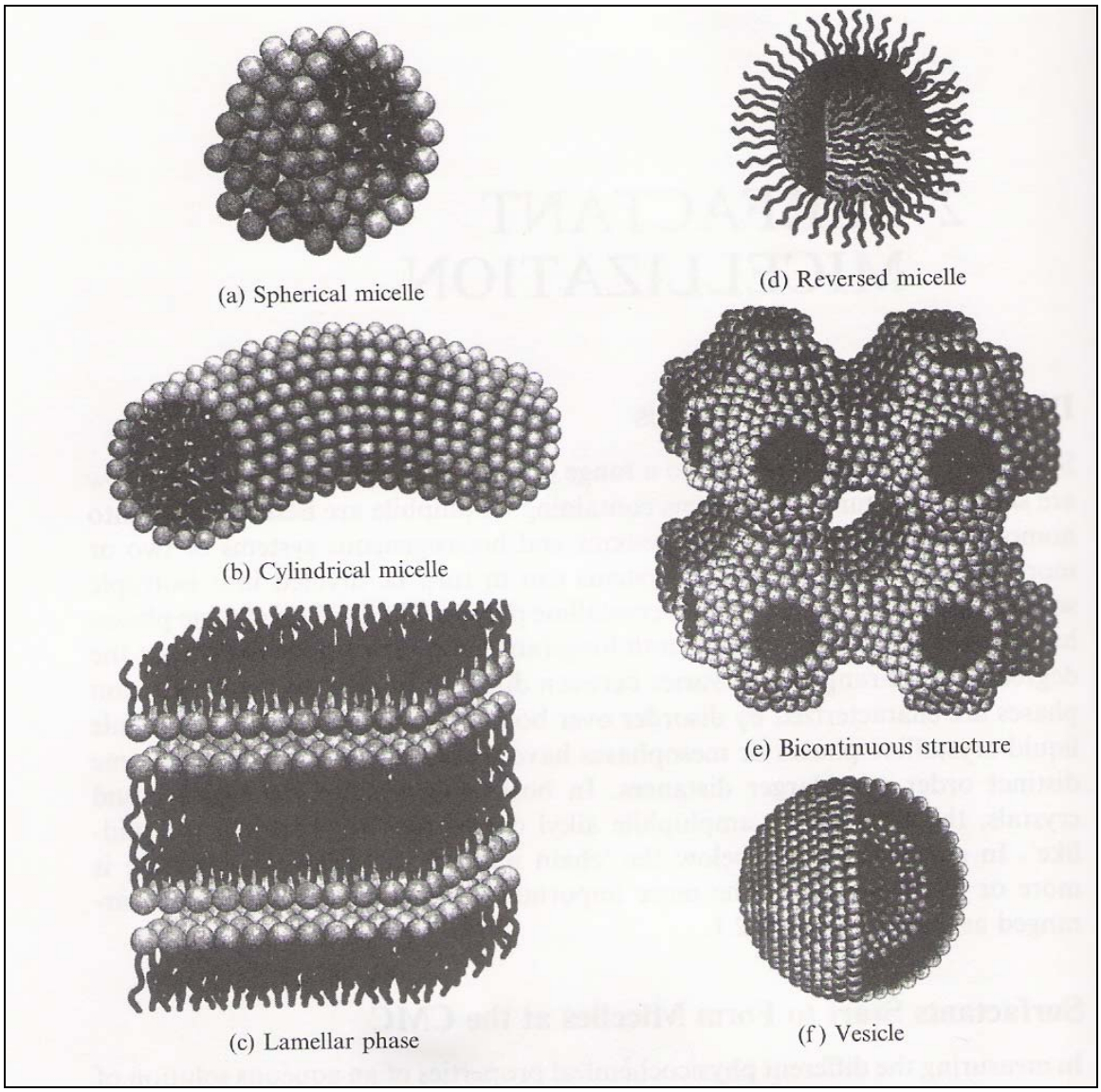


**Figure 2.3: Self-assembly structures of micelles formed at increased surfactant concentrations [18].**

The concentration at which micelles appear is called the critical micelle concentration (cmc) [6,21]. Surfactant properties such as surface tension, viscosity, conductivity, turbidity, nuclear magnetic resonance etc. vary above and below the cmc (*see Figure 2.4*) [18,23]. Some of the techniques used for the determination of the cmc of surfactants and polymeric surfactants include light-scattering changes, hydrodynamic and surface tension properties and changes in absorbance or fluorescence upon dye solubilization [24].

Thermodynamic parameters such as Gibbs energy, enthalpy and entropy, associated with surfactant micellization, can be determined from calorimetric, ultraviolet (UV) and isodine solubilization (IS) techniques [25].

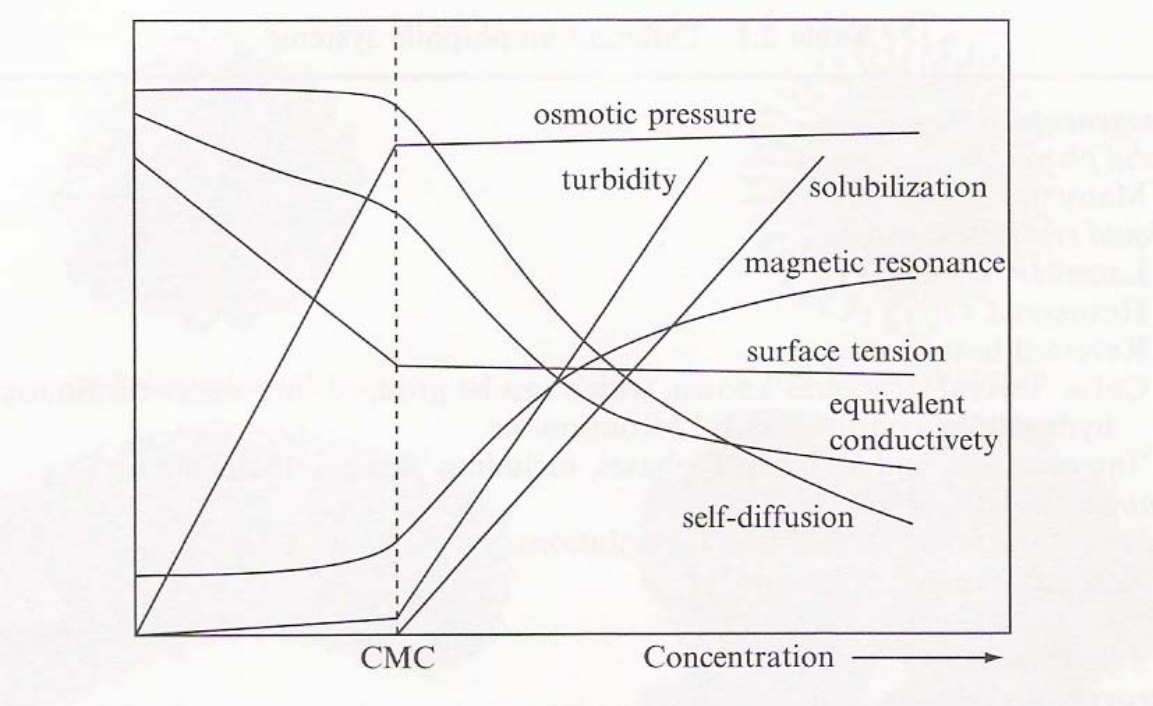


**Figure 2.4: Schematic representation of the variation in surfactant properties above and below the CMC [18].**

Polymeric micelles are a separate class of micelles formed from copolymers consisting of both hydrophilic and hydrophobic monomer units [21]. They are becoming important carriers for the delivery of bioactive materials such as water-insoluble drugs, hormones and plasmid DNA [26]. Polymerized micelles, or polysoaps, also exhibit a potential to function as catalysts because they form stable micelle associations (*see Figure 2.5*). Conventional micelles, on the other hand, rapidly dissociate at equilibrium conditions and are therefore not favourable for catalytic processes [27].

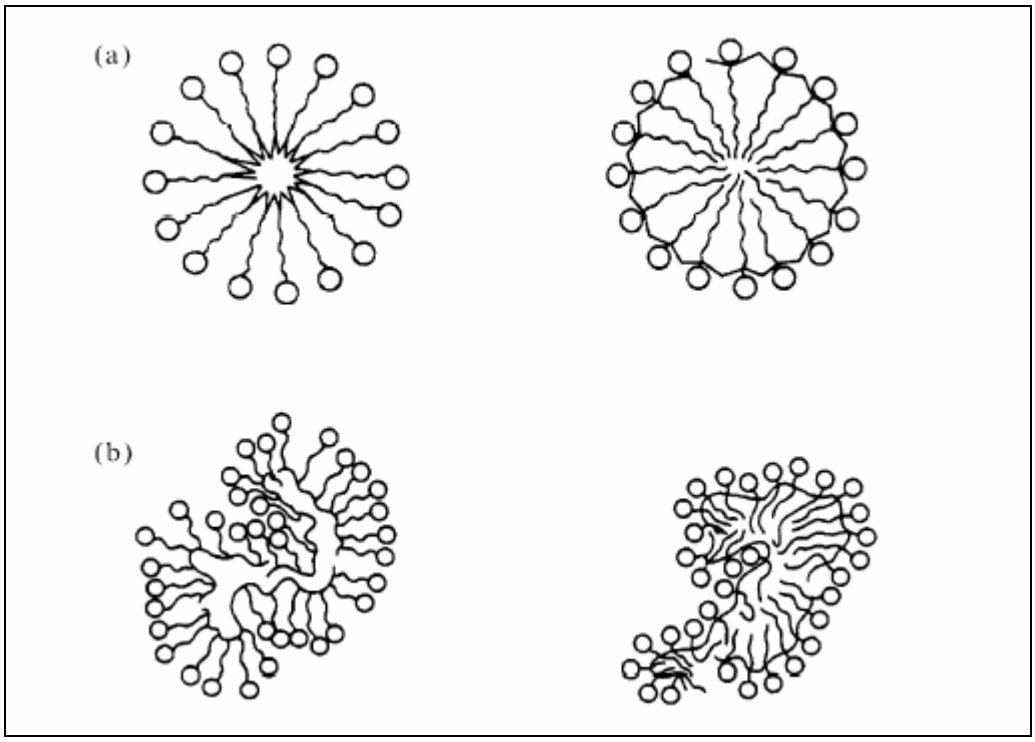


**Figure 2.5: Schematic representation of a) a polymerized micelle and b) a polysoap [27].**

The applications of colloidal particles, such as micelles, are becoming important in the cosmetic, foods, detergent and petrochemical industries [28]. The drug carrying ability of micelles provide numerous advantages such as the solubilization of poorly soluble drugs, the accumulation in body regions with leaky vasculature, attachment of specific ligands to their outer surface and large scale reproducibility on a commercial level. Micelles also increase the bioavailability of drugs by protecting them from inactivation by the body's defense mechanisms without causing undesirable side effects [29].

### 2.1.2.3. Hydrophile-Lipophile balance (HLB value)

The activity of surfactants is usually related to their hydrophile and lipophile balance (HLB) [30]. The HLB values of surfactants are related to their properties such as the cmc, the solubility parameter (σ) and their ability to promote inversion of emulsions [31,32].

These values can be calculated using either the surfactant molecular structure or they can be determined experimentally by the emulsion comparison method found by Griffin in 1949 [32]. Griffin proposed that the effectiveness of a surfactant in an emulsion system could be calculated via the HLB of the surfactant, which is calculated from its chemical structure, and the HLB of the oil phase involved [33]. In ideal cases, the HLB can be calculated according to the formula:

$$HLB = 20\left(\frac{M_h}{M}\right) \quad (2.1)$$

where:

$M_h$: the molecular mass of the hydrophilic fraction in the molecule
M: the total molecular mass of the surfactant [34].

Surfactants with the following HLB values are used as the following: 3-6, as water-in-oil emulsifiers; 7-9, as wetting agents; 8-15 as oil-in-water emulsifiers; 13-15, as detergents and 15-18 as solubilizers [18].

### 2.1.3. Surfactant classes

Surfactants are classified according to their polar head group or to their dissociation in water [2,35]. There are four classes of surfactants: anionic, cationic, nonionic and zwitterionic surfactants [36]. Polymeric surfactants are a separate class of surfactants which offer improved properties by chemically linking surface-active molecules [35,37]. Surfactants can also have functional groups that can chemically react with surfaces [38].

#### 2.1.3.1. Anionic surfactants

An anionic surfactant is the reaction product of an organic compound such as an acid or alcohol with an inorganic compound such as sodium hydroxide [39]. They are the most

commonly used surfactants and include alkylbenzene sulphonates (detergents), soaps (fatty acids), lauryl sulphate (foaming agent), di-alkyl sulfosuccinate (wetting agent), lignosulfonates (dispersants) etc. [35]. Figure 2.6 gives the structure of an anionic surfactant.

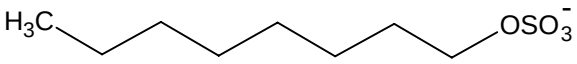


**Figure 2.6: An example of an anionic surfactant: an alkyl sulfate.**

Anionic surfactants have the advantage of being stable foaming agents but they also have the disadvantage of being sensitive to minerals (calcium, magnesium, etc.) and to the presence of minerals in water (hard water) or pH changes [33]. The amphoteric character of anionic surfactants allows them to accumulate in living organisms, rivers, seas and sewage sludge. Their modification of protein structure and disfunctioning of enzymes and phospholipid membranes causes toxic symptoms in organs of animal and human organisms [40]. The industrial scale production and application of anionic surfactants arose because of their advantageous physico-chemical character. They have many beneficial effects but also show marked toxicity and cause marked environmental pollution [17].

### 2.1.3.2. Cationic surfactants

Cationic surfactants are formed in reactions of alkyl halides with primary, secondary and tertiary amines [36]. Figure 2.7 gives the structure of a cationic surfactant.

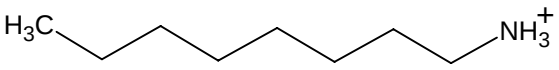


**Figure 2.7: An example of a cationic surfactant: a fatty amine salt.**

The majority of cationic surfactants have an ammonium head group which undergoes Hofmann degradation*, resulting in temperature sensitivity and an amine odor. Amine derivatives are also sensitive toward oxidation, resulting in, for example, the yellowing of paper products or coatings [42]. Cationic surfactants reduce surface tension and are used as wetting agents in acidic media but they do not have detergent action when formulated into alkaline solutions. These surfactants, though readily biodegradable in aerobic environments, are toxic even at low concentrations, and their application to agricultural soil may have detrimental effects on soil biota [43]. They are also used in applications ranging from fabric softeners and toiletries to adhesion promoters in asphalt and corrosion inhibitors [36].

### 2.1.3.3. Nonionic surfactants

Nonionic surfactants have a hydrophobic/hydrophilic balance and have neither a negative nor a positive charge in either part of the molecule (*see Figure 2.8*). They are not affected by water hardness or pH changes as the anionic and cationic surfactants are, and they are considered as medium- to low-foaming agents [33]. Contrary to ionic surfactants, nonionic surfactants also become less water soluble and more hydrophobic at higher temperatures [13].

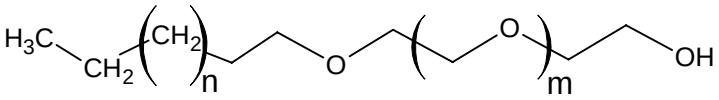


**Figure 2.8: An example of a nonionic surfactant: a fatty alcohol ethoxylate, where n and m is the number of repeating units.**

Most nonionic surfactants are ethylene oxide derivatives and include polyoxyethylene alkyl ethers, alkyl glyceryl ethers, polysorbates (Tween) etc. [44,45]. Nonionic surfactants are becoming increasingly more important since they are compatible with many other

* Hoffmann degradation occurs when the quaternary ammonium salt undergoes elimination to give an alkene [41].

types of surfactants and are soluble in water and many organic solvents [25]. The growth of the nonionic surfactant industry in recent years has been aided by an environmental concern over the non-biodegradable nature of most anionic surfactants [16]. Polyethoxy alkylphenols are nonionic surfactants that are biodegradable in water but their biodegradation yields phenol and alkylphenol compounds that are persistent and toxic [19]. Nonionic surfactants with hydroxyl groups, for example sugar esters, possess stronger hydrophilicity and hydrophobicity than those containing polyoxyethylene groups.

### 2.1.3.4. Zwitterionic surfactants

Zwitterionic surfactants consist of both positive and negatively charged groups. They should not be confused with amphoteric surfactants which are pH dependent [13]. Figure 2.9 gives the structure of a zwitterionic surfactant.

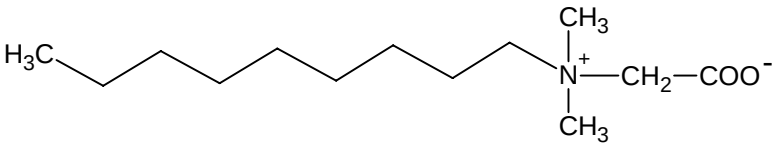


**Figure 2.9: An example of a zwitterionic surfactant: a betaine**

Zwitterionic surfactants have excellent dermatological properties, have a low eye irritation potential and are frequently used in shampoos and other cosmetic products. They also function well in high electrolyte formulations because, like the nonionic surfactants, they have no net charge [13].

### 2.1.3.5. Polymeric surfactants

The polymerization of surfactants can lead to well defined polymeric surfactants (*see Figure 2.10*) and to polymeric micelles [37]. Compared to low molecular weight surfactants, polymeric surfactants with their high molecular weight are considered to have weak abilities to reduce surface/interfacial tensions [46]. They do however have higher

micelle stability due to factors such as low critical concentration, slow exchange between free polymers and micelles, low mobility in the core, higher molecular mass, etc. [47].

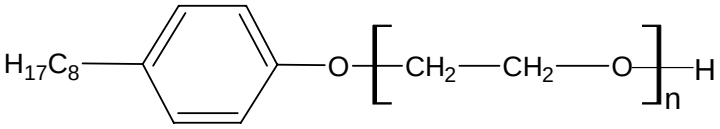


**Figure 2.10: Structure of polyetoxylated octyl phenol where n is the number of repeating units.**

Oligomeric surfactants are low molecular weight 'polymeric' surfactants which have a limited number of repeating groups. They are excellent wetting agents, dispersants, low-foaming agents and are used in non-aqueous dispersions [48].

Polymeric and oligomeric surfactants are more effective in the stabilization of emulsions than ionic and nonionic surfactants [49]. They provide steric stabilization that makes emulsions less sensitive to fluctuations and increases in electrolyte concentrations and they can be applied at high temperatures [49,50]. These surfactants are equally effective at high and low solids contents and they stabilize aqueous and nonaqueous dispersions equally well [50]. The polymeric molecule can be specifically designed for the suitability of a specific application [49]. Those containing the anhydride group are reactive [51].

### 2.1.3.6. Industrial surfactants

#### *1) Sodium lauryl sulphate (SDS)*

Sodium lauryl sulphate *(see Figure 2.11)*, also known as sodium dodecyl sulphate, is an anionic surfactant. It causes severe skin dehydration and has a high eye and skin irritation potential [40].

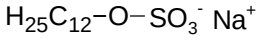

**Figure 2.11: Structure of sodium lauryl sulphate.**

***2) Sucrose esters (SE)***

Sucrose esters are nonionic surfactants consisting of a sugar (e.g. glucose or sucrose) as the hydrophilic group and a fatty acid as the hydrophobic group [52,4]. The structure of a sugar ester is given in the figure below.

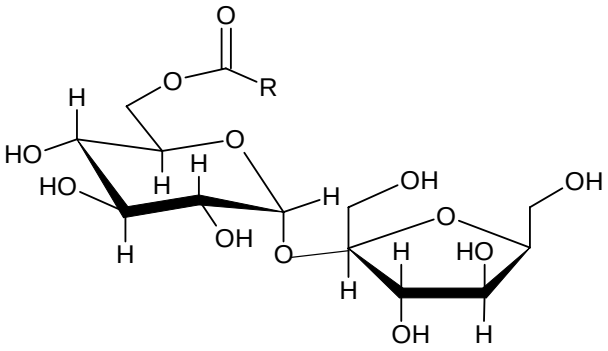

**Figure 2.12: Structure of a sucrose ester where R is an alkyl chain.**

Sugar esters were first recorded in the literature in 1880 but extensive investigations of other esters and esterification processes did not take place until the 1950's. Japan was the first country to undertake the industrial production of sugar esters [53].

Sugar esters are tasteless, odorless, nontoxic, a nonirritant to the eyes and skin, highly biodegradable and have favourable properties with respect to applications in the food industry, cosmetics, detergents, oral-care products and medical supplies [52,4,5,54]. The breadth of their functional properties can be attributed to the fact that they can be manufactured with an extremely wide range of HLB values, e.g. HLB 1-18 [55-56]. Their surface properties, including their HLB value, are controlled by the type of acyl group, the degree of substitution and the degree of polymerization of the carbohydrate [57]. They

also have excellent surface-tension-reducing capacity, dispersion and detergent power [1,55,58,59]. An important feature of sugar surfactants is the temperature-insensitivity of their physical-chemical properties [60,61]. This insensitivity results from the strength of the hydrogen bonds between the hydroxyl groups of the sugar unit and water which prevents any significant dehydration of the head group [60].

***3) Alkenyl succinic anhydride (ASA)***

ASA (*labeled 1 in Figure 3.5*) is an extensively used sizing agent (reactive surfactant) and is produced from the reaction of an olefin with maleic anhydride (*see Figure 3.5*) [62,38]. It is a liquid, is insoluble in water, and must be emulsified for use in a papermaking system. A cationic emulsifying agent such as starch must be used in order for the ASA to be deposited onto the negatively charged cellulose surface. It is thought that the cellulose surface develops a negative charge due to the ionization of molecules or the adsorption of ions from the surrounding solution. The retention of ASA on the cellulose surface is thus the result of the ionic attraction of the cationic emulsion droplets to the negatively charged cellulose fiber. When ASA is retained on the fiber, its functional end group reportedly reacts with the cellulosic hydroxyl groups to form covalent bonds [63]. The reactivity of ASA indicates that it hydrolyzes rapidly. This results in press picking, deposits and sheet defects such as de-sizing [62].

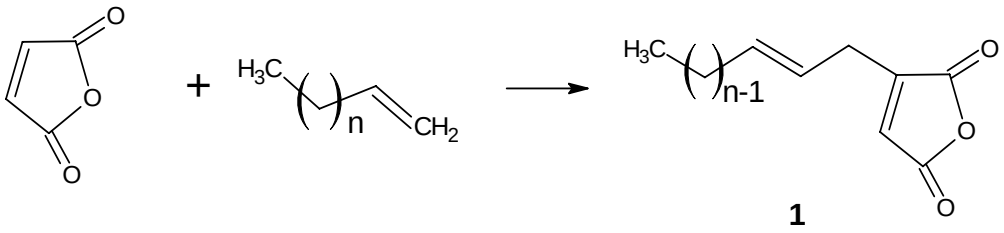


**Figure 2.13: Formation of ASA where n is the number of reacting units.**

The functional end group of ASA that reportedly reacts with the hydroxyl groups of cellulose, starch and water, is maleic anhydride [38]. Maleic anhydride hydrolyzes to maleic

acid in the presence of water at room temperature or can form a half ester with the hydroxyl groups of cellulose [51].

### 2.1.4. General applications of surfactants

The choice of surfactant generally depends on its application because there is no universally good surfactant suitable for all uses [13]. They find one of their major pharmaceutical uses as solubility enhancers in aqueous formulations. Generally, only nonionic surfactants are used in parenteral formulations [64].

A range of potentially new or improved applications have recently emerged. For example, cationic surfactants have been shown to be effective at condensing, and thereby accelerating, the transport of genetic material (DNA) across biological membranes. Vesicles formed by mixtures of anionic and cationic surfactants have been used as templates for polymerization, thus leading to the formation of hollow polymeric capsules. Recently, ionic amphiphiles have formed the basis of so-called ionic liquids that can serve as novel reaction media [65]. A starch graft, poly(methyl acrylate) copolymer, that degrades during the growing season, has also been developed for use in agricultural mulching [66]. Chemically synthesized surfactants have been used in the oil industry to aid in the clean up of oil spills, as well as to enhance oil recovery from oil reservoirs. These compounds are not biodegradable and can be toxic to the environment [17].

### 2.1.5. Application of surfactants to paper

Surfactants are used as sizing agents for paper to help improve the paper's water-fastness, dimensional stability and wet strength [67].

## 2.2. Paper

## 2.2.1. Introduction

Paper is usually made from the pulping of wood but occasionally synthetic fibers and cellulose fibers from other plant sources are also used [68,69]. Wood, used in the pulp and paper industry, is composed of cellulose fibers which are held together by hydrogen bonds, carbohydrates such as starch and sugars, and lignin which act as an adhesive substance for the cellulose fibers [68,70]. In the processing of wood (*see Figure 2.11*), it is broken down to separate the cellulose from the non-cellulose substances and the raw material is chemically reduced to form a pulp [70].

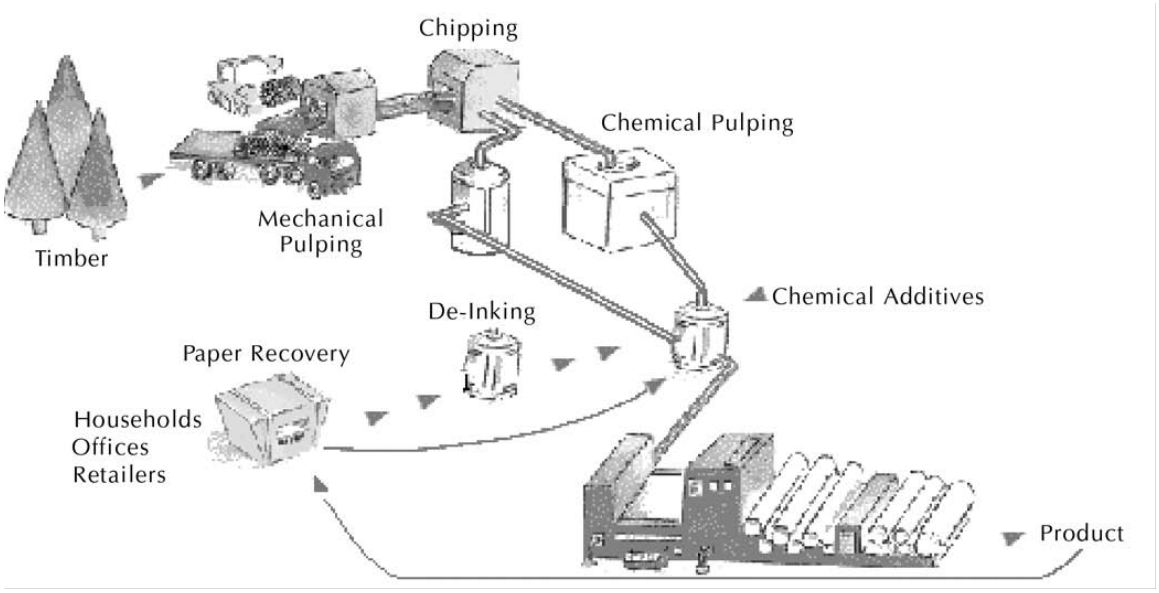


**Figure 2.14: Simplified scheme of the paper production process [71].**

Some of the components in wood are difficult to bio- or chemically degrade and they are washed away from the fibers during the washing, dewatering and screening processes [72]. Cellulose fibers are retained in the paper web by the chemical addition of polyelectrolytes which flocculate mineral fillers and fibrous fine material onto the cellulose fibers' surfaces [73]. The required quality of paper is produced by the further addition of chemicals which help to give the desired physical, optical or electrical properties to the paper [68,70]. These chemicals include dyes and optical brighteners to enhance appearance, resins to

lend wet strength, rosins or starch size to reduce penetration of aqueous liquids, pigment coatings to provide a smooth surface for printing, mineral fillers to increase opacity, polymers applied by saturation or extrusion to give mechanical or barrier properties, and cationic polyelectrolytes and resistive polymers used in the interior and on the surface of paper for dielectric recording [68,72]. Polymeric additives used to improve the retention of pigments and fine material and the formation and drainage properties of the paper web etc., form undesirable deposits, known as pitch deposits, in the paper web or on the surfaces of press rolls and other machinery [74]. The properties of paper are also directly affected by the fibers' chemical composition including color, opacity, strength and electrical properties [68].

### 2.2.2. Cellulose, the basic constituent of paper

Cellulose is the most abundant natural polymer and is extensively used as a renewable raw material for many products in paper, paint, food, textile and pharmaceutical industries [75]. It is a complex polysaccharide composed of long unbranched microfibrils which consist of glucose units that give support to the cell wall of higher plants [76]. Because of the strong hydrogen bonds (*see Figure 2.12*) that occur between cellulose chains in the crystalline regions, cellulose does not melt or dissolve in common solvents [77]. The insolubility of cellulose means that technological processes are also based on colloid systems, for example, fiber suspension in papermaking. Therefore, interfacial interactions involving cellulose are of particular interest for cellulose material production and utilization. These interactions not only govern processes of manufacturing, recycling, coating, etc. but also determine the physical properties of cellulose-based products. Cellulose is often modified by physical, chemical, enzymatic and genetic means in order to increase its industrial use. Modification of cellulose leads to substitution of its free hydroxyl groups and to changes in its properties. In the less ordered regions of cellulose, the chains are further apart and more available for bonding to other molecules. Like alcohols, cellulose can engage in primary and secondary bonding [78].

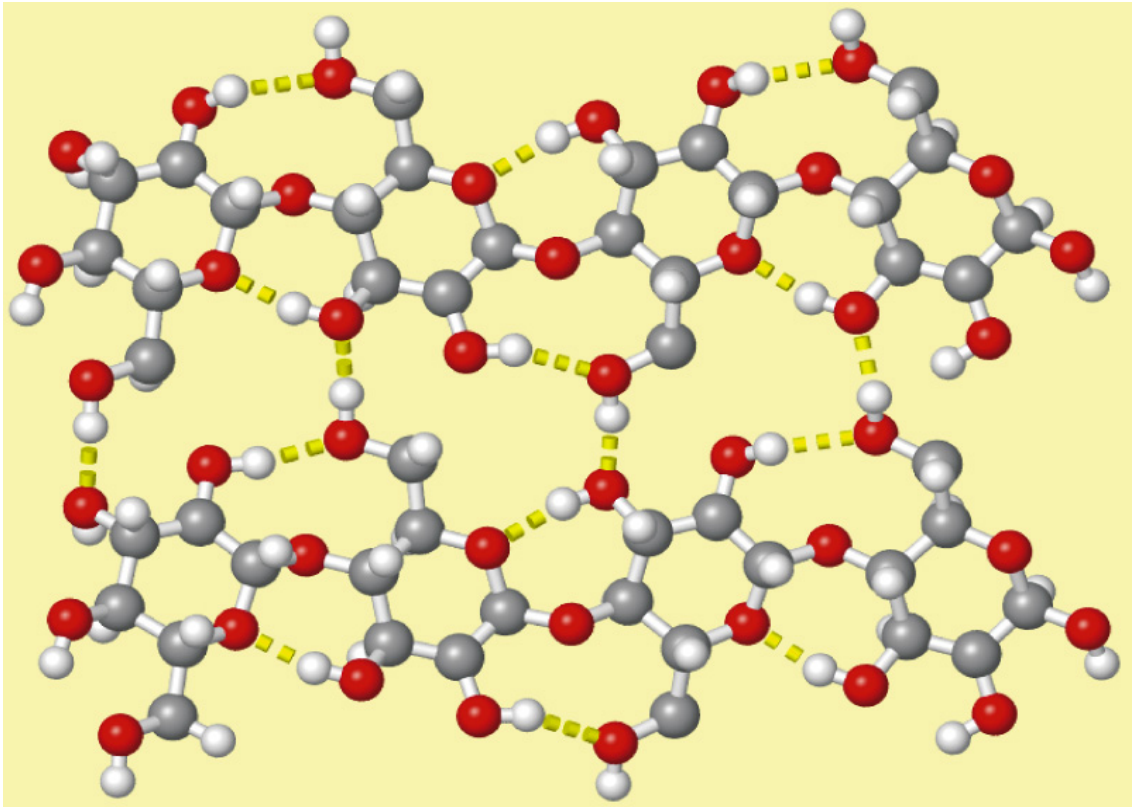

**Figure 2.15: 3D structure of cellulose where the red balls = oxygens, white = hydrogens, gray = carbons and yellow lines = hydrogen bonds [79].**

### 2.2.3. Paper sizing

Various paper grades are sized by the addition of chemicals to improve the mechanical and water-repellent properties of the paper [80,81]. Improved hydrophobicity of paper is important for printing purposes [82]. Sizing allows for the interaction between the paper and ink to be controlled [81,83]. Initially, starch was the only additive applied to the paper surface but today, rosin and synthetic polymers such as alkenyl succinic anhydride (ASA) and alkyl ketene dimer (AKD) are more commonly used [84]. These agents not only improve the sizing, printability and writability of paper, but they also improve the runnability of the paper production machinery [81,83]. Rosin sizing, a precipitation between rosin acid and aluminium resinate, occurs under acidic conditions and the sizing effect is achieved by electrostatic interaction between the cellulosic surface and the highly

hydrophobic agent [82]. AKD and ASA are used in alkaline systems and presumably form ester bonds with the hydroxyl (OH) groups on the fiber surface [84,85]. Many paper mills have changed from acidic to neutral or alkaline conditions because of the higher chemical stability of neutral papers and due to the availability of inexpensive calcium carbonate used as a filler [82]. Additional benefits of alkaline conditions include the buffering of acid which hydrolyses the wood fibers during long term storage, thus decreasing the aging properties of the paper. Alkaline paper also loses less strength than acidic paper during the recycling process [85].

***a) Requirements of sizing agents***

Sizing agents must produce a contact angle greater than $90^0$ to retard liquid penetration. They can achieve this by orientating their hydrophobic tails such that a barrier is presented to the penetrant. Orientation provides a surface of low energy and is therefore important. Sizing agents must also be well anchored and distributed on the fiber surface. When a sizing agent has all the above requirements only a small quantity will be needed to sufficiently protect the fiber against penetration [63].

***b) Mechanism of the sizing process***

The mechanism of the proposed sizing process is not completely understood but the literature contains some proposals. In the proposed mechanism shown in Figure 2.16, the lactone ring of AKD is opened at the acyl-oxygen bond and a β-keto ester is formed between AKD and free OH groups on the cellulosic fibers [82].

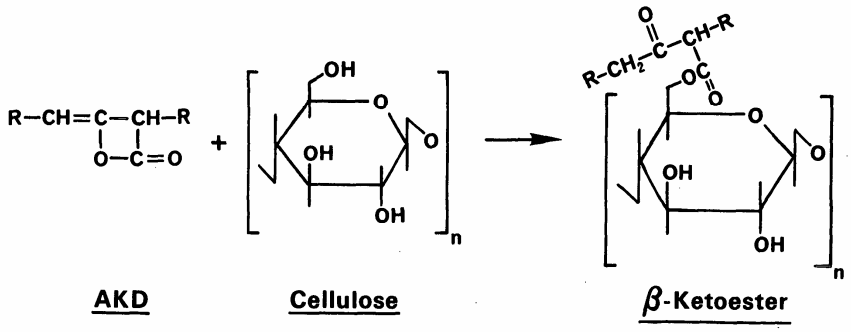


**Figure 2.16: Mechanism of the sizing process by the reaction of AKD with the OH groups of cellulose [63].**

ASA, with its maleic anhydride head group, follows the same mechanism as AKD but produces an ester-acid (*see Figure 2.17*) [63].

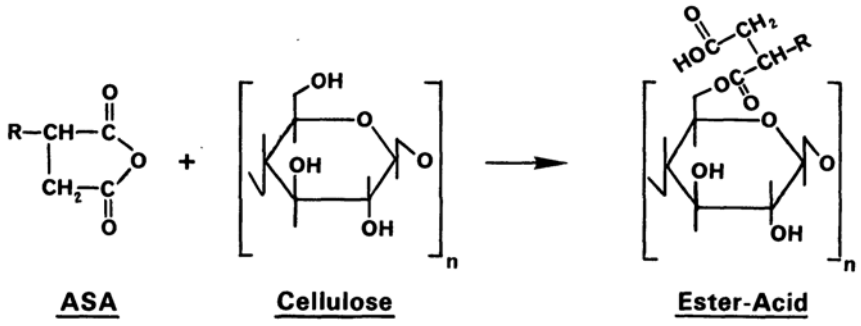


**Figure 2.17: Mechanism of the sizing process by the reaction of ASA with the OH groups of cellulose [63].**

Both AKD and ASA can undergo hydrolysis in water to form unstable β-keto acids. AKD can also react further to yield a ketone [63]. See Figure 2.15 for ASA hydrolysis and Figure 2.16 for AKD hydrolysis.

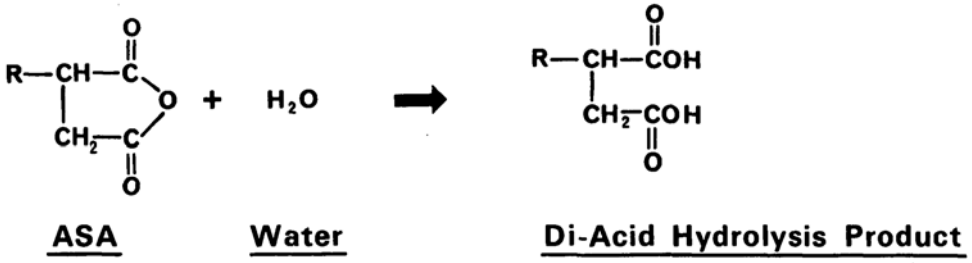


**Figure 2.18: Hydrolysis of ASA in water [63].**

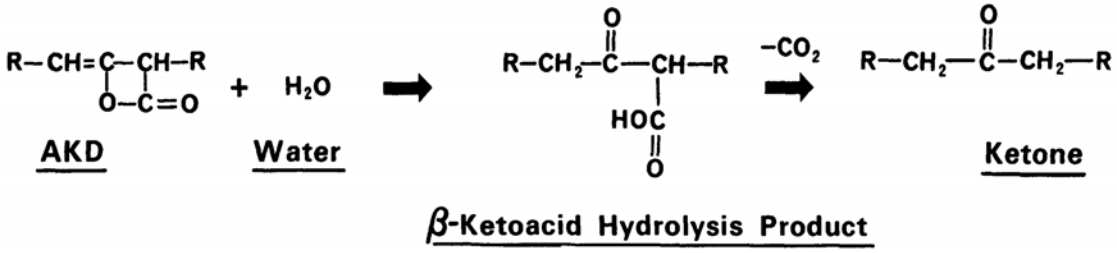


**Figure 2.19: Hydrolysis of AKD in water [82].**

Paper can be sized manually with a brush or by the dipping method [86]. The dipping method is used in this study (*see Chapter 3, Section 3.2.3*). The sizing process is dependent on different parameters such as the type of sizing agent (its viscosity, pH and concentration), time and method of drying of paper sheets, the temperature at which the sized paper is dried, and paper coating machine speed [80,82]. A strong sizing effect can take place after the sized paper is cured or exposed to elevated temperatures between 100 and 120 $^{0}$C [83]. The types of sizing agents used depend on the end use of the paper product [87]. Examples of sizing agents are styrene maleic anhydride and styrene acrylic acid, used for printing and copy papers. Polyurethanes, which provide effective hydrophobicity, cannot be used on copy papers because they prevent important powdered toner adhering to the paper [68]. Conventionally, a sizing dispersion consists of dissolved starch that provides stiffness and strength, and a suspended sizing agent that makes the paper surface hydrophobic [80]. The combination of the starch and sizing agent reduces linting, dusting,

the picking of vessel segments during offset printing, and even improves the performance of hydrophobic polyelectrolytes added with the size-press starch solution [68,88]. The majority of sizing agents are used in the production of paper and paperboard [89].

### 2.2.4. Properties of the pore spaces of paper

The pore spaces of paper, which are the channels between the fibers, are anisotropic* (*see Figure 2.17*).

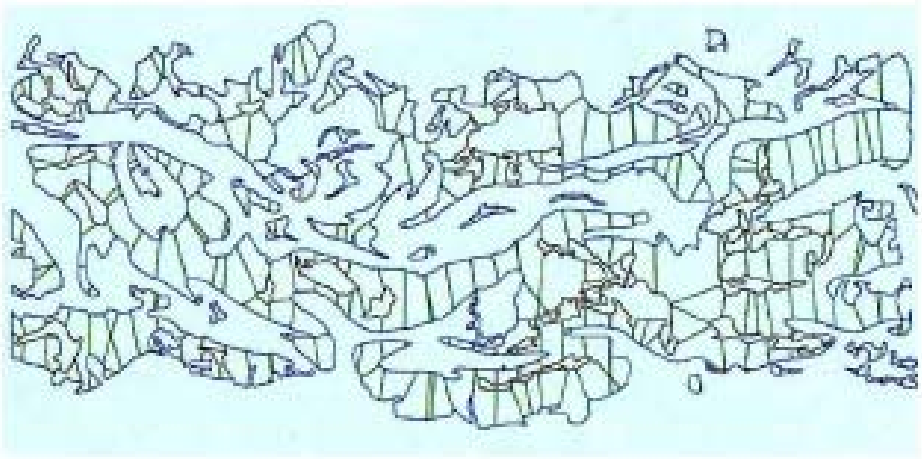

**Figure 2.20: An example of the image of a paper's pore space. The regions without the straight lines represent the pore spaces [91].**

The penetration, flow and spreading of fluids in the pore spaces of paper occur during the papermaking process, coating of the paper surface and printing [91]. The rate of liquid penetration into a pore can be described by the Washburn equation:

$$\frac{dl}{dt} = \frac{\gamma r}{4\eta l} \text{Cos}\,\theta \qquad (2.2)$$

* Anisotropic means that the pore spaces of paper have physical properties that are different in different directions [90].

where:

r: the pore radius (m)

γ: the surface tension (mJ/m)

η: the viscosity of the fluid (Pas)

$l$ : the pore length (m)

θ: the contact angle ($^0$)

t: the time of fluid penetration, flow and spreading (s)

Liquid penetration can best be controlled by altering the contact angle. The pore radius, pore length, surface tension and liquid viscosity are difficult to control. Altering of the contact angle can be accomplished by the use of sizing agents [63]. The fluid flow within the pore spaces, the mechanical properties and surface appearance of paper are affected by the fiber-to-fiber contacts, the hydrogen bonds between the fibers and the fibers' orientation [91].

Paper's pore space morphology comprises its porosity, the effective radii, the lengths of the channels between the fibers, the interconnectivity of the fibers, as well as the thickness of the paper. The morphology of the pore space of a paper product is controlled by the types of fibers used. For example, dense paper with small pores and low porosity is generated from short fibers subject to a high degree of refining. The pore space morphology of paper can be changed by factors such as the spatial distribution of fibers, the degree of refining, the use of fillers, calendaring (pressing), sizing, etc. The paper's porosity and the connectivity of the flow channels between the fibers can also be varied. An example of a non-porous material is greaseproof paper and that of a porous material is filter paper [91]. A wide variety of types and grades of paper are made to serve many functions, such as writing and printing, wrapping and packaging, kitchen towels, building materials etc. [86].

In this study paperboard is used; paperboard is generally thicker, heavier and less flexible than conventional paper [68].

## 2.3. Free radical polymerization

### 2.3.1. Introduction

Polymers can be synthesized via many pathways, but the most widely used process is free radical polymerization [8]. Free radical polymerization is a chain growth polymerization process which has the advantage of being less sensitive to traces of impurities than other polymerization techniques, such as ionic and coordination polymerizations [92]. The disadvantage of this technique is that it exhibits very little control over the molecular weight distribution and the chemical composition of the polymer chain [93]. The effective control of molecular weight is important because polymer properties are strongly dependent on it [94]. The molecular weight is affected by several parameters such as temperature, pressure, initiator concentration and chain transfer agents. An increase in temperature, initiator concentration and concentration of chain transfer agents leads to a lower molecular weight. Chain transfer agents have the added advantage of producing polymers with a narrow molecular weight distribution [95].

### 2.3.2. Copolymerization

Homopolymerization refers to the polymerization of a single monomer and copolymerization refers to the polymerization of a mixture of two or more monomers [96]. Copolymerization allows the synthesis of polymers with a wide range of physical and mechanical properties. The reactivity and relative concentrations of the two monomers determine the concentration and distribution of each comonomer incorporated into the polymer chain [97]. The composition of a copolymer is usually different to the composition of the monomer mixture from which it is produced. This results from the fact that the monomers have different tendencies to be incorporated into the copolymer and thus react at different rates with the two free radical species present [98]. Different types of copolymer structures can be formed if, for example, monomers A and B copolymerize. The copolymer structures *(see Figure 2.21)* include random, alternating, block, and graft

copolymers. Random copolymerization depends on the rate of incorporation of each comonomer. Alternating copolymerization is an example of chain copolymerization where each of the monomers preferentially adds to the other and homopolymerization is absent. Block copolymers contain long sequences of each comonomer along its backbone. Graft copolymers contain long sequences of one monomer with the other comonomer as side chains or grafts [99].

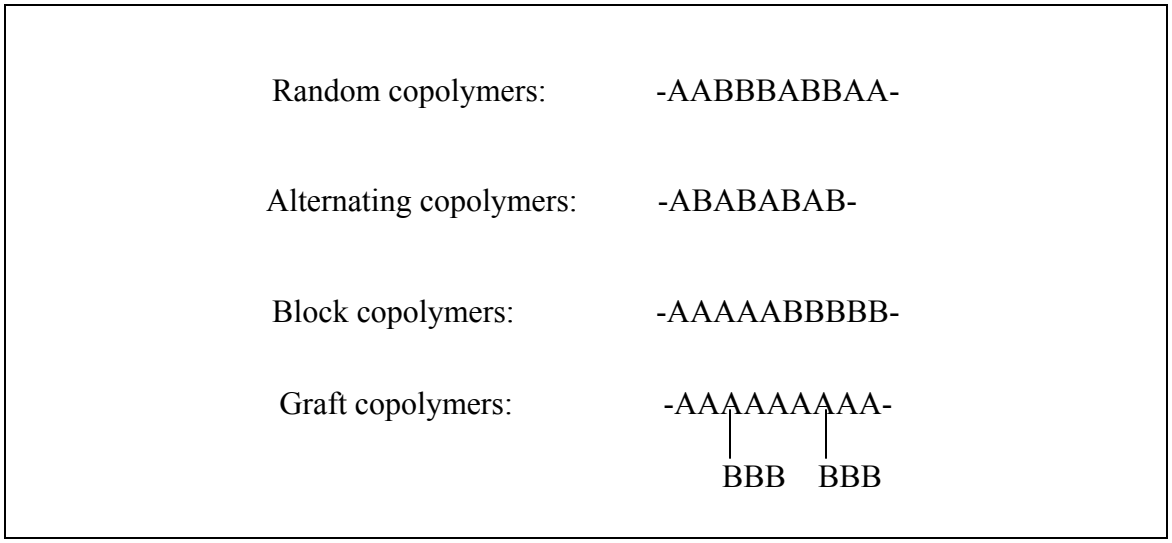


**Figure 2.21: Types of copolymer structures.**

This study will use in situ $^{1}$H NMR to determine the type of copolymer structures formed in the synthesis of the surface-active alkanes *(see Chapter 4)*.

### 2.3.2.1. Monitoring of polymerization processes via in situ $^{1}$H NMR

In the determination of copolymer composition, it is necessary to distinguish between the overall- and instantaneous composition for a given copolymer system. The former gives the copolymer composition formed up to a given % conversion, while the latter gives the copolymer composition that is formed at less than 10% conversion. Knowledge of the overall copolymer composition can sometimes be of more practical importance than the knowledge of the instantaneous copolymer composition. This applies to some copolymer

systems where the overall copolymer composition varies with % conversion, thus forming a copolymer with differing properties [100]. This study will focus on the overall copolymer composition.

Various analytical methods such as $^{1}H$ NMR, $^{13}C$ NMR and Fourier Transform Infrared Spectroscopy (FTIR) can be used to determine copolymer compositions [101]. In situ $^{1}H$ NMR, where the polymerization is performed in an NMR tube, was used in this study to determine the overall composition of the synthesized surface-active alkanes. Optimization of the NMR technique has permitted its use in the study of chemical reactions instead of just chemical structure identification and elucidation [102]. A major advantage of the in situ study is that it determines the copolymer composition directly in solution and the monomer conversions can be observed by monitoring the decrease in the peak intensities that are associated with each monomer. This makes the process of determining copolymer composition very easy, quick and accurate [101].

### 2.3.3. Solution polymerization

Free radical polymerization reactions can be performed in bulk, emulsion, suspension and solution systems. This study was limited to solution polymerization. Solution polymerization eliminates the problems associated with bulk polymerization, which is the simplest of all polymerization processes. In bulk polymerization a small amount of initiator is added to the pure monomer and the reaction is heated to a temperature at which the initiator breaks down to give free radicals. Although this leads to the formation of highly pure products, it has several disadvantages and limited applicability. Solution polymerization gives easier thermal control and improved heat transfer through the dissolution of the monomer in a suitable solvent. Heat removal is easily facilitated by carrying out the reaction at the reflux temperature of the solvent. The heat is then removed as the latent heat of vaporization [92]. The major disadvantage of this polymerization process is the difficulty in removing and handling large quantities of solvent [96].

## 2.4. References


(1) Sarney, D.B.; Vulfson, E.V. *Trends in Biotechnology* **1995**, *13*, 164-172.

(2) Lim, M-Y.; Chou, T-C.; Lin, X-Z.; Chen, C-Y.; Ling, T-R.; Shiesh, S-C. *Colloids and Surfaces B: Biointerfaces* **2000**, *17*, 265-274.

(3) Bognolo, G. In *ICI Surfactants*; Central Science Laboratory Agency: York, 1998; pp 1-9.

(4) Voutsas, E.C.; Tsavas, P.; Magoulas, K.; Tassios, D.; Ferrer, M.; Plou, F.J.; Ballesteros, A. *Journal of Chemical Engineering Data* **2002**, *47*, 1517-1520.

(5) Tarahomjoo, S.; Alemzadeh, I. *Enzyme & Microbial Technology* **2003**, *33*, 33-37.

(6) Thomas, H.G.; Lomakin, A.; Blankschtein, D.; Benedek, G.B. *Langmuir* **1997**, *13*, 209-218.

(7) Chevalier, Y. *Current Opinion in Colloid & Interface Science* **2002**, *7*, 3-11.

(8) Chernikova, E.; Terpugova, P.; Bui, C.; Charleux, B. *Polymer* **2003**, *44*, 4101-4107.

(9) Varade, D.; Bahadur, P. *Journal of Surfactants and Detergents* **2004**, *7*, 257-261.

(10) Liu, S.; Armes, S.P. *Current Opinion in Colloid & Interface Science* **2001**, *6*, 249-256.

(11) Ottewill, R.H. *Surface Active Agents*; The Society of Chemical Industry: London, 1979.

(12) Rahman, R.A.; Herawan, T. *Journal of Oil Palm Research* **2000**, *12*, 117-122.

(13) Holmberg, K.; Jonsson, B.; Kronberg, B.; Lindman, B. *Surfactants and Polymers in Aqueous Solution*, In*: Surfactants and Polymers in Aqueous Solution*, 2nd ed.; John Wiley & Sons: West Sussex, 2003; p 545.

(14) Atkins, P.W. *Physical Chemistry*, 6th ed.; Oxford University Press: Oxford, 1998; Vol. 6.

(15) Adamson, A.W. *Physical Chemistry of Surfaces*, 3rd ed.; John Wiley & Sons: New York, 1976.

(16) Musselman, S.W.; Chander, S. *Colloids and Surfaces A: Physicochemical and Engineering Aspects* **2002**, *206*, 497-513.

(17) Banat, I.M. *Bioresource Technology* **1995**, *51*, 1-12.

(18) Piispanen, P.S., 2002. Synthesis and Characterization of Surfactants Based on Natural Products, Kungl Tekniska Hogskolan, Stockholm, 1-60 pp.

(19) Barhoumi, M.; Beurroies, I.; Denoyel, R.; Said, H.; Hanna, K. *Colloids and Surfaces A: Physicochemical and Engineering Aspects* **2003**, *223*, 63-72.

(20) Goodwin, J. *Colloids and Interfaces with Surfactants and Polymers*; John Wiley & Sons, Ltd: England, 2004.

(21) Torchilin, V.P. *Journal of Controlled Release* **2001**, *73*, 137-172.

(22) http://sun.science.wayne.edu/~bio669. 2000. *Fundamental Principles of Membrane Biophysics*. University of Wayne State. Accessed August 2005.

(23) Priyanto, S.; Mansoori, G.A.; Suwono, A.; University of Illinois: Chicago, 2001; pp 1-10.

(24) Zhang, X.; Jackson, J.K.; Burt, H.M. *Journal of Biochemical and Biophysical Methods* **1996**, *31*, 145-150.

(25) Dai, S.; Tama, K.C. *Colloids and Surfaces A: Physicochemical and Engineering Aspects* **2003**, *229*, 157-168.

(26) Ngimhuang, J.; Furukawa, J-I.; Satoh, T.; Furuike, T.; Sakairi, N. *Polymer* **2004**, *45*, 837-841.

(27) Summers, M.; Eastoe, J. *Advances in Colloid and Interface Science* **2003**, *100-102*, 137-152.

(28) Weiss, J.; Coupland, J.N.; Brathwaite, D.; McClements, D.J. *Colloids and Surfaces A: Physicochemical and Engineering Aspects* **1997**, *121*, 53-60.

(29) Torchilin, V.P. *Advanced Drug Delivery Reviews* **2002**, *54*, 235-252.

(30) Holmberg, K. *Current Opinion in Colloid & Interface Science* **2001**, *6*, 148-159.

(31) Proverbio, Z.E.; Bardavid, S.M.; Arancibia, E.L.; Schulz, P.C. *Colloids and Surfaces A: Physicochemical and Engineering Aspects* **2003**, *214*, 167-717.

(32) Trapani, G.; Altomare, C.; Franco, M. ; Latrofa, A.; Liso, G. *International Journal of Pharmaceutics* **1995**, *116*, 95-99.

(33) Ganeva, D.E., 2003. Nanochemistry Through Self-assembly: Polymerisation of the Organised Phases of Polyelectrolyte-Surfactant Complexes. PhD Thesis, University of Stellenbosch, 135 pp.

(34) Yan, Y., 2001. Enzymatic Production of Sugar Fatty Acid Esters. PhD Thesis, University of Stuttgart, 104 pp.

(35) Salager, J-L. *Surfactants: Types and uses*; Laboratory of formulation, interfaces, rheology and processes: Merida-Venezuela, 2002; Vol. 2.

(36) de Paz Banez, M.V.; Robinson, K.L.; Vamvakaki, M.; Lascelles, S.F.; Armes, S.P. *Polymer* **2000**, *41*, 8501-8511.

(37) Joynes, D.; Sherrington, D.C. *Polymer* **1997**, *38*, 1427-1438.

(38) Jenkins, S.; Cytec Industries: U.K., 2002; p 9.

(39) Piasecki, A. *Biodegradable and Chemically Degradable Anionic Surfactants*; Encyclopedia of Surface and Colloid Science: New York, 2002.

(40) Cserha´ti, T.; Forga´cs, E.; Oros, G. *Environment International* **2002**, *28*, 337-348.

(41) McMurry, J. *Organic Chemistry*, 5th ed.; Brooks/Cole: USA, 2000.

(42) zu Putlitz, B.; Hentze, H-P.; Landfester, K.; Antonietti, M. *Langmuir* **2000**, *16*, 3214-3220.

(43) Scott, M.J.; Jones, M.N. *Biochimica et Biophysica Acta* **2000**, *1508*, 235-251.

(44) Shinoda, K.; Carlsson, A.; Lindman, B. *Advances in Colloid and Interface Science* **1996**, *64*, 253-271.

(45) Prete, P.S.C.; Gomes, K.; Malheiros, S.V.P.; Meirelles, N.C.; de Paula, E. *Biophysical Chemistry* **2002**, *97*, 45-54.

(46) Cao, Y.; Li, H. *European Polymer Journal* **2002**, *38*, 1457-1463.

(47) Duval-Terrie, C.; Huguet, J.; Muller, G. *Colloids and Surfaces A: Physicochemical and Engineering Aspects* **2003**, *220*, 105-115.

(48) Karsa, D.R. In *Household and Personal Care Today*, 2003; Vol. 1, pp 22-24.

(49) Tadros, T.F.; Vandamme, A.; Levecke, B.; Booten, K.; Stevens, C.V. *Advances in Colloid and Interface Science* **2004**, *108-109*, 207-226.

(50) Piirma, I. *Polymeric Surfactants*; Dekker: New York, 1992.

(51) Felthouse, T.R.; Burnett, J.C.; Horrell, B.; Mummey, M.J.; Kuo, Y-J.*Maleic Anhydride, Maleic Acid, and Fumaric Acid*, In *Kirk-Othmer Encyclopedia of Chemical Technology*, 4th ed.; John Wiley & Sons: Texas, 2001; Vol. 15, pp 893-928.

(52) Garofalakis, G.; Murray, B.S.; Sarney, B.D. *Journal of Colloid and Interface Science* **2000**, *229*, 391-398.

(53) Colbert, J.C. *Sugar Esters: Preparation and Applications*; Noyes Data Corporation: New Jersey, 1974.

(54) Soderberg, I.; Drummond, C.J.; Furlong, D.N.; Godkin, S.; Matthews, B. *Colloids and Surfaces A: Physicochemical and Engineering Aspects* **1995**, *102*, 91-97.

(55) Sadtler, V.M.; Guely, M.; Marchal, P.; Choplin, L. *Journal of Colloid and Interface Science* **2004**, *270*, 270-275.

(56) Glatter, O.; Orthaber, D.; Stradner, A.; Scherf, G.; Fanun, M.; Garti, N.; Clement, V.; Leser, M.E. *Journal of Colloid and Interface Science* **2001**, *241*, 215-225.

(57) Pedersen, N.R.; Wimmer, R.; Emmersen, J.; Degn, P.; Pedersen, L.H. *Carbohydrate Research* **2002**, *337*, 1179-1184.

(58) Muller, A.S.; Gagnaire, J.; Queneau, Y.; Karaoglanian, M.; Maitre, J.P.; Bouchu, A. *Colloids and Surfaces A: Physicochemical and Engineering Aspects* **2002**, *203*, 55.

(59) Ferrer, M.; Comelles, F.; Plou, F.J.; Cruces, M.A.; Fuentes, G.; Parra, J.L.; Ballesteros, A. *Langmuir* **2002**, *18*, 667-673.

(60) Stubenrauch, C. *Current Opinion in Colloid & Interface Science* **2001**, *6*, 160-170.

(61) Garti, N.; Clement, V.; Fanun, M.; Leser, M. E. *J. Agric. Food Chem.* **2000**, *48*, 3945-3956.

(62) Lee, H.L.; Kim, J.S.; Youn, H.J. *Tappi* **2004**, *3*, 4.

(63) McCarthy, W.R., 1987. An Investigation of the Mechanism of Alkaline Sizing with Alkenyl Succinic Anhydride. Doctoral Thesis, Lawrence, New York, 122 pp.

(64) Soderlind, E.; Wollbratt, M.; von Corswant, C. *International Journal of Pharmaceutics* **2003**, *252*, 61-71.

(65) Luk, Y-Y.; Abbott, N.L. *Current Opinion in Colloid & Interface Science* **2002**, *7*, 267-275.

(66) Tharanathan, R.N. *Trends in Food Science & Technology* **2003**, *14*, 71-78.

(67) Zhmud, B. In *Pira International*; Institute for Surface Chemistry: Belgium, 2003; p 10.

(68) Kroschwitz, J.I.; Howe-Grant, M. *Paper*, In*: Encyclopedia of Chemical Technology*, 4th ed.; John Wiley & Sons: New York, 1996; Vol. 18.

(69) Rousu, P.; Rousu, P.; Anttila, J. *Resources, Conservation and Recycling* **2002**, *35*, 85-103.

(70) Thompson, G.; Swain, J.; Kay, M.; Forster, C.F. *Bioresource Technology* **2001**, *77*, 275-286.

(71) Ottenio, D.; Escabasse, J-Y.; Podd, B.; International Life Sciences: Belgium, 2004; p 48.

(72) Pokhrel, D.; Viraraghavan, T. *Science of the Total Environment* **2004**, *333*, 37-58.

(73) Osterberg, M. *Journal of Colloid and Interface Science* **2000**, *229*, 620-627.

(74) Kekkonen, J.; Laukkanen, A.; Stenius, P.; Tenhu, H. *Colloids and Surfaces A: Physicochemical and Engineering Aspects* **2001**, *190*, 305-318.

(75) Park, J-W.; Park, K.; Song, H.; Shin, H. *Journal of Biotechnology* **2002**, *93*, 203-208.

(76) Mathews, C.K.; van Holde, M. *Biochemistry*; Benjamin/Cummings: Redwood, 1990.

(77) Eriksson, T.; Borjesson, J.; Tjerneld, F. *Enzyme & Microbial Technology* **2002**, *31*, 353-364.

(78) Richardson, S.; Gorton, L. *Analytica Chimica Acta* **2003**, *497*, 27-65.

(79) Horton, H.R.; Moran, L.A.; Ochs, R.S.; Rawn, J.D.; Scrimgeour, K.G. *Principles of Biochemistry*, 3rd ed.; Prentice-Hall Inc., 2002.

(80) Andersson, C.; Jarnstrom, L.; Mesic, B. In *5th International Paper and Coating Chemistry Symposium*; University of Karlstad and Packforsk: Montreal, 2003; pp 1-6.

(81) Brinen, J.S.; Kulick, R.J. *International Journal of Mass Spectrometry and Ion Processes* **1995**, *143*, 177-190.

(82) Zule, J.; Dolenc, J. *Acta Chim. Slov.* **2003**, *50*, 115-122.

(83) Shen, W.; Parker, I.H. *Journal of Colloid and Interface Science* **2001**, *240*, 172-181.

(84) Sain, M.; Rousin, D.; Schmidhauser, J.; Sartomer Company Inc.: USA pp 1-9.

(85) Mattsson, R., 2002. AKD Sizing - Dispersion Colloidal Stability, Spreading and Sizing with Pre-flocculated Dispersion. Licentiate Thesis, Lulea University of Technology, Sweden, 34 pp.

(86) http://developmentbookshop.com. *Small-Scale Paper Making*. Intermediate Technology Development Group Inc. Accessed October 2004.

(87) Au, C.O.; Thorn, I. *Applications of Wet-End Paper Chemistry*, 1st ed.; Blackie Academic & Professional: Glasgow, 1995.

(88) Hubbe, M.A. *Additives and Ingredients, their Composition, Functions, Strategies for Use*; Mini-Encyclopedia of Papermaking Wet-End Chemistry: North Carolina, 2003.

(89) http://www.freedoniagroup.com. May 2002 *Sizing & Thickening Agents*. The Freedonia Group Inc. Accessed October 2004.

(90) Allen, R.E. *The Concise Oxford Dictionary of Current English*, 8th ed.; BCA, 1991.

(91) Ghassemzadeh, J.; Sahimi, M. *Chemical Engineering Science* **2004**, *59*, 2265-2280.

(92) Bovey, F.A.; Winslow, F.H. *Macromolecules: An Introduction to Polymer Science*; Academic Press, Inc.: New Jersey, 1979.

(93) Bussels, R., 2004. (Multi)block copolymer synthesis via controlled radical polymerization in aqueous dispersions. Doctoral Thesis, Eindhoven, Eindhoven, 227 pp.

(94) El Rezzi, V., 2001. Chain-transfer kinetics for free-radical homo- and copolymerizations of styrene and methyl methacrylate in supercritical carbon dioxide. PhD Thesis, Georg-August University of Gottingen, Beirut, 158 pp.

(95) Haramina, T.; University of Gottingen: Beirut, 2004; p 3.

(96) Kaufman, H.S.; Falcetta, J.J. *Introduction to Polymer Science and Technology: An SPE Textbook*; John Wiley & Sons: New York, 1977.

(97) Lovell, P.A.; El-Aasser, M.S. *Emulsion Polymerization and Emulsion Polymers*; Wiley & Sons: New York, 1997.

(98) Ham, G.E. *Copolymerization*; Interscience: Kansas, 1964; Vol. XVII.

(99) Pasquale, A.J., 2002. Synthesis and Characterization of Multi-Component Polymeric Materials Prepared via Free Radical Polymerization. Doctoral Thesis, University of Virginia, Virginia, 255 pp.

(100) Miller, M.L. *The structure of Polymers*; Reinhold Book Corporation: New York, 1966.

(101) Wiles, K.B., 2002. Determination of Reactivity Ratios for Acrylonitrile/Methyl Acrylate Radical Copolymerization via Nonlinear Methodologies Using Real Time FTIR. MSc. Thesis, Virginia, Blacksburg, Virginia, 96 pp.

(102) Alvares, D.R.S.; Menezes, S.M.C.; Lucas, E.F. *Polymer International* **2004**, *53*, 1639-1643.

# CHAPTER 3

# PRE-SCREENING EXPERIMENT: INVESTIGATION OF THE EFFECT OF SURFACTANT STRUCTURE ON THE SIZING EFFICIENCY OF RECYCLED PAPERBOARD

## 3.1. Introduction

The adsorption of surfactants at solid surfaces is determined by their interaction with the surface, and their hydrophobicity. A strong attraction between surfactant head groups and a solid surface creates a monolayer, where the surfactant head groups are in contact with the surface and the surfactant tail groups are in contact with the surrounding environment. This adsorption structure occurs, for example, in the adsorption of charged surfactants at oppositely charged surfaces, which creates a hydrophobic surface with a surfactant bilayer forming at higher surfactant concentrations. When there is a chemical reaction between the surfactant head groups and the surface, a hydrophobic monolayer is formed. If, however, there is a weak attraction between the surfactant head groups and the surface, micelles or other surfactant aggregates form at higher surfactant concentrations. This is because the attraction between the surfactant tail groups is stronger than the attraction between the surfactant head groups and the surface [1]. The efficiency and effectiveness with which the surfactant adsorbs at the surface is influenced by the nature of the structural groups on the surface, the molecular structure of the surfactant and the nature of the surrounding environment [2].

The surface of paper can be characterized in terms of its roughness, porosity and compressibility. Sizing improves the paper finish by modifying the surface of its pores and also by changing its surface structural behaviour. Good sizing efficiency is dependent

on the surfactant's ability to form covalent bonds with the hydroxyl groups of cellulose [3]. The evaluation of paper's surface is important in understanding the surfactant's behaviour during coating [4].

In this chapter, an anionic, non-ionic and reactive surfactant are used respectively, to size recycled paperboard. The sizing efficiency of these three respective surfactants will be evaluated in order to establish the surfactant structure best suited for sizing recycled paperboard.

## 3.2. Experimental

### 3.2.1. Materials

The materials used for the sizing of paperboard are summarized in the table below.

**Table 3.1: Industrial surfactants used to size paperboard**

| **Material** | **Material code** | **Supplier** |
|---|---|---|
| Sucrose ester | SE (P1670) | Mitsubishi-Kagaku Foods Corporation (Japan) |
| Sodium lauryl sulfate | SDS | Saarchem (SA) |
| Alkenyl succinic anhydride | ASA | Buckman Laboratories Inc. (Manchester) |
| Starch (Stysol 70) | | African Products (Pty Limited) (SA) |

Paperboard was supplied by Mondi Packaging. Distilled deionized (DDI) water, obtained from a Millipore Milli-Q purification system, was used. All other materials were used as received from the suppliers.

### 3.2.2. Preparation

The three industrial surfactant solutions were all prepared in 100 ml screw-top glass bottles. The maximum concentration (wt %) of all three surfactants was to be 10%, because SE starts to gel at 4% and reaches a maximum at 10% concentration. The surfactants were prepared as follows:

1) Solutions of SDS with concentrations of 2, 4, 6, 8 and 10% in DDI water were prepared at room temperature.

2) Solutions of SE P1670 with concentrations of 2, 4, 6, 8 and 10% in DDI water were prepared at $70^0$C in a water bath.

3) Emulsions of ASA with concentrations of 2, 4, 6, 8 and 10% in starch were prepared at room temperature. The starch (15%) was prepared by dissolving in DDI water and boiling at $90^0$C for 3 h.

### 3.2.3. Application

Uncoated paperboard sheets (148 x 210 mm) were dipped into the respective surfactant solutions *(see Figure 3.1)* as follows:

- The uncoated paperboard was dipped into a pan containing the surfactant solutions and pulled along the length of the pan underneath the surface of the liquid and not along the breadth of the pan, as shown by Figure 3.1.
- The surfactant coated paperboard was then dried in an oven at 110 $^0$C for 3 min to evaporate the solvents used.

The amount of surfactant adsorbed by the paperboard was calculated according to:

$$\text{Surfactant weight}\left(g/m^2\right) = \left(a - b\right) \qquad (3.1)$$

where:

a: is the weight ($g/m^2$) of the surfactant coated paperboard
b: is the weight ($g/m^2$) of the uncoated paperboard.

The results of the amount of surfactant adsorbed by the paperboard are given in Table 3.2, Section 3.3.

**Figure 3.1: Coating pan in which paperboard sheets were dipped into surfactant solutions.**

### 3.2.4. Testing of surfactant coated paperboard

The surfaces of the uncoated and surfactant coated paperboard were evaluated via SEM, which is described in Section 3.2.4.1. The sizing efficiency and hydrophobibcity of the surfactant coated paperboard were determined via the Cobb test and contact angle measurements. These two tests are respectively described in Sections 3.2.4.2 and 3.2.4.3.

#### 3.2.4.1. Scanning electron microscopy (SEM)

A SEM instrument, model ABT-60 from Topcon, was used to evaluate the surface characteristics of the paperboard surface and the general appearance of coatings on a micro-meter scale. Data were generated as j-peg or gif images obtained at 7 kV and a distance of 10 mm.

Samples were prepared by cutting uncoated as well as coated paperboard into small blocks of about 1 $cm^2$. The small blocks were then coated with a thin micro-layer of 24 carat gold to increase the sample's transferring ability so as to obtain clearer images.

#### 3.2.4.2. The Cobb test

The Cobb test *(see Figure 3.2)* or Hercules Size tester are commonly used to measure the water-repellent properties of sized paper [5]. This test measures the total amount of water absorbed by paper or paperboard from one side in a certain amount of time [6]. The Cobb test equipment consists of:

- Cobb tester (metal ring fitted with a rubber seal and a metal base board)
- analytical balance (accuracy: 0.01g)
- blotting paper
- solid brass roller
- graduated cylinder (capacity: 100ml)
- stopwatch

- distilled water

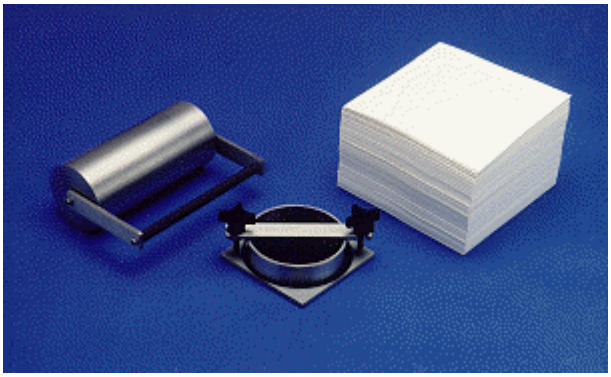

**Figure 3.2: Cobb test equipment [7].**

'60-second Cobbs' were used to measure the amount of water absorbed by the two-sided coated paperboard. The Cobb values were calculated according to:

$$'60\text{-second Cobb}' = 100(a - b) \qquad (3.2)$$

where:

a: is the weight ($g/m^2$) of the surfactant coated paperboard sheet exposed to water
b: is the weight ($g/m^2$) of the coated paperboard sheet before exposure.

### 3.2.4.3. Contact angle measurement

Contact angle measurements are indirect methods for measuring the surface energies of solid samples. This is done by measuring the interactions between the solid sample and probe liquids. When measuring the degree of sizing and evaluating the surface energies of paper sheets, an understanding of the factors affecting the contact angles is important. The reason for this is because of the topographical and chemical heterogeneity of the paper sheets [8].

In this study the static contact angle method was used to measure the surface tension of coated paperboard. A 4-µl droplet of distilled water was placed on the surface of the paperboard and a photograph was then taken with a stereomicroscope that was connected to a computer. The contact angle of the water droplet on the surface of the paperboard was measured and reported as angle theta (θ) (*see Figure 3.3.)*. The reported contact angle is the average of five individual measurements.

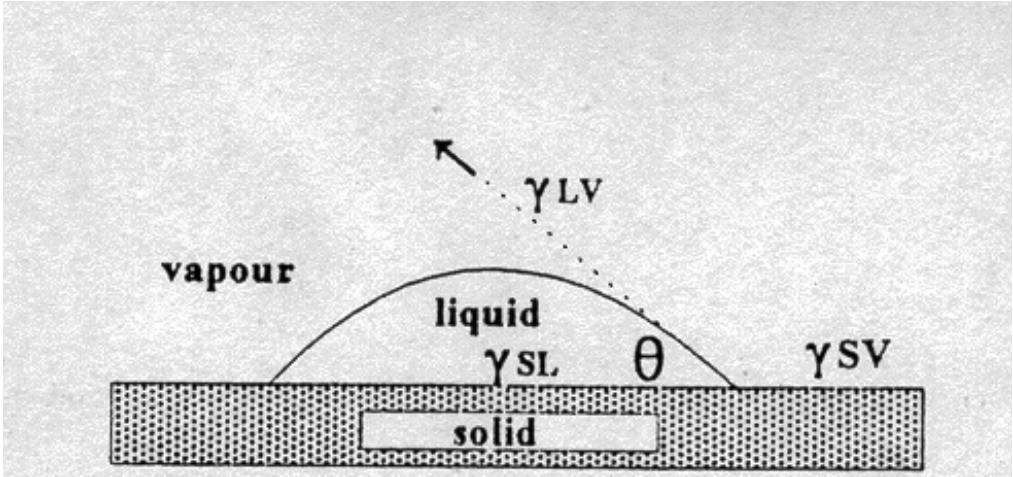


**Figure 3.3: Hydrophobicity calculation of a water droplet on a surface.**

The wetting process is a three-phase equilibrium that is described by Young's equation [9]:

$$\mathrm{Cos}\theta = \frac{\gamma_{SV} - \gamma_{SL}}{\gamma_{LV}} \qquad (3.3)$$

where:

θ: is the contact angle ($^0$)

$\gamma_{SV}$: the surface tension (mJ/m$^2$) at the solid/vapour interface

$\gamma_{SL}$: the surface tension (mJ/m$^2$) at the solid/liquid interface

$\gamma_{LV}$: the surface tension (mJ/m$^2$) at the liquid/vapour interface.

When $\theta = 0$ complete wetting occurs and when it is $\geq 90^0$ water penetration into the fiber structure does not occur [2,10].

### 3.3. Results and discussion

The amounts of surfactant adsorbed by the uncoated paperboard and the amount of water absorbed by the surfactant coated paperboard were determined. Uncoated paperboard, used as a reference, was found to have a Cobb value of 593. The results are summarized in Table 3.2.

**Table 3.2: Surfactant concentrations used, surfactant weight adsorbed and surfactant Cobb values**

| ASA in starch | | | SE | | | SLS | | |
|---|---|---|---|---|---|---|---|---|
| Surfactant Conc. (wt %) | Surfactant Weight adsorbed ($g/m^2$) | Cobb values | Surfactant Conc. (wt %) | Surfactant Weight adsorbed ($g/m^2$) | Cobb values | Surfactant Conc. (wt %) | Surfactant Weight adsorbed ($g/m^2$) | Cobb values |
| 2 | 37.07 | 47 | 2 | 5.99 | 463 | 2 | 9.26 | 494 |
| 4 | 46.50 | 64 | 4 | 12.64 | 458 | 4 | 19.04 | 502 |
| 6 | 57.79 | 74 | 6 | 21.23 | 382 | 6 | 28.81 | 507 |
| 8 | 49.20 | 76 | 8 | 24.77 | 251 | 8 | 37.91 | 519 |
| 10 | 60.49 | 73 | 10 | 27.80 | 134 | 10 | 49.53 | 499 |

The three surfactants have different hydrophilic head groups, which will interact differently with the hydrophilic paperboard surface. SDS, an anionic surfactant, will have an electrostatic interaction with the paperboard surface. SE, a non-ionic surfactant, will form hydrogen bonds with the paperboard surface. ASA, a reactive surfactant, will form an ester bond with the paperboard surface because of its hydrolyzable maleic anhydride head group. The structures, type of bonding interactions with paperboard and alkyl chain lengths of the three surfactants are given in Table 3.3.

**Table 3.3: Structures, type of bonding interaction with cellulose and the alkyl chain lengths of SDS, SE and ASA**

| **Compound** | **Bonding interaction** | **R = Alkyl chain length** |
|---|---|---|
| SDS 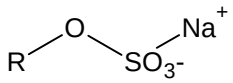 | Ionic | C12 |
| SE 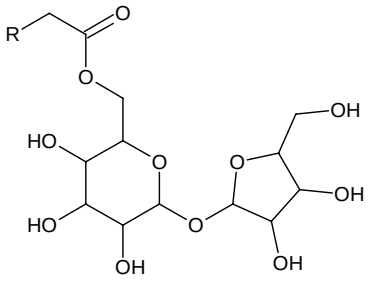 | Hydrogen | C18 |
| ASA 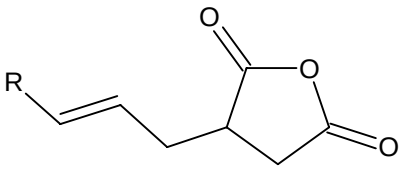 | Ester | C18-24 |

The amount of surfactant adsorbed by the uncoated paperboard is graphically illustrated in Figure 3.4.

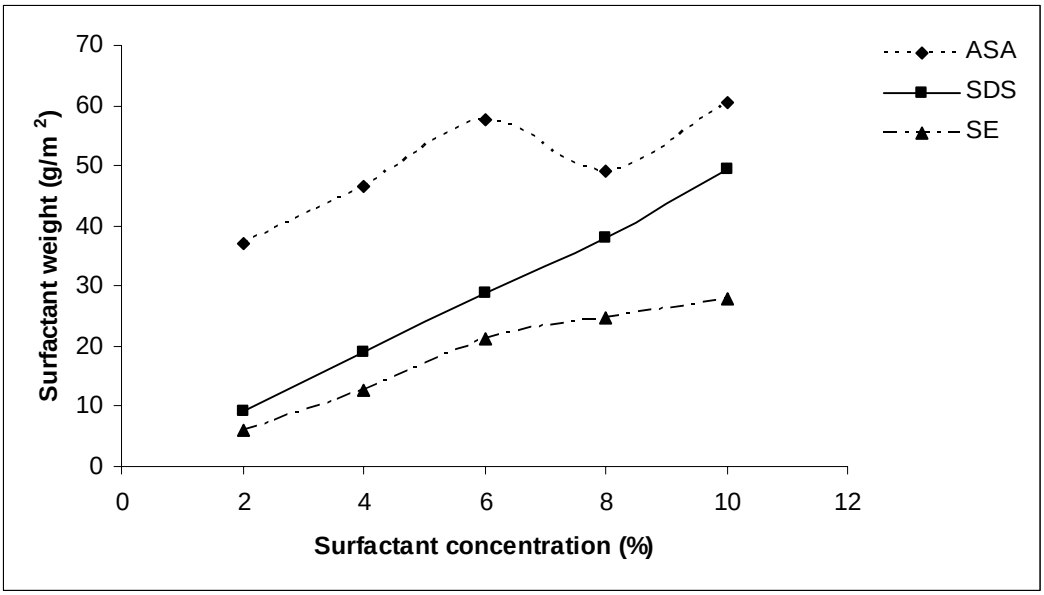


**Figure 3.4: Amount of surfactant adsorbed by uncoated paperboard.**

Surfactant adsorption is of the order: ASA>SDS>SE. The result indicates that the type of bonding interaction of the surfactants with paperboard is of the order: ester->ionic->hydrogen bond [11]. There is also an increase in surfactant adsorption with increasing surfactant concentration [1]. The fluctuations in the graphs are due to defects in the recycled paperboard such as holes in the fibers and wide pore throats* [12]. These defects can be seen in the SEM image of uncoated paperboard in Figure 3.5.

* Pore throats are the channels formed between the fibers [12].

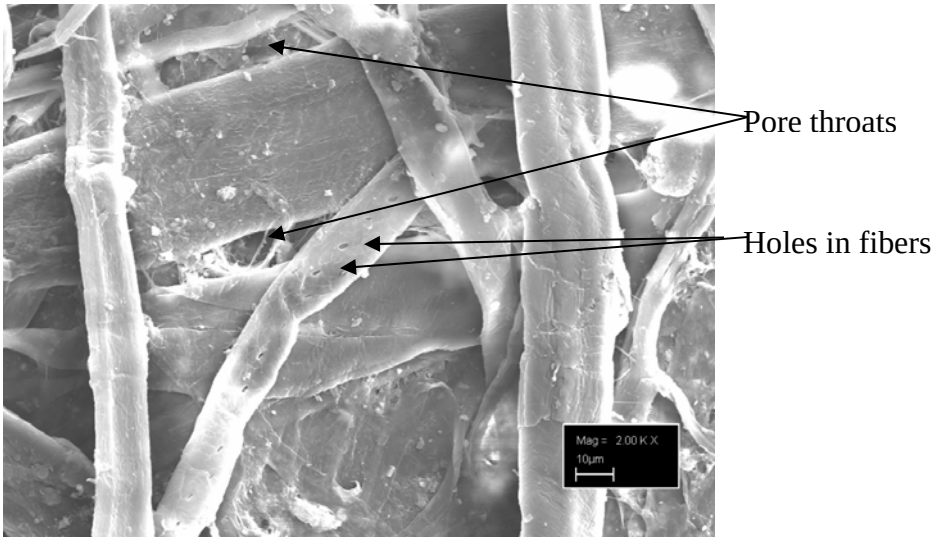


**Figure 3.5: SEM image of uncoated paperboard (Magnification = 2.00K X 10µm).**

The respective SEM images of paperboard coated with 10% SE, ASA and SDS can be seen in Figures 3.6 to 3.8. The SEM images show the paperboard surface covered with the three surfactants. Pinholes are still visible on the surface of the surfactant coated paperboard. This means that the surfactants did not fully cover the paperboard surface and they also did not completely fill the fiber pinholes and pore throats.

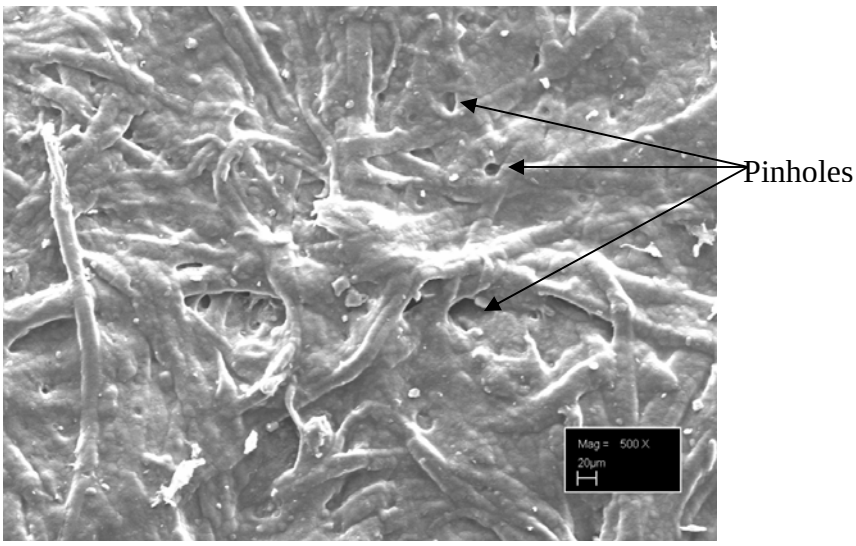


**Figure 3.6: SEM image of 10% SE coated paperboard (Magnification = 500 X 20 µm).**

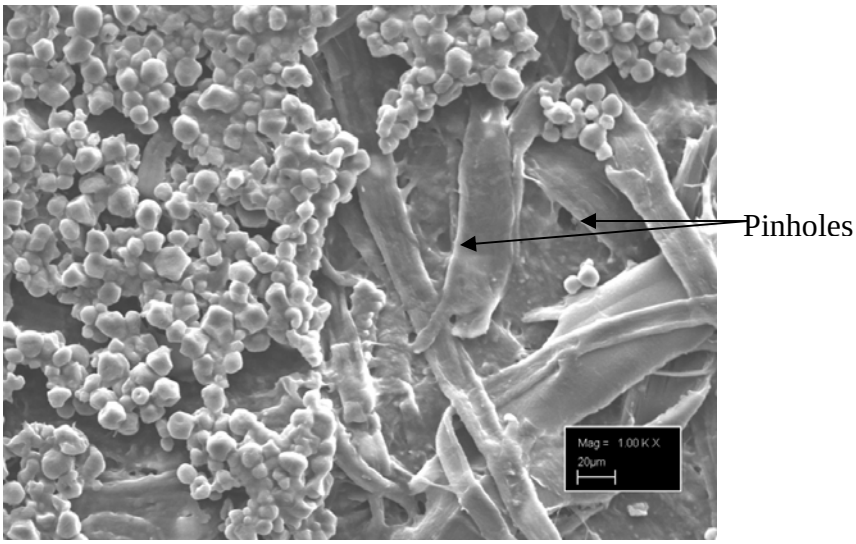


**Figure 3.7: SEM image of 10% ASA coated paperboard (Magnification = 1.00K X 20µm).**


**Figure 3.8: SEM image of 10% SDS coated paperboard (Magnification = 1.00K X 20µm).**

The hydrophobicity and sizing efficiency of the surfactants were determined by measurement of the amount of water absorbed by each surfactant coated paperboard. This was done with the use of the Cobb test and contact angle measurements. The amount of

water absorbed, given as Cobb values, by each surfactant is graphically illustrated in Figure 3.9. The hydrophobicity of the three industrial surfactants was compared and it was found that ASA absorbed the least and SDS the most water.

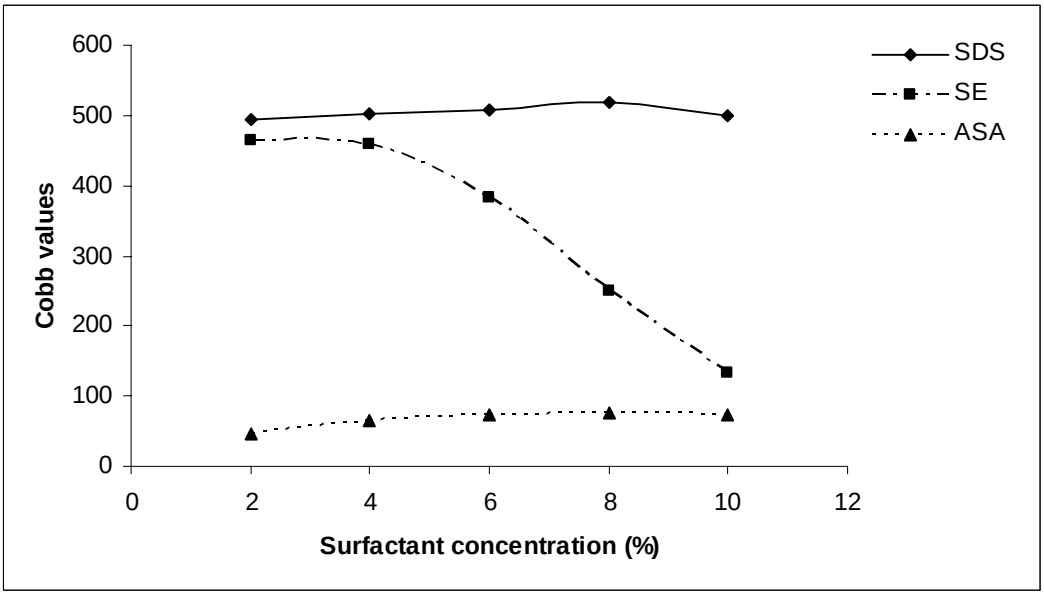


**Figure 3.9: Amount of water absorbed by surfactant coated paperboard (Cobb values).**

The fast decrease in the amount of water absorbed by SE is due to its gelation after 4% concentration. SE gels because it consists of mono-, di- and tri-substituted molecules which make its hydrophobicity increase with increased concentration.

SDS and SE gave zero contact angles which are in good agreement with the high Cobb values obtained for them. The contact angle measurements of ASA are tabulated in Table 3.4 and graphically illustrated in Figure 3.10. The high contact angle at 2% [ASA] is in good agreement with the low Cobb value obtained at the same [ASA]. There are, however, a lot of variations in the contact angles from 4% to 10% [ASA]. This can be ascribed to the roughness and geometry of the paper surface [1].

**Table 3.4: Contact angles of ASA**

| ASA in starch | |
|---|---|
| Conc. (wt %) | Contact angle |
| 2 | 98.0 |
| 4 | 87.9 |
| 6 | 89.0 |
| 8 | 83.9 |
| 10 | 90.7 |

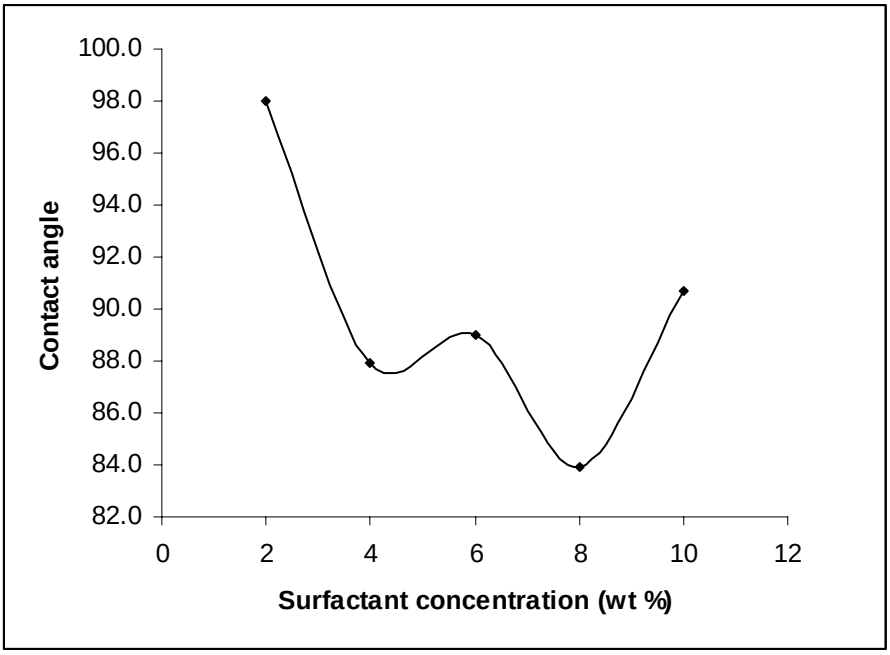


**Figure 3.10: Contact angles of ASA.**

## 3.4. Conclusions

The results from the pre-screening experiment indicate that ASA has the best sizing efficiency, which results in it absorbing the least amount of water, compared to SDS and SE. It can be concluded from these results that:

- Reactive surfactants are best suited for the sizing of recycled paperboard.
- Maleic anhydride, the polar headgroup of ASA, adheres best to cellulose because of its covalent bond formation with the hydroxyl groups of cellulose.

## 3.5. References


(1) Holmberg, K.; Jonsson, B.; Kronberg, B.; Lindman, B. *Surfactants and Polymers in Aqueous Solution*, In*: Surfactants and Polymers in Aqueous Solution*, 2nd ed.; John Wiley & Sons: West Sussex, 2003; p 545.

(2) Musselman, S.W.; Chander, S. *Colloids and Surfaces A: Physicochemical and Engineering Aspects* **2002**, *206*, 497-513.

(3) Sain, M.; Fortier, D. *Industrial Crops and Products* **2002**, *15*, 1-13.

(4) Conners, T.E.; Banerjee, S. *Surface Analysis of Paper*; CRC Press: Boca Raton, 1995.

(5) Andersson, C.; Jarnstrom, L.; Mesic, B. In *5th International Paper and Coating Chemistry Symposium*; University of Karlstad and Packforsk: Montreal, 2003; pp 1-6.

(6) Kroschwitz, J.I.; Howe-Grant, M. *Paper*, In*: Encyclopedia of Chemical Technology*, 4th ed.; John Wiley & Sons: New York, 1996; Vol. 18.

(7) http://www.gpi-test.com/Cobb.gif. 2001. *Gurley Cobb Tester*. Gurley Precision Instruments. Accessed October 2004.

(8) Shen, W.; Filonanko, Y.; Truong, Y.; Parker, I.H.; Brack, N.; Pigram, P.; Liesegang, J. *Colloids and Surfaces A: Physicochemical and Engineering Aspects* **2000**, *173*, 117-126.

(9) Adamson, A.W. *Physical Chemistry of Surfaces*, 3rd ed.; John Wiley & Sons: New York, 1976.

(10) Mattsson, R., 2002. AKD Sizing - Dispersion Colloidal Stability, Spreading and Sizing with Pre-flocculated Dispersion. Licentiate Thesis, Lulea University of Technology, Sweden, 34 pp.

(11) Cartmell, E.; Fowles, G.W.A. *Valency and Molecular Structure*, 2nd ed.; Butterworths: London, 1961.

(12) Ghassemzadeh, J.; Sahimi, M. *Chemical Engineering Science* **2004**, *59*, 2265-2280.

# CHAPTER 4

# SYNTHESIS OF SURFACE-ACTIVE ALKANES

## 4.1. Introduction

The interest in polymerizable single-chain surfactants containing groups such as allyl, acrylate, methacrylate, styryl and acrylamido, has accelerated over the last 20 years [1]. Acrylic copolymers have become the main component in many automotive coating formulations due to their excellent resistance to chemicals, solvents, ultraviolet light, abrasion and exterior durability [2]. The polymers of (alkyl)methacrylates, with their low glass transition temperatures, draw significant importance in material science even though the higher (alkyl)methacrylates have a low solubility in common solvents at low temperatures [3]. The ester substituent is an effective electron-withdrawing group and activates the double bond towards anionic and radical initiation as well as coordination polymerization [4]. Acrylic and methacrylic monomers are thus readily incorporated into copolymers with monomers of almost every type, even those which may otherwise be difficult to polymerize [5].

Maleic anhydride (MAH), an electron accepting monomer, has been shown to homopolymerize poorly via free radical methods [6,7]. The rates of free radical polymerizations of maleic anhydride copolymers depend on polar and steric factors. Maleic anhydride has been extensively studied and produces alternating copolymers with good adhesion and solubility properties [8]. It is an important raw material that is used in the manufacture of phtalic-type alkyd and unsaturated polyester resins, surface coatings, lubricant additives, plasticizers, copolymers and agricultural chemicals [9].

In the present work, MAH was copolymerized with butyl methacrylate (BMA) (see Scheme 4.1) and lauryl methacrylate (LMA) (see Scheme 4.2) respectively. A kinetics study as well as bench-scale experiments were done for the two copolymerization systems. In situ $^{1}H$ NMR was used to monitor reaction parameters such as monomer conversion and co-monomer content in the copolymers in the kinetics study, while quantitative $^{13}C$ NMR was used to quantify the co-monomer content of the isolated copolymers in the bench-scale experiments.

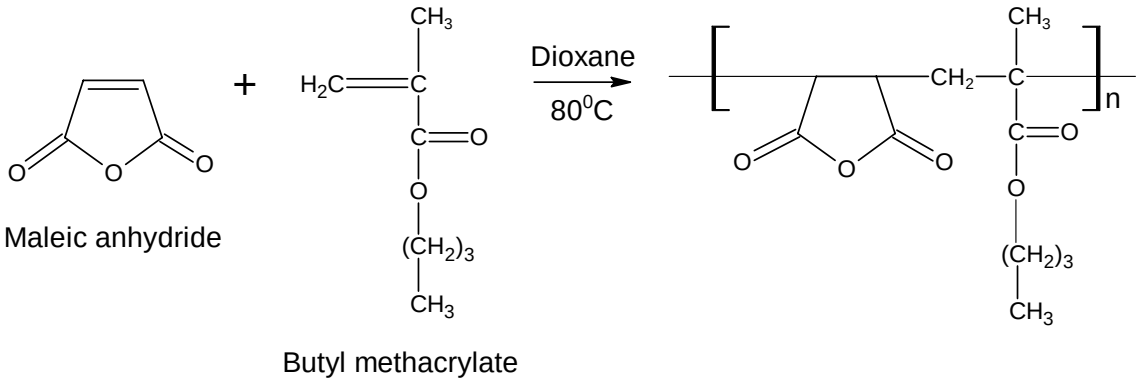


**Scheme 4.1: Reaction scheme for the synthesis of the MAH/BMA copolymer.**

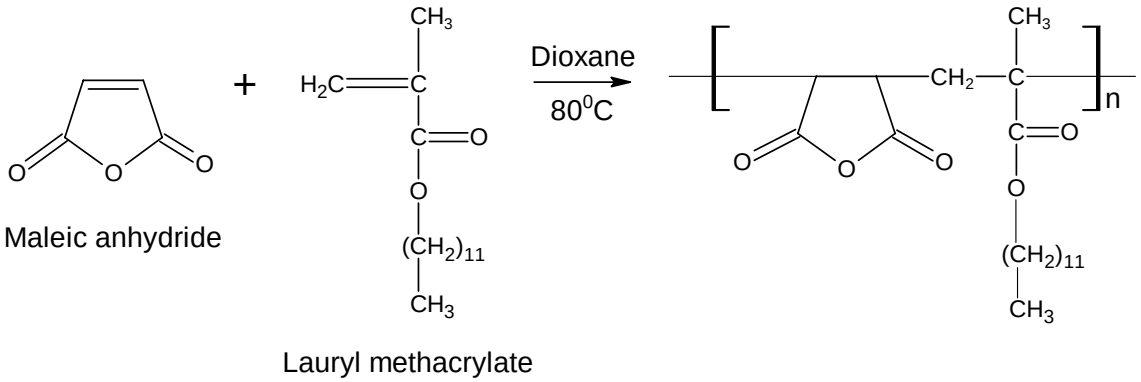


**Scheme 4.2: Reaction scheme for the synthesis of the MAH/LMA copolymer.**

## 4.2. Experimental

### 4.2.1. Materials

The materials used in both the kinetics study and bench-scale experiments of the MAH/BMA and MAH/LMA copolymer systems are summarized in Table 4.1.

**Table 4.1: Materials used in the kinetics study and bench-scale experiments of the two copolymer systems**

| Material | Abbreviation | Supplier |
|---|---|---|
| Maleic anhydride (99%) | MAH | Acros Organics (USA) |
| Butyl methacrylate | BMA | Sigma-Aldrich (SA) |
| Lauryl methacrylate | LMA | Cognis Performance Chemicals (UK) |
| Magnesium sulphate (anhydrous) | $MgSO_4$ | Saarchem (SA) |
| 2,2'-Azobisisobutyronitrile | AIBN | Sigma-Aldrich (SA) |
| Deuterated chloroform ($CDCl_3$) | | Sigma-Aldrich (SA) |
| Deuterated benzene ($C_6D_6$) | | Acros Organics (USA) |
| 1,4-Dioxane | | Saarchem (SA) |
| Acetone-$d_6$ | | Sigma-Aldrich (SA) |
| Tetrahydrofuran | THF | BDH Chemicals (England) |
| Diethylether | | BDH Chemicals (England) |

BMA and LMA were washed free of inhibitor with 0.3M KOH solution, washed with distilled water, dried with anhydrous magnesium sulphate ($MgSO_4$) and stored at 0 $^0$C. $^{13}$C NMR analysis showed no impurities present in MAH but a resonance peak after 200

ppm and the low intensity of its carbonyl resonance peak revealed some hydrolysis. MAH was dried at 20 $^{0}$C under reduced pressure for 24 h. AIBN was purified by recrystallization from methanol. All other materials were used as received from the suppliers.

### 4.2.2. Characterization

#### a) Nuclear Magnetic Resonance (NMR)

$^{1}$H NMR was used for the kinetics study and characterization of the isolated copolymers, while $^{13}$C NMR was used for the quantitative analysis of the isolated copolymers in the bench-scale experiments. $^{1}$H- and $^{13}$C NMR were recorded on a Varian Unity Inova 600 MHz spectrometer. The 600 MHz spectrometer is equipped with an Oxford magnet (14.09 T) and a 5 mm inverse detection PFG probe. Standard pulse sequences were used for obtaining both $^{1}$H and $^{13}$C spectra.

The copolymerization kinetics analyses via in situ $^{1}$H NMR were recorded on a 400 MHz Varian Unity Inova spectrometer. A 5 mm dual broadband PFG probe was used for the experiments and the sample cavity in the probe was calibrated in the manner suggested by the NMR instrument manufacturer. Samples were inserted into the magnet at 25 ˚C and the magnet fully shimmed. A spectrum was collected at 25 ˚C to serve as a reference. The sample was then removed from the magnet and the cavity of the magnet raised to the required temperature. Once the magnet cavity had stabilised at the required temperature the sample was re-inserted and allowed to equilibrate for approximately 5 min. Additional shimming was then carried out to fully optimize the system and the experiments started between 5 and 10 min after the sample was inserted in the magnet, the exact time being noted

The in situ $^{1}$H NMR analyses were performed in benzene-$d_6$. Quantitative $^{13}$C NMR analysis of the isolated MAH/BMA copolymer was performed in acetone-$d_6$, while that of the isolated MAH/LMA copolymer was performed in 90% THF and 10% acetone-$d_6$.

**b) Gel Permeation Chromatography (GPC)**

Gel permeation chromatography (GPC), better known as size exclusion chromatography (SEC), was used to determine the molecular weights of the isolated copolymers. The GPC instrument consists of a Waters 410 Differential Refractometer, Waters 717 Plus Autosampler, Waters 610 Fluid Unit Pump and Waters 600E System Controller. Molecular weights are obtained from refractive index data analyzed with Millenium V3.05 software, relative to polystyrene standards. Separation according to molar mass was obtained through the size exclusion effect, made possible by a series of columns with different pore sizes.

The respective MAH/BMA (5 mg) and MAH/LMA (5mg) copolymers were dissolved in 1 ml of THF (HPLC-grade). A 0.45 μm filter was connected to a 1 ml glass syringe which was used to filter the sample solutions before injection into GPC vials. The GPC instrument was calibrated with narrow molar mass polystyrene standards, supplied by Polymer Laboratories. The flow rate and temperature were 1 ml/min and 30 $^{0}$C, respectively.

## 4.2.3. Synthesis of the MAH/BMA and MAH/LMA copolymers

### 4.2.3.1. Bench-scale experiments

**a) MAH/BMA copolymerization**

MAH (8.108 g) and BMA (11.510 g) were weighed off in a three-neck round-bottom flask. A solvent mixture containing 60 ml toluene and 12 ml of dry acetone, as well as a magnetic stirrer bar, were added to the flask. The round-bottom flask was fitted with a reflux condenser, bubbler, septum, and nitrogen gas-line. The reaction mixture was placed in an oil bath which was fitted with a thermostat for temperature regulation. The reaction mixture was then degassed with nitrogen for 30 min, after which the temperature

was raised to 80 $^0$C. When the oil bath stabilized at 80 $^0$C, AIBN (0.189 g), dissolved in a small volume of toluene, was added through the septum. The reaction was terminated after 6 h and the copolymer precipitated in hexane. The copolymer was dried in a vacuum oven for 24 h, weighed, and characterized via NMR and GPC.

**b) MAH/LMA copolymerization**

MAH (8.042 g) and LMA (20.768 g) were weighed in a three-neck round-bottom flask. A solvent mixture containing 60 ml toluene and 12 ml acetone, as well as a magnetic stirrer bar, were added to the flask. The round-bottom flask was fitted with a reflux condenser, bubbler, septum, and nitrogen gas-line. The reaction mixture was placed in an oil bath which was fitted with a thermostat for temperature regulation. The reaction mixture was then degassed with nitrogen for 30 min, after which the temperature was raised to 80 $^0$C. When the oil bath stabilized at 80 $^0$C, AIBN (0.189 g), dissolved in a small volume of toluene, was added through the septum. The reaction was terminated after 6 h and the copolymer precipitated in hexane. The copolymer was dried in a vacuum oven for 24 h, weighed, and characterized via NMR and GPC.

### 4.2.3.2. Copolymerization kinetics analysis via in situ $^1$H NMR

In situ $^1$H NMR was used to study the kinetics of the MAH/BMA and MAH/LMA copolymer systems. A series of mixtures containing different mole percentages of the monomers was used in each of the two respective copolymer systems. The feed ratios, masses and moles of co-monomers used for the two copolymer systems are tabulated separately in Tables 4.2 and 4.3. The polymerizations were performed in 5 mm diameter NMR tubes with benzene-$d_6$ as NMR solvent and 1,4-dioxane as reference solvent.

A representative example of the sample preparation for the NMR kinetics procedure is as follows:
MAH (0.03110g), BMA (0.00491g) and AIBN (0.00062g) were dissolved in 0.873g of benzene-$d_6$ in a small vial. 1,4-Dioxane (0.00200g) was weighed into the NMR tube. The

sample solution and NMR tube were flushed with nitrogen to remove oxygen present. The sample solution was transferred to the NMR tube and flushed again with nitrogen. The NMR tube was sealed with parafilm, placed in the spectrometer and the polymerizations performed at 80 $^0$C for 1 h. Data were collected every 30 seconds and the decrease in intensity of the double bond proton signals of the vinyl groups of the monomers used in each copolymer system, relative to the 1,4-dioxane reference signal, was followed during the course of the reactions.

**Table 4.2: Feed ratios (%), masses (m) and moles (n) for the MAH/BMA copolymer system**

| mol % BMA | mol% MAH | mass BMA(g) | mass MAH(g) | n BMA | n MAH | mass AIBN(g) | mass Benzene-$d_6$ (g) |
|---|---|---|---|---|---|---|---|
| 11.11 | 88.89 | 0.049 | 0.031 | 0.00004 | 0.00032 | 0.00062 | 0.873 |
| 30.56 | 69.44 | 0.015 | 0.024 | 0.00011 | 0.00025 | 0.00057 | 0.815 |
| 50.00 | 50.00 | 0.025 | 0.018 | 0.00018 | 0.00018 | 0.00049 | 0.825 |
| 70.59 | 29.41 | 0.033 | 0.010 | 0.00024 | 0.00010 | 0.00041 | 0.797 |
| 91.18 | 8.82 | 0.043 | 0.003 | 0.00031 | 0.00003 | 0.00046 | 0.804 |

**Table 4.3: Feed ratios (%), masses (m) and moles (n) for the MAH/LMA copolymer system**

| mol % LMA | mol % MAH | mass LMA(g) | mass MAH(g) | n LMA | n MAH | mass AIBN(g) | mass Benzene-$d_6$ (g) |
|---|---|---|---|---|---|---|---|
| 10.71 | 89.29 | 0.007 | 0.024 | 0.00003 | 0.00025 | 0.00032 | 0.814 |
| 29.63 | 70.37 | 0.021 | 0.019 | 0.00008 | 0.00019 | 0.00043 | 0.825 |
| 50.00 | 50.00 | 0.036 | 0.014 | 0.00014 | 0.00014 | 0.00049 | 0.816 |
| 70.37 | 29.63 | 0.049 | 0.008 | 0.00019 | 0.00008 | 0.00061 | 0.813 |
| 89.29 | 10.71 | 0.064 | 0.003 | 0.00025 | 0.00003 | 0.00070 | 0.797 |

## 4.3. Results and discussion

### 4.3.1. Bench-scale experiments

#### 4.3.1.1 Characterization of the MAH/BMA and MAH/LMA copolymer systems via $^1$H NMR

The isolated MAH/BMA and MAH/LMA copolymers were characterized via $^1$H NMR. Figure 4.1 only gives the assigned resonance peaks for the MAH/BMA copolymer because the MAH/LMA copolymer gives similar resonance peaks. The co-monomer content of the two copolymers could not be quantified via $^1$H NMR. This was due to the low concentration and broadness of proton (a) between the regions of 2.5 ppm and 3.5 ppm. The broadness of the area under the $CH_3$ peak of toluene and peak c, in the region of 2 ppm, is due the $CH_2$ resonance of BMA in the copolymer and to the formation of BMA homopolymer also formed during the polymerization.

There is also some solvent and unreacted MAH left in both copolymer systems. This is seen between the regions of 6 ppm and 8 ppm. MAH should only give one resonance peak but the spectrum reveals two MAH peaks, at 6.2 ppm and 7.2 ppm. This is due to the hydrolyzed ring that was also formed. The hydrolyzed MAH peak is at 6.4 ppm while that of the non-hydrolyzed MAH is at 7.2 ppm. This is in accordance to the predicted NMR spectrum.

It was assumed that all the BMA and LMA monomers were incorporated in the respective copolymers, because their two respective resonance peaks, between 5.0 ppm and 6.0 ppm, were absent.

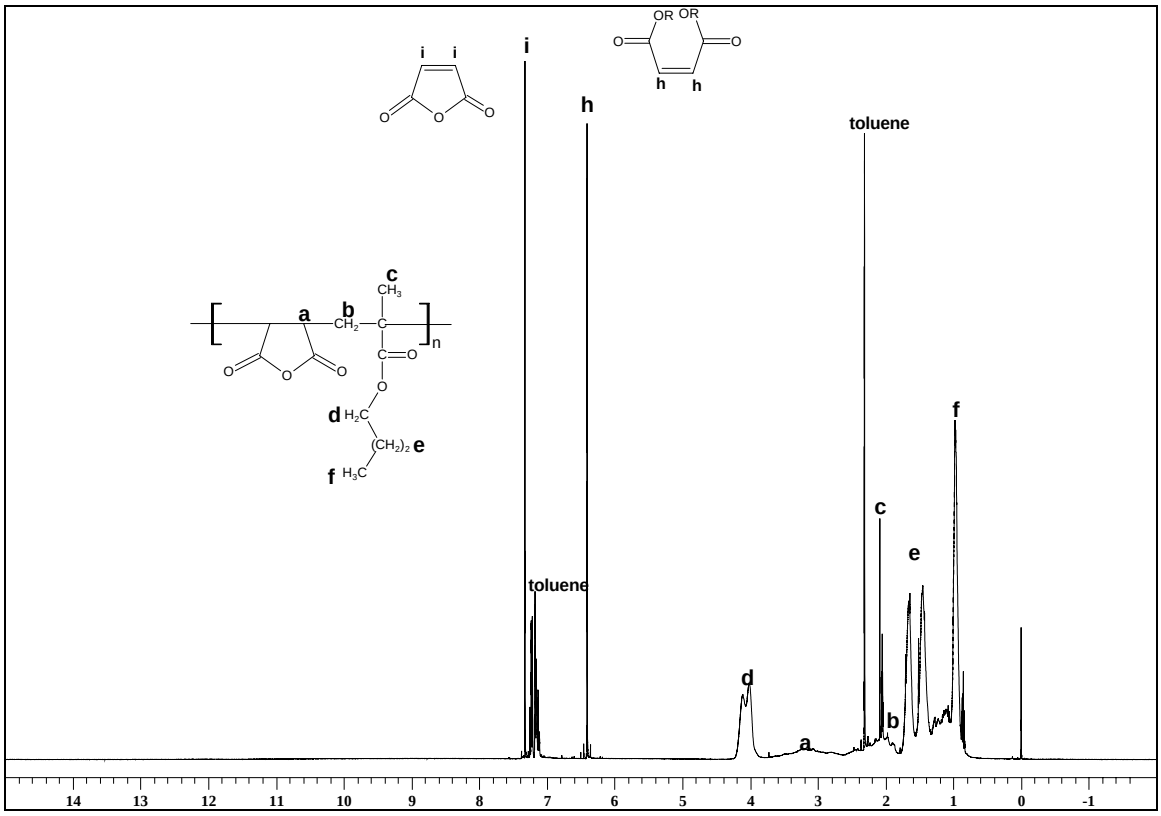


**Figure 4.1: $^{1}$H NMR spectrum of the MAH/BMA copolymer.**

### 4.3.1.2. Quantification of the isolated MAH/BMA and MAH/LMA copolymer systems via $^{13}$C NMR

The carbonyl signals of BMA and LMA are distinct from the two carbonyl signals of MAH. Quantitative $^{13}$C NMR was thus used to determine the co-monomer content of the two respective copolymers.

Routine $^{13}$C spectra only give qualitative information due to the distortion of their peak intensities, which results from the following two effects:

1) The nuclear Overhauser enhancement (nOe), which operates as a result of proton decoupling, leads to the enhancement of protonated carbons as opposed to non-protonated carbons.

2) The insufficient time ($T_1$) allowed for complete relaxation of specific $^{13}C$ nuclei in a molecule results in the peak integrals not being proportional to the number of nuclei they represent.

In order to use quantitatively these two problems are overcome as follows:
1) The nOe effect is overcome by the use of inverse gated decoupling where the decoupler is only applied during the acquisition period and not during the delay between the pulses where the nOe enhancement would take place.
2) The relaxation times ($T_1$) of a sample must first be measured in order to overcome the insufficient time problem. When the longest $T_1$ has been determined the delay between the pulses needs to be at least five times the longest $T_1$, but only if a $90^0$ pulse is to be used. Smaller angles can also be used and are calculated using the Ernst equation (4.8) which allows the conditions required for complete decay of transverse magnetization between scans to be determined:

$$\mathrm{Cos}\,\alpha_e = e^{-\tau_r / T_1} \qquad (4.8)$$

where:
$\alpha_e$: Ernst angle
$\tau_r$: delay between pulses (including acquisition time).

Obtaining quantitative information from $^{13}C$ spectra is time consuming for two reasons: the nOe effect and allowing for the full relaxation of nuclei [10].

The $^{13}C$ NMR spectra of both copolymers gave two distinguishable $^{13}C$ resonance peaks between 160 ppm and 180 ppm. The $^{13}C$ NMR spectra of the MAH/BMA and MAH/LMA copolymers are shown in Figures 4.10 and 4.11 respectively.

A 1:1 molar ratio of MAH:BMA and of MAH:LMA was used in the respective bench-scale experiments. The % copolymer yield obtained for the MAH/BMA copolymer was

95.04% and for the MAH/LMA copolymer was 94.79%. The results from the quantitative $^{13}C$ NMR analysis, shown in Figures 4.2 and 4.3, indicate that there was a 0.3:1.0 molar ratio of MAH:BMA and a 0.15:1.0 molar ratio of MAH:LMA incorporated in the respective copolymers. The resonance peak of MAH, at 165.36 ppm, is due to two carbonyls and thus should be divided by a factor of 2. The exact molar ratios are thus 0.15:1.0 for MAH:BMA and 0.075:1.0 for MAH:LMA.

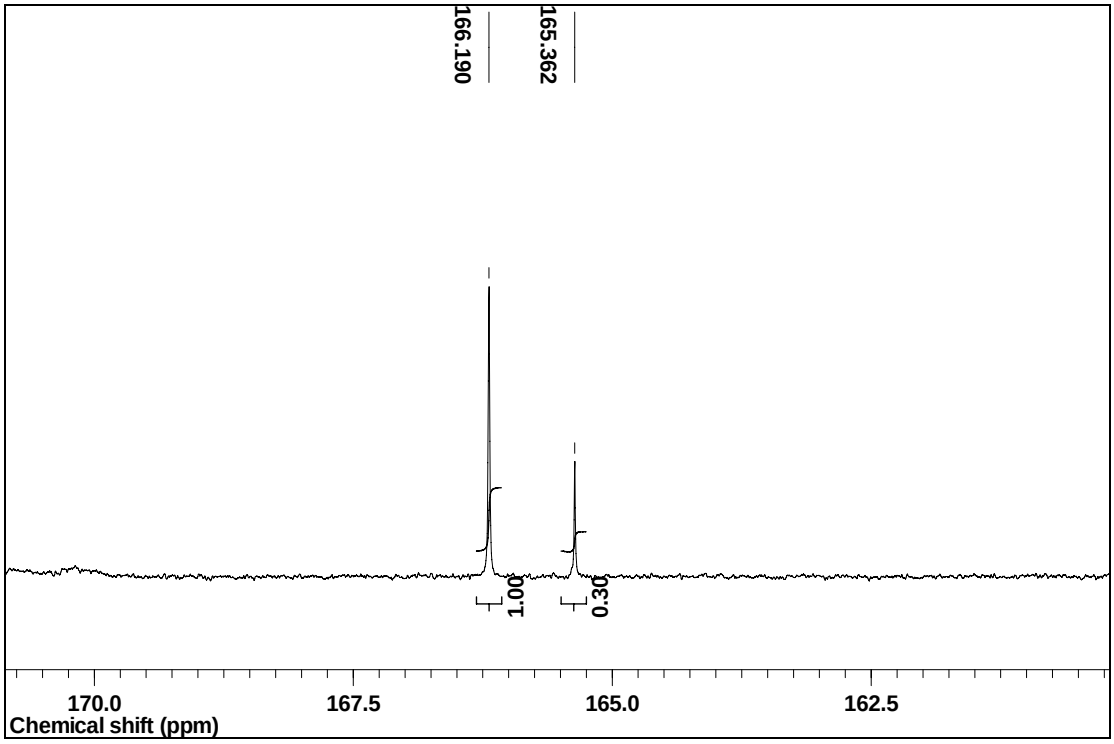


**Figure 4.2: $^{13}C$ NMR spectrum of the MAH/BMA copolymer in acetone-$d_6$.**

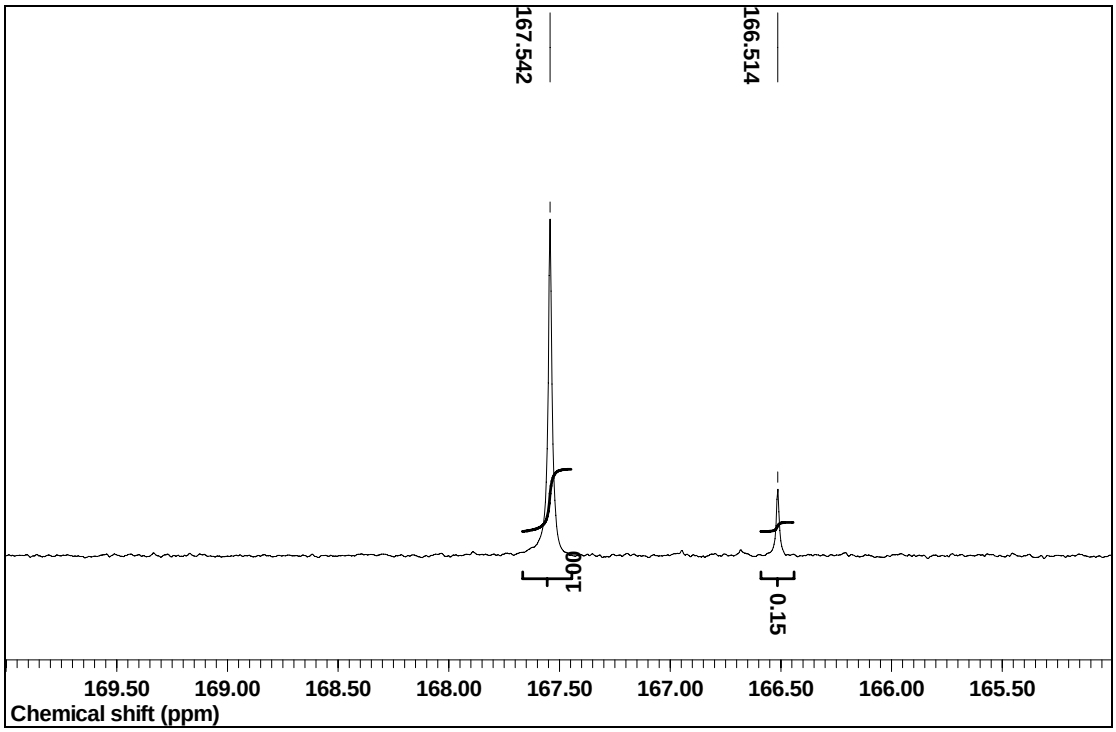


**Figure 4.3: $^{13}$C NMR spectrum of the MAH/LMA copolymer in 90% THF and 10% acetone-$d_6$.**

Results of the $^{13}$C NMR spectra and the absence of BMA and LMA monomer resonance peaks in the $^{1}$H NMR spectra, indicate that 100% BMA and 100% LMA were incorporated in the respective copolymers.

The initial % [BMA] and % [MAH], calculated from the total [monomer] and [initiator], was 58.1% and 40.9% respectively for the MAH/BMA copolymer. This means that if 58.1% of BMA was incorporated in the copolymer, then 36.94% of MAH must have been incorporated in the copolymer. The $^{13}$C NMR analysis shows that only 15% of MAH was incorporated in the copolymer. This means that 21.94% of the % copolymer yield was due to unreacted MAH, initiator and solvent present in the copolymer.

The initial % [LMA] and % [MAH], calculated from the total [monomer] and [initiator], was 71.72% and 27.63% respectively for the MAH/LMA copolymer. This means that if

71.72% of LMA was incorporated in the copolymer, then 23.07% of MAH must have been incorporated in the copolymer. The $^{13}C$ NMR analysis shows that only 7.5% of MAH was incorporated in the copolymer. This means that 15.57% of the % copolymer yield was due to unreacted MAH, initiator and solvent present in the copolymer.

#### 4.3.1.3. GPC analysis

GPC analysis of the MAH/BMA and MAH/LMA copolymers revealed that low molecular weight polymers with broad polydispersities were formed. The results are given in Table 4.4.

**Table 4.4: GPC analysis of MAH/BMA and MAH/LMA**

| GPC analysis | | | |
|---|---|---|---|
| **Polymer** | **Mn** | **Mw** | **Mw/Mn** |
| MAH/BMA | 5936 | 40527 | 6.83 |
| MAH/LMA | 26205 | 146893 | 5.61 |

### 4.3.2. Copolymerization kinetics analysis via in situ $^{1}H$ NMR

The in situ $^{1}H$ NMR experiments produced fairly resolved peaks that corresponded to the double bond protons of each of the monomers used in both copolymer systems. The insensitivity of the technique is however well apparent and will be seen in the fluctuations in the data obtained in Sections 4.3.2.1 and 4.3.2.2 [11].

The disappearance of the co-monomers was detected by the area under their proton peaks. The two protons of MAH resonated at the same frequency because they are chemically equivalent by symmetry considerations [10]. The MAH proton signal usually resonates at 7.0 ppm in acetone-$d_6$ but it was found that it resonated at 5.6 ppm when benzene-$d_6$ was used as NMR solvent. This effect is due to dipole interactions between the polar solvents and the polar MAH bonds which causes a solvent-induced shift [10]. The

effect can also be ascribed to the positive magnetic anisotropy ($\sigma_A$) normally found for aromatic solvents such as benzene. Studies on the variation in chemical shifts of protons in large molecules have shown considerable regularity in solvent effects. A solvent shift in going from $CDCl_3$ to $C_6D_6$ as solvent, can be denoted as:

$$\Delta_{C_6D_6}^{CDCl_3} = \delta_{CDCl_3} - \delta_{C_6D_6} \qquad (4.1)$$

where:

$\sigma$: the shielding factor

$\Delta$: the difference in the shielding factors of the two solvents [12].

Thus an upfield shift of the MAH proton resonance occurs due to the positive value of $\Delta$ [12].

The double bond proton signals of the vinyl groups of BMA (*see Figure 4.4*) and LMA have the same chemical shifts because their structures only differ in the number of carbon atoms after the ester function. The two protons of both BMA and LMA resonated at two different frequencies due to the different chemical environments experienced by them. The different chemical environments experienced by the two protons are created by the anisotropic field of the carbonyl group of the ester function in both BMA and LMA, which has a deshielding effect on one of the protons and shifts it downfield [10].

There is a direct correlation between the concentration of the monomers and the reduction in their double bond proton area caused by the development of the copolymerization reaction [13]. This permitted a direct quantitative measurement of the amount of respective co-monomers incorporated into each copolymer system.

The copolymerization kinetics analysis for the MAH/BMA copolymer is discussed in Section 4.3.2.1, and that of the MAH/LMA copolymer in Section 4.3.2.2.

### 4.3.2.1. MAH/BMA copolymerization

The decrease in intensity of the double bond proton signals of MAH (a, at 5.6 ppm)$_{average}$ and BMA (b, at 5.2 ppm and c at 6.0 ppm)$_{average}$ relative to the proton signals of 1,4-dioxane (i, at 3.7 ppm)$_{average}$ reference signal was followed during the course of the reaction (*see Figure 4.4*).

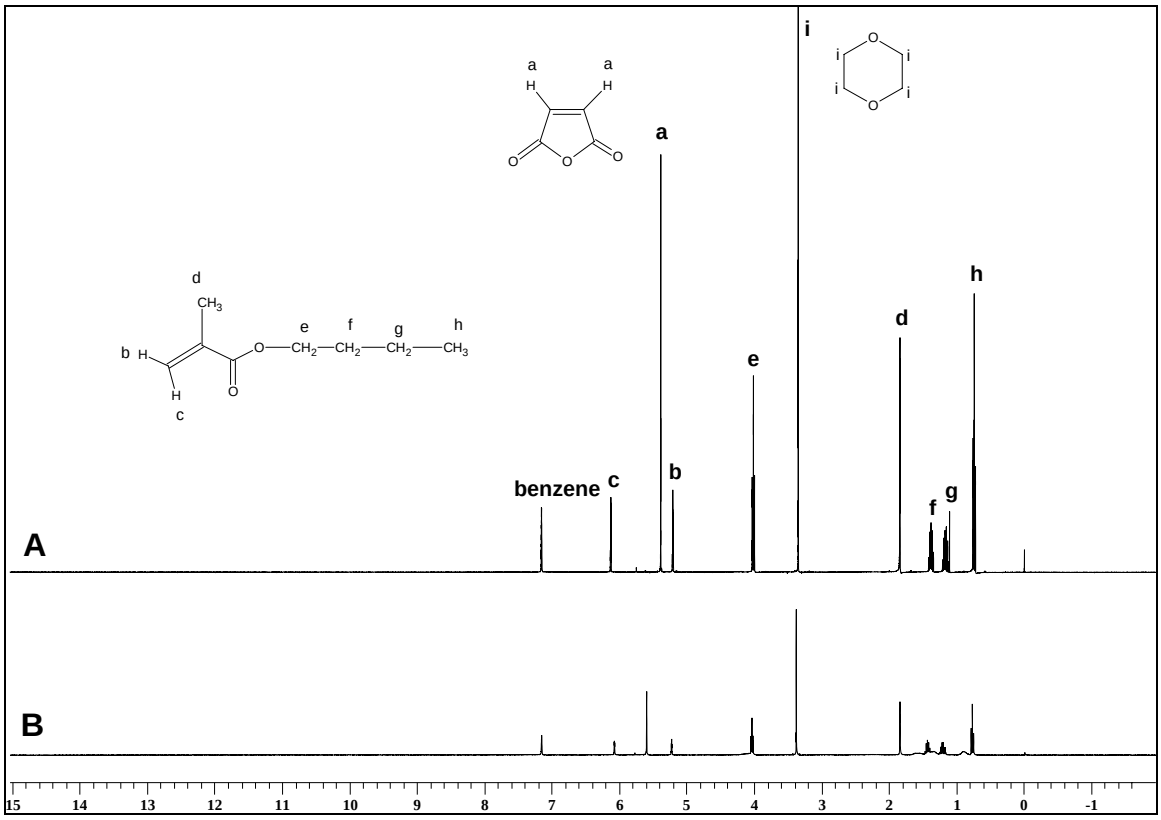


**Figure 4.4: $^{1}$H NMR spectra of the MAH/BMA (50/50 molar ratio) copolymerization at 80 $^{0}$C in benzene-d$_6$. A is the spectrum of the monomers at t = 0 and B the spectrum of the monomers at t = 1 h.**

Spectrum A shows the proton signals of the monomers at the start of the reaction while B shows the decrease in the vinyl proton signals of the monomers as the copolymerization proceeded (after 1 h). Spectrum B also shows the formation of MAH/BMA copolymer

and BMA homopolymer. This is seen in Figure 4.5 when the size of all the resonance peaks in spectrum B is increased.

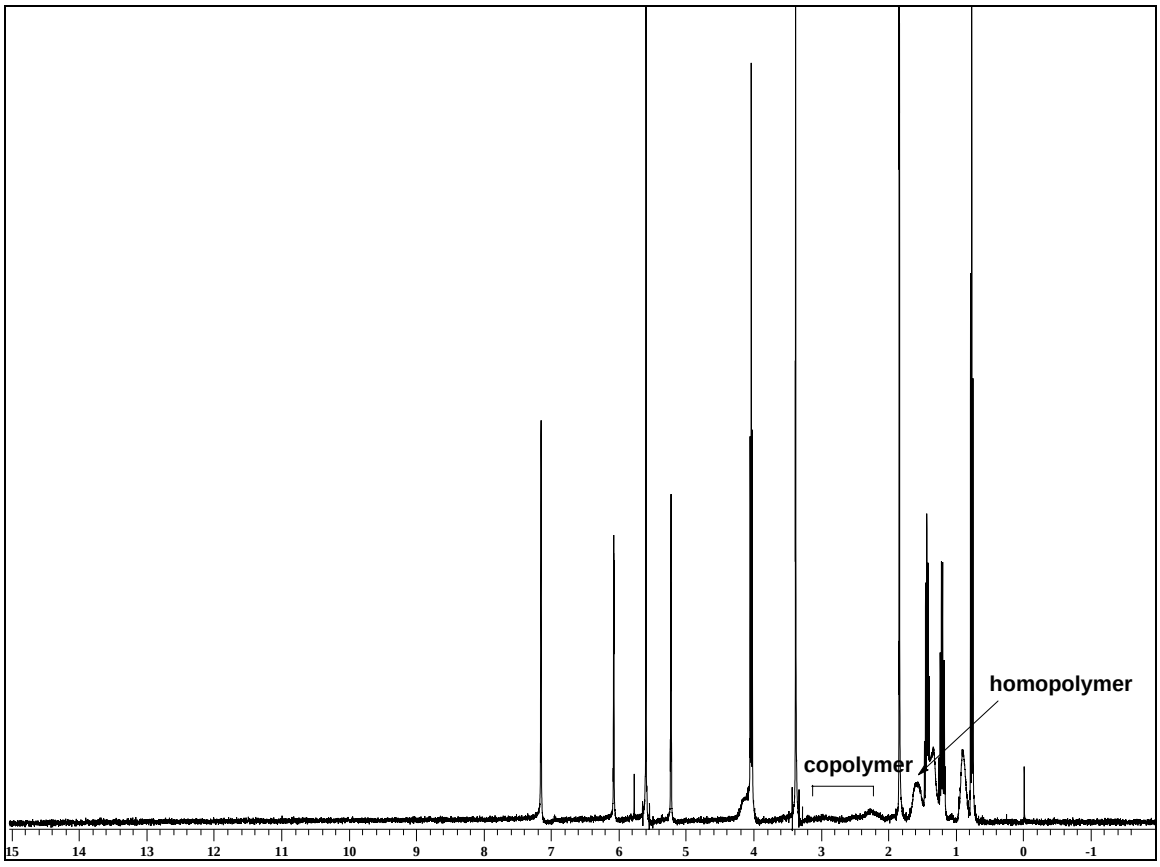


**Figure 4.5: $^{1}$H NMR spectrum of MAH/BMA copolymer and BMA homopolymer.**

The decreasing concentrations of the co-monomers in the reaction mixture or feed were calculated by integrating their peaks with respect to the reference peak of 1,4-dioxane. Figure 4.6 gives the monomer consumption as normalized (integrated) peak intensities for the 50/50 molar ratio of the MAH/BMA copolymer. The two proton signals of BMA were summed in order to determine the initial monomer concentrations at the start of the reaction. The initial concentrations of the monomers, as calculated from the normalized peak intensities, were 0.79 mol/L for BMA and 0.79 mol/L for MAH. The exact mol % concentrations of the monomers thus were 49.94% for BMA and 50.06% for MAH.

The results gave rise to two problems. Firstly, there is an increase and then a decrease in the consumption curve of BMA at the start of the reaction (from t = 0 s to t = 210 s). Secondly, the MAH consumption curve also decreases faster than that of BMA at the start of the reaction, which should not be the case since MAH cannot homopolymerize. There is also no ring opening of MAH, as the peak that should appear in this case at 6.5 ppm (*refer back to Figure 4.1*) did not. A possible reason for these problems could be the high reactivity of MAH towards AIBN, which was studied by Ito et al.[14], but since only 1% AIBN was used this reason is unlikely. Another reason could be poor integration, but since integration was done in duplicate (and by two people), and the same results obtained, it is not likely to be the case.

The two most likely reasons could be the long equilibration period of the spectrometer and the fluctuations measured in the intensity of the reference solvent, 1,4-dioxane. The equlibration takes 5 to 10 min, which means that data is obtained 5 to 10 min after the actual reaction had started. The resonance integral of the reference solvent, dioxane, was also found to first decrease and then increase by up to 40% during the experiment. Evaporation of the reference was investigated but since its resonance signal increased instead of decreased, this could not be the case. A concrete reason for the fluctuations in the resonance signal of the reference could thus not be obtained at this stage but the fluctuations do give a reason for the problems obtained in the results. It is also reasonable to assume that fluctuations also occur in the integrals especially in the early stages of reaction. The BMA and MAH resonance signals are integrated with respect to dioxane which means that their integrals will be affected by any fluctuations in the integrals of dioxane. Due to these problems therefore actual reactivity ratios, which are calculated at less than 10% conversion, could not be calculated [13]. This was mainly due to negative values being obtained at the start of the copolymerization when the amount of BMA incorporated in the copolymer was calculated and the excessive drop in MAH concentration. The drop in MAH is erroneous as is evident when referring back to the bulk copolymerization analysis (*Section 4.3.1.2*) where a +/- 1:1 monomer ratio gave only 15% MAH incorporated into the MAH/BMA copolymer.

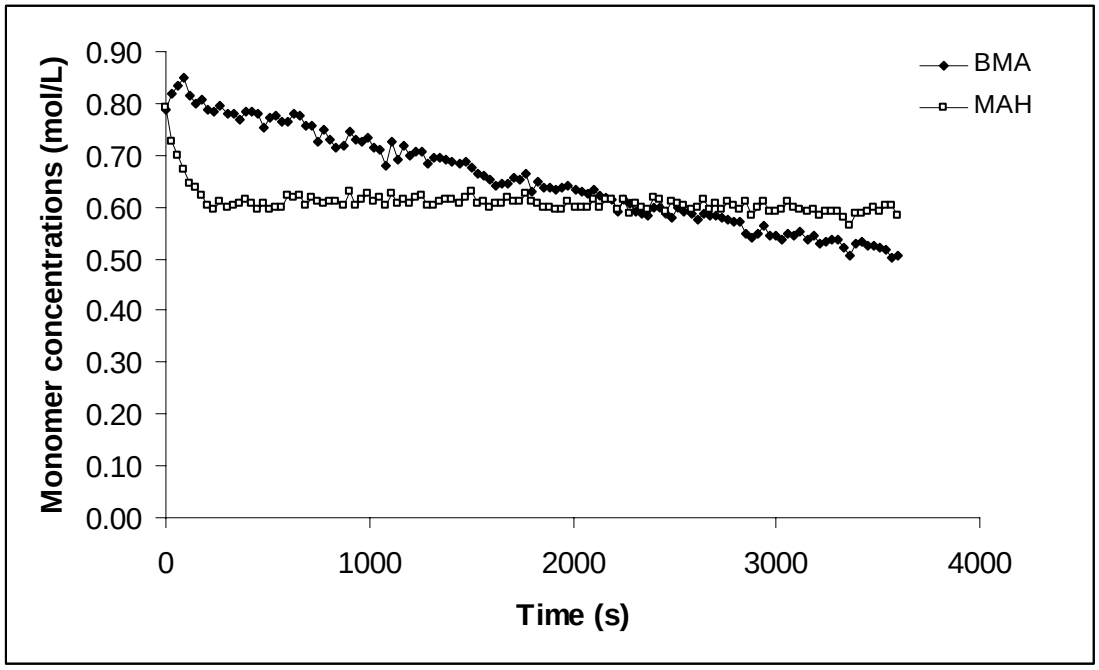


**Figure 4.6: Monomer consumption curves for the MAH/BMA (50/50 molar ratio) copolymerization at 80 $^0$C in benzene-$d_6$.**

The copolymer conversion for the different molar ratios of the MAH/BMA reaction mixture was calculated as follows:

$$\left( \frac{[\mathrm{MAH}]_{co} + [\mathrm{BMA}]_{co}}{[\mathrm{MAH}]_0 + [\mathrm{BMA}_0]} \right) \mathrm{x}\,100\% \qquad (4.2)$$

where:

$[MAH]_{co}$: concentration of MAH in the copolymer at time t

$[BMA]_{co}$: concentration of BMA in the copolymer at time t

$[MAH]_0$: initial concentration of MAH in the feed

$[BMA]_0$: initial concentration of BMA in the feed.

Figure 4.7 shows the copolymer conversions for the different molar ratios of the MAH/BMA reaction mixture as a function of time. The higher the MAH content in the reaction mixture, the higher the copolymer conversion (wt %) at the start of the reaction. This can be seen for the 89% MAH/11% BMA, 66% MAH/34% BMA and 50% MAH/50% BMA copolymer systems. The copolymer conversions for these systems tend to get slower after about 15% conversion. This tendency is more predominant for the 89% MAH/11% BMA system, which has the lowest conversion at t = 3600 s even though it has the highest conversion in the beginning stages of the reaction. At 11% BMA only an equal percentage or less of MAH is possible as it can only copolymerize not homopolymerize, hence the low conversion. The higher the BMA content in the reaction mixture, the lower the copolymer conversion (wt %) at the start of the reaction. This tendency is predominant for the 9% MAH/91% BMA and 27% MAH/73% BMA copolymer systems, which has high conversions at 3600 s even though they have the lowest conversions in the beginning stages of the reactions. It should also be noted that the graphs do not start at zero, which again highlights the problems encountered at the start of the copolymerization reactions.

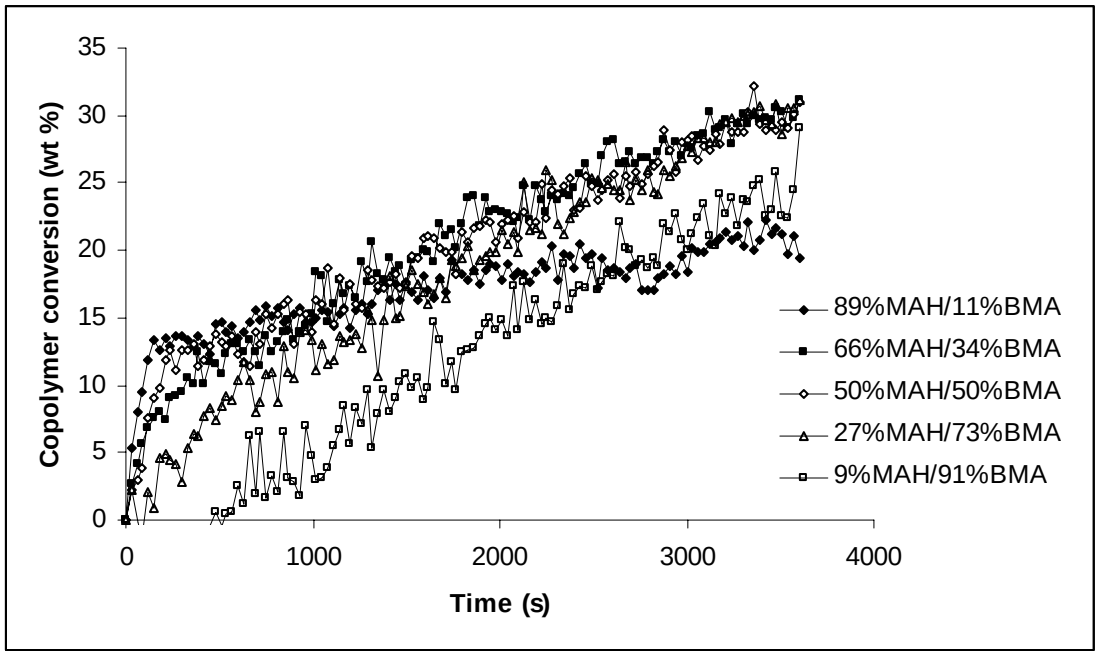


**Figure 4.7: MAH/BMA copolymer conversion as a function of time.**

The amounts of MAH and BMA incorporated in the MAH/BMA copolymer were calculated as follows:

$$(\%\,\mathrm{BMA})_{co} = \left(\frac{[\mathrm{BMA}]_{co}}{[\mathrm{BMA}]_0 + [\mathrm{MAH}]_0}\right) \mathrm{x}\,100\% \qquad (4.3)$$

$$(\%\,\mathrm{MAH})_{co} = \left(\frac{[\mathrm{MAH}]_{co}}{[\mathrm{MAH}]_0 + [\mathrm{BMA}]_0}\right) \mathrm{x}\,100\%$$

Figure 4.8 shows the % copolymer conversion and % monomers incorporated in the MAH/BMA (50/50 molar ratio) copolymer as a function of time. Initially there is a higher content of MAH than BMA, but after about 10% conversion there is a faster incorporation of BMA and slower incorporation of MAH. The result indicates that MAH has a higher reactivity than BMA in the beginning stages of the reaction but after about 12% conversion the reactivity of MAH stabilizes and the reactivity of BMA increases continuously.

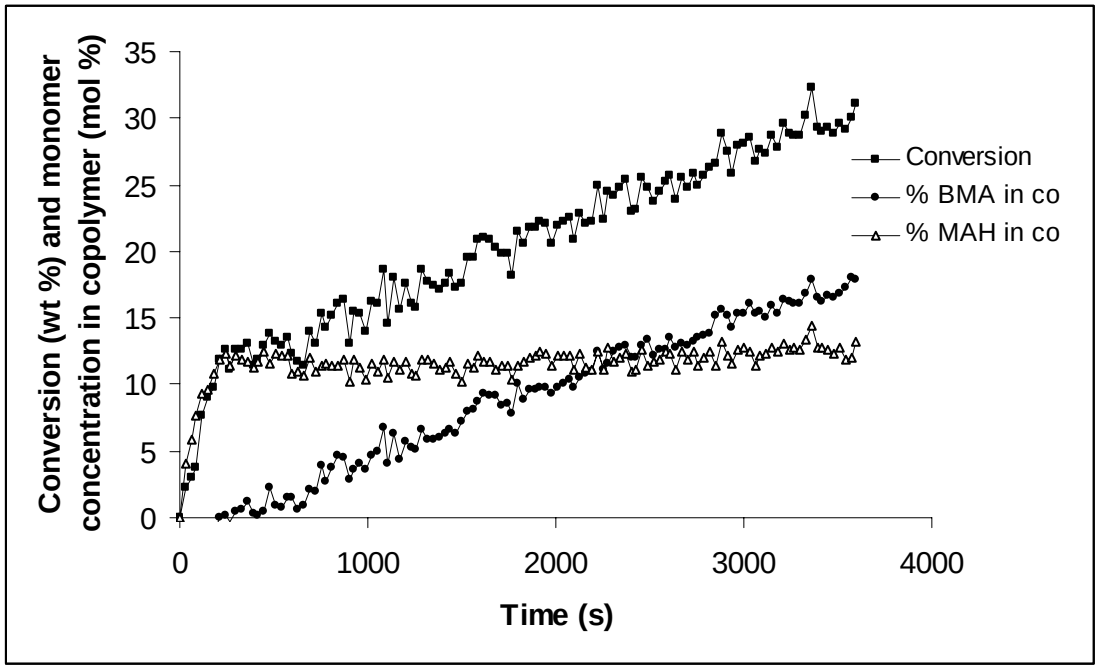


**Figure 4.8: Copolymer conversion and monomer concentration in the MAH/BMA (50/50 molar ratio) copolymer as a function of time.**

The amounts of MAH and BMA still left in the feed after 1 h were calculated as follows:

$$(\%\,\mathrm{BMA})_f = \left(\frac{[\mathrm{BMA}]_f}{[\mathrm{BMA}]_0 + [\mathrm{MAH}]_0}\right) \mathrm{x}\,100\% \qquad (4.4)$$

$$(\%\,\mathrm{MAH})_f = \left(\frac{[\mathrm{MAH}]_f}{[\mathrm{MAH}]_0 + [\mathrm{BMA}]_0}\right) \mathrm{x}\,100\%$$

where:

$(\%\ \mathrm{BMA})_f$: % BMA in the feed at time t

$[\mathrm{BMA}]_f$: concentration of BMA in feed at time t

$(\%\mathrm{MAH})_f$: % MAH in the feed at time t

$[\mathrm{MAH}]_f$: concentration of MAH in the feed at time t.

Table 4.5 summarizes the initial concentrations, initial molar ratios, copolymer conversions, % monomers incorporated in the MAH/BMA copolymer and the % monomers still left in the feed after 1 h.

**Table 4.5: Copolymer conversions and compositions of MAH/BMA at t = 3600 s**

| Molar Ratios | | [Monomer]$_0$ (mol/L) | | Conv. (wt%) | Mole % Monomer in copolymer | | Mole % Monomer in feed | |
|---|---|---|---|---|---|---|---|---|
| MAH | BMA | MAH | BMA | | MAH | BMA | MAH | BMA |
| 89.36 | 10.64 | 0.71 | 0.09 | 19.36 | 8.73 | 10.63 | 80.63 | 0.01 |
| 66.27 | 33.74 | 2.82 | 1.44 | 31.09 | 10.85 | 20.24 | 55.42 | 13.49 |
| 50.06 | 49.94 | 0.79 | 0.79 | 31.06 | 13.24 | 17.82 | 36.82 | 32.12 |
| 27.17 | 72.83 | 2.92 | 7.84 | 31.20 | 7.12 | 24.08 | 20.05 | 48.75 |
| 8.86 | 91.14 | 0.42 | 4.34 | 29.03 | 3.14 | 25.89 | 5.72 | 65.25 |

### 4.3.1.2. MAH/LMA copolymerization

The decrease in intensity of the double bond proton signals of MAH (5.6 ppm)$_{average}$ and LMA (5.2 ppm and 6.0 ppm)$_{average}$ relative to the 1,4-dioxane (3.7 ppm)$_{average}$ reference signal was followed during the course of the reaction (*see Figure 4.4*).

The decreasing concentrations of the co-monomers in the reaction mixture were calculated by integrating the peaks with respect to the reference peak of 1,4-dioxane.

Figure 4.9 gives the monomer consumption as normalized (integrated) peak intensities for the 50/50 molar ratio of the MAH/LMA copolymer. The two proton signals of LMA were summed in order to determine the initial monomer concentrations at the start of the reaction. The initial concentrations of the monomers, as calculated from the normalized peak intensities, were 4.06 mol/L for LMA and 4.57 mol/L for MAH. The exact mol % concentrations of the monomers thus were 47.04% for LMA and 52.96% for MAH.

The same problems obtained for the MAH/BMA copolymer system occurred for the MAH/LMA copolymer system.

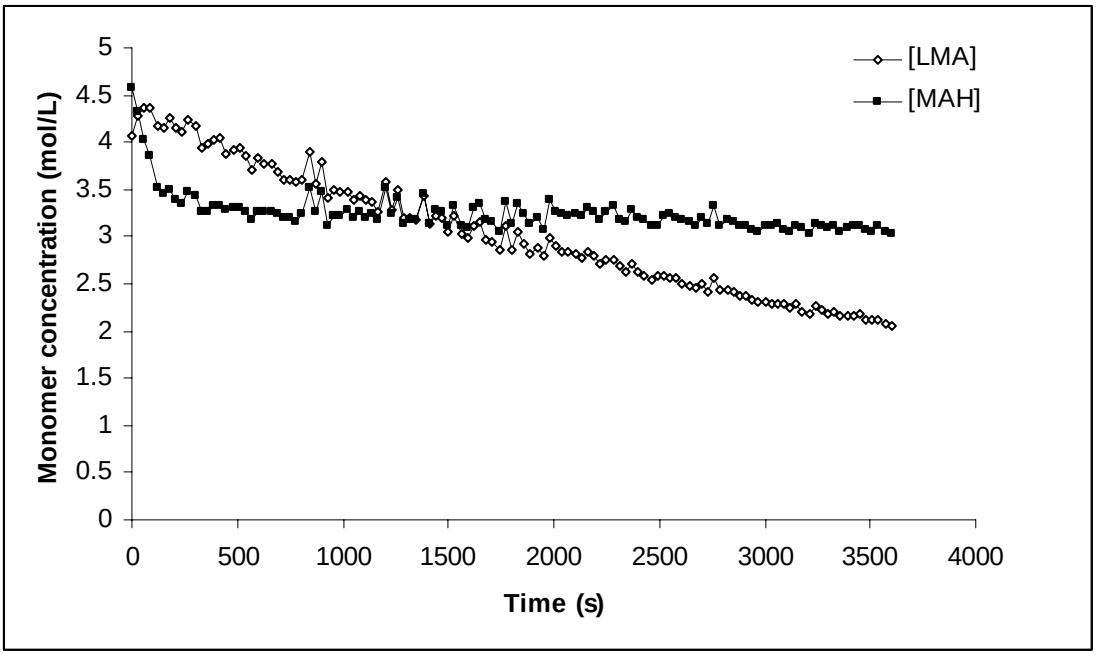


**Figure 4.9: Monomer consumption curves for the MAH/LMA (53/47 molar ratio) copolymerization at 80 $^0$C in benzene-$d_6$.**

The copolymer conversion for the different molar ratios of the MAH/LMA reaction mixture was calculated as follows:

$$\left( \frac{[\text{MAH}]_{co} + [\text{LMA}]_{co}}{[\text{MAH}]_0 + [\text{LMA}]_0} \right) \text{x}\, 100\% \qquad (4.5)$$

where:

$[MAH]_{co}$: concentration of MAH in the copolymer at time t

$[LMA]_{co}$: concentration of LMA in the copolymer at time t

$[MAH]_0$: initial concentration of MAH in the reaction mixture

$[LMA]_0$: initial concentration of LMA in the reaction mixture.

Figure 4.10 shows the copolymer conversions for the different molar ratios of the MAH/LMA reaction mixture as a function of time. The higher the MAH content in the reaction mixture, the higher the copolymer conversion (wt %) at the start of the reaction. This can be seen for the 92% MAH/8% LMA, 70% MAH/30% LMA and 53% MAH/47% LMA copolymer systems. The copolymer conversions for these systems tend to get slower after about 15% conversion. This tendency is more predominant for the 92% MAH/8% LMA system, which has the lowest conversion at t = 3600 s even though it has a high conversion in the beginning stages of the reaction. Again this is to be expected as the amount of LMA is 8% and it will copolymerize with the MAH which cannot homopolymerize, therefore maximum conversion can theoretically be 16.48%. The higher the LMA content in the reaction mixture, the lower the copolymer conversion (wt %) at the start of the reaction. This tendency is predominant for the 10% MAH/90% LMA and 29% MAH/71% LMA copolymer systems, which have high conversions at 3600 s although they have the lowest conversions in the beginning stages of the reactions. It should also be noted that the graphs do not start at zero, which again highlights the problems encountered at the start of the copolymerization reactions.

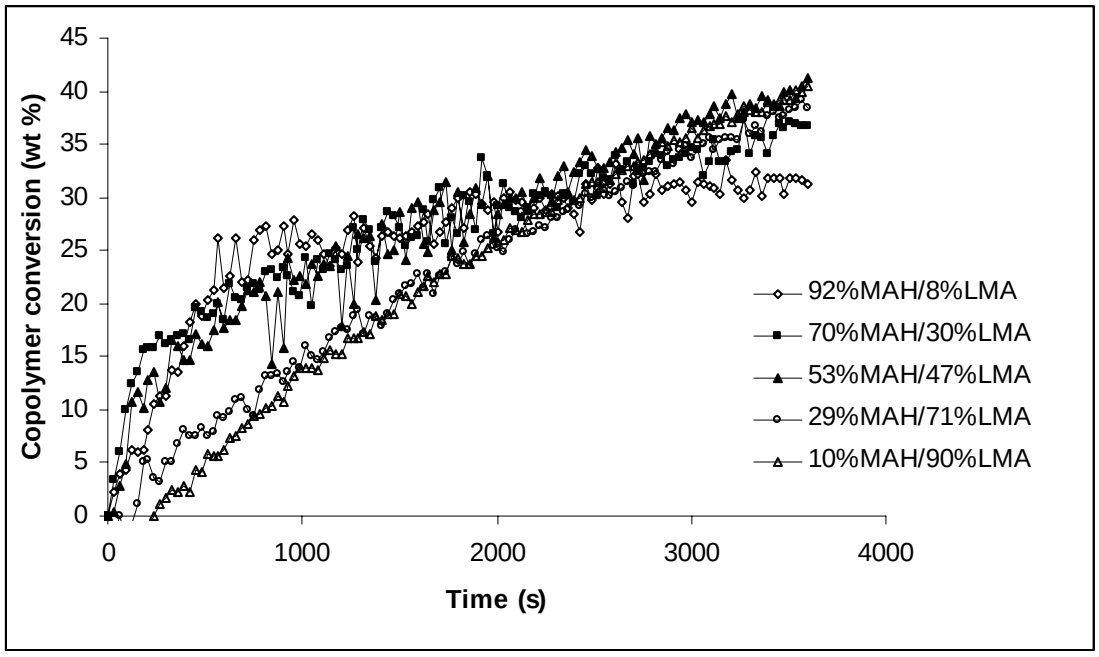


**Figure 4.10: MAH/LMA copolymerization conversion as a function of time.**

The amounts of MAH and LMA incorporated in the MAH/LMA copolymer were calculated as follows:

$$(\%\,\mathrm{LMA})_{co} = \left( \frac{[\mathrm{LMA}]_{co}}{[\mathrm{LMA}]_0 + [\mathrm{MAH}]_0} \right) \mathrm{x}\,100\% \qquad (4.6)$$

$$(\%\,\mathrm{MAH})_{co} = \left( \frac{[\mathrm{MAH}]_{co}}{[\mathrm{MAH}]_0 + [\mathrm{LMA}]_0} \right) \mathrm{x}\,100\%$$

Figure 4.11 shows the % copolymer conversion and % monomers incorporated in the MAH/LMA (53% MAH/47% LMA) copolymer as a function of time. Initially there is a higher content of MAH than LMA, but after about 15% conversion there is a faster incorporation of LMA and slower incorporation of MAH. The result indicates that MAH has a higher reactivity than LMA in the beginning stages of the reaction but after about 15% conversion the reactivity of MAH stabilizes and the reactivity of LMA increases continuously.

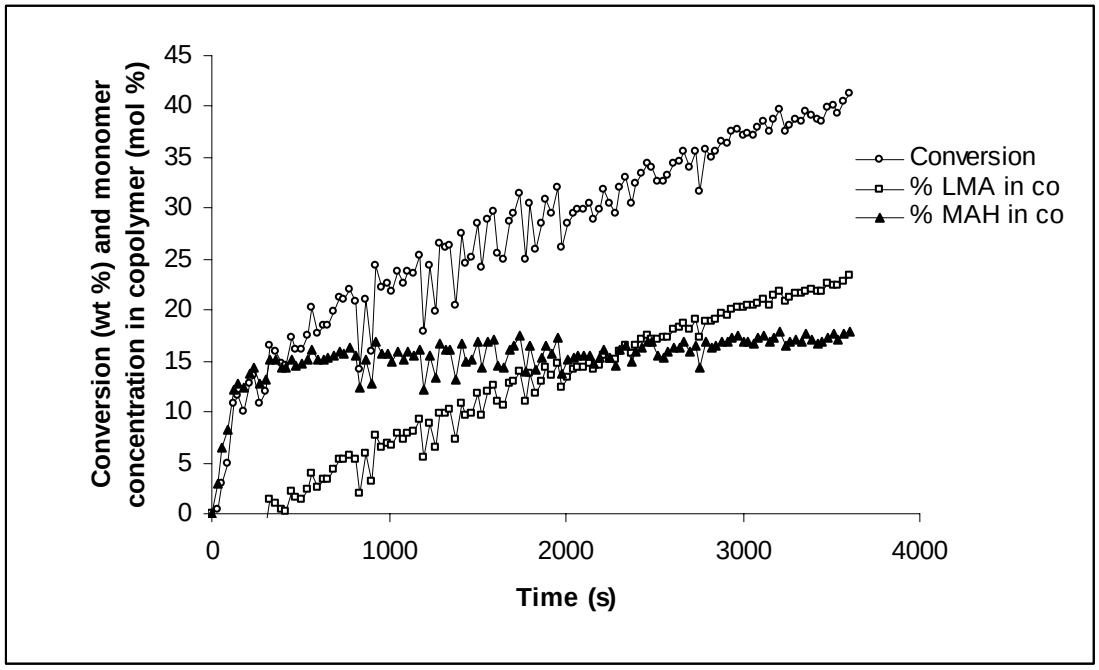


**Figure 4.11: Copolymer conversion and monomer concentration in the MAH/LMA (53/47 molar ratio) copolymer as a function of time.**

The amounts of MAH and LMA still left in the feed after 1 h were calculated as follows:

$$(\%\,\mathrm{LMA})_f = \left(\frac{[\mathrm{LMA}]_f}{[\mathrm{LMA}]_0 + [\mathrm{MAH}]_0}\right) \mathrm{x}\,100\%$$

$$(\%\,\mathrm{MAH})_f = \left(\frac{[\mathrm{MAH}]_f}{[\mathrm{MAH}]_0 + [\mathrm{LMA}]_0}\right) \mathrm{x}\,100\% \qquad (4.7)$$

where:

$(\%\ \mathrm{LMA})_f$: % LMA in the feed at time t

$[\mathrm{LMA}]_f$: concentration of LMA in feed at time t

$(\%\mathrm{MAH})_f$: % MAH in the feed at time t

$[\mathrm{MAH}]_f$: concentration of MAH in the feed at time t.

Table 4.6 summarizes the initial concentrations, initial molar ratios, copolymer conversions, % monomers incorporated in the MAH/LMA copolymer and the % monomers still left in the feed after 1 h.

**Table 4.6: Copolymer (co) conversions and compositions (f) of MAH/LMA at t = 3600 s**

| Molar Ratios | | $[Monomer]_0$ (mol/L) | | Conv. (wt %) | Mole % Monomer in copolymer | | Mole % Monomer in feed | |
|---|---|---|---|---|---|---|---|---|
| MAH | LMA | MAH | LMA | | MAH | LMA | MAH | LMA |
| 91.77 | 8.24 | 3.81 | 0.34 | 31.30 | 25.53 ∗ | 5.77 | 66.24 | 2.47 |
| 69.86 | 30.14 | 2.98 | 1.28 | 36.81 | 19.51 | 17.30 | 50.35 | 12.84 |
| 52.96 | 47.04 | 4.57 | 4.06 | 41.26 | 17.97 | 23.29 | 35.00 | 23.75 |
| 28.52 | 71.48 | 1.77 | 4.44 | 38.39 | 9.22 | 29.17 | 19.30 | 42.31 |
| 10.07 | 89.93 | 0.29 | 2.56 | 40.39 | 3.95 | 36.44 | 6.13 | 53.48 |

∗ This value is definitely in error because MAH does not homolymerize.

Although the kinetic study failed to give accurate quantitative data for the monomer incorporation in the respective copolymer systems, it nonetheless gives a clear picture of the reactivity of MAH towards BMA and LMA.

## 4.4. Conclusions

The main conclusion reached from both the in situ $^{1}H$ NMR experiments and the quantitative $^{13}C$ NMR analyses is that the copolymerization of MAH with BMA and with LMA forms random copolymers and not alternating copolymers. It was found from the kinetic study via $^{1}H$ NMR that both BMA and LMA have a higher reactivity than MAH even though MAH has a high reactivity at the start of the copolymerization reactions. This was seen in the monomer consumption data, where the graphs of BMA and LMA continued while that of MAH stabilized after a certain percentage conversion. The reactivity of MAH should be further investigated in order to establish or confirm that MAH has a higher reactivity towards AIBN than towards BMA and LMA in the early

stages of these copolymerizations as stated in the literature by Ito et al. [14]. Quantitative $^{13}C$ NMR analysis which showed the low incorporation of MAH in the two respective copolymers, further showed that MAH has a low reactivity towards BMA and LMA. In criticism of the NMR technique, it is felt that it is too insensitive for work involving largely dissimilar monomers.

## 4.5. References

(1) Joynes, D.; Sherrington, D.C. *Polymer* **1997**, *38*, 1427-1438.

(2) Li, D.; Grady, M.C.; Hutchinson, R.A. *Industrial & Engineering Chemistry Research* **2005**, *44*, 2506-2517.

(3) Raghunadh, V.; Baskaran, D.; Sivaram, S. *Polymer* **2004**, *45*, 3149-3155.

(4) Haddleton, D.M.; Crossman, M.C.; Hunt, K.H. *Macromolecules* **1997**, *30*, 3992-3998.

(5) Ham, G.E. *Copolymerization*; Interscience: Kansas, 1964; Vol. XVII.

(6) Pasquale, A.J., 2002. Synthesis and Characterization of Multi-Component Polymeric Materials Prepared via Free Radical Polymerization. Doctoral Thesis, University of Virginia, Virginia, 255 pp.

(7) Davies, M.C.; Dawkins, J.V.; Hourston, D.J. *Polymer* **2005**, *46*, 1739-1753.

(8) Li, H-M.; Chen, H-B.; Shen, Z-G.; Lin, S. *Polymer* **2002**, *43*, 5455-5461.

(9) Felthouse, T.R.; Burnett, J.C.; Horrell, B.; Mummey, M.J.; Kuo, Y-J.*Maleic Anhydride, Maleic Acid, and Fumaric Acid*, In *Kirk-Othmer Encyclopedia of Chemical Technology*, 4th ed.; John Wiley & Sons: Texas, 2001; Vol. 15, pp 893-928.

(10) Pavia, D.L.; Lampman, G.M.; Kriz, G.S. *Introduction to Spectroscopy*, 3rd ed.; Thomson Learning: USA, 2001.

(11) Christian, G.D.; O'Reilly, J.E. *Instrumental Analysis*, 2nd ed.; Allyn and Bacon Inc.: Massachusetts, 1986.

(12) Becker, E.D. *High Resolution NMR: Theory and Chemical Applications*, 2nd ed.; Academic Press: New York, 1980.

(13) Alvares, D.R.S.; Menezes, S.M.C.; Lucas, E.F. *Polymer International* **2004**, *53*, 1639-1643.

(14) Ito, H.; Miller, D.; Sveum, N.; Sherwood, M. *Polymer Science* **2000**, *38*, 3521-3542.

# CHAPTER 5

# CELLULOSE MODIFICATION WITH POLYMERIC SURFACTANTS

## 5.1. Introduction

The growing interest in polymeric surfactants is due to their strong driving force to move to interfaces. The main driving force for this is an effective interaction between polymer segments and the surface. Their tendency to collect at interfaces is not as dependent on the physical variables generally observed for normal, low molecular weight surfactants. This means that they are effective at low total concentrations and have little sensitivity towards salts, temperature changes, etc. [1].

Polymer adsorption involves a number of various interactions but one of the most fundamental considerations is the conformation of polymer molecules at an interface [2]. In literature, it is found that most polymer systems adsorb at surfaces in a coiled conformation and the amount of polymer adsorbed is molecular weight dependent [1]. Several theories also exist that describe the process of polymer adsorption. These theories were developed either using statistical mechanical approaches or quasi-lattice models. The latter was developed by Roe, Scheutjens and Fleer. One of the predictions from the theories is that the higher the molecular weight of a polymer, the higher the amount of adsorption [2].

An understanding of polymer mobility near the polymer-solid interface is important in many different applications, including adhesion, electronics packaging, coatings and composites. The physical properties of polymers near interfaces are strongly influenced by changes in their mobility. Available data have shown that the chain mobility of polymers are dramatically reduced near surfaces with attractive polymer-solid interaction energies [3].

In this chapter, the industrial reactive surfactant, ASA, and the two synthesized surfactants, MAH/BMA and MAH/LMA, are used respectively, to size recycled paperboard. The sizing efficiency of these three respective surfactants will be evaluated in order to establish which surfactant has the best performance in terms of sizing paperboard.

## 5.2. Experimental

### 5.2.1. Materials

The materials used for the sizing of paperboard are summarized in the table below.

**Table 5.1: Polymeric surfactants and materials used to size paperboard**

| Materials | Material code | Supplier |
|---|---|---|
| Maleic anhydride/butyl methacrylate copolymer | MAH/BMA | |
| Maleic anhydride/lauryl methacrylate copolymer | MAH/LMA | |
| Alkenyl succinic anhydride | ASA | Buckman Laboratories Inc. (Manchester) |
| Starch (Stysol 70) | | African Products (Pty Limited) SA |
| Acetone | | BDH Chemicals (England) |
| Tetrahydrofuran | THF | BDH Chemicals (England) |

Paperboard was supplied by Mondi Packaging. Distilled deionized (DDI) water, obtained from a Millipore Milli-Q purification system, was used. All other materials were used as received from the suppliers.

### 5.2.2. Preparation

MAH/BMA, MAH/LMA and ASA solutions were all prepared in 100 ml screw-top glass bottles. The surfactants were prepared as follows:

1) Solutions of MAH/BMA with concentrations of 2, 4, 6, 8 and 10% in acetone were prepared at room temperature.
2) Solutions of MAH/LMA with concentrations of 2, 4, 6, 8 and 10% in THF were prepared at room temperature.
3) Emulsions of ASA with concentrations of 2, 4, 6, 8 and 10% in starch were prepared at room temperature. The starch (15%) was prepared by dissolving in DDI water and boiling at 90 $^{0}$C for 3 h.

### 5.2.3. Application

Uncoated paperboard sheets (148 x 210 mm) were dipped into the respective surfactant solutions. See Chapter 3, Section 3.2.3 for the dipping and drying methods. The results of the amount of surfactant adsorbed by the paperboard are given in Table 5.2, Section 5.3.

### 5.2.4. Testing of polymeric surfactant coated paperboard

The surfaces of the uncoated and surfactant coated paperboard were evaluated via SEM, which is described in Chapter 3, Section 3.2.4.1. The sizing efficiency and hydrophobicity of the surfactant coated paperboard were determined via the Cobb test and contact angle measurements. These two tests are described in Chapter 3, Sections 3.2.4.2 and 3.2.4.3 respectively.

## 5.3. Results and discussion

The amounts of surfactant adsorbed by the uncoated paperboard and the amount of water absorbed by the surfactant coated paperboard were determined. Uncoated paperboard, used as a reference, was found to have a Cobb value of 593. The results are summarized in Table 5.2.

**Table 5.2: Surfactant concentrations used, surfactant weight adsorbed and surfactant Cobb values**

| LMA in THF | | | BMA in acetone | | | ASA in starch | | |
|---|---|---|---|---|---|---|---|---|
| Surfactant Conc. (wt %) | Surfactant Weight adsorbed ($g/m^2$) | Cobb values | Surfactant Conc. (wt %) | Surfactant Weight adsorbed ($g/m^2$) | Cobb values | Surfactant Conc. (wt %) | Surfactant Weight adsorbed ($g/m^2$) | Cobb values |
| 2 | 5.02 | 14 | 2 | 3.37 | 18 | 2 | 37.07 | 47 |
| 4 | 9.97 | 9 | 4 | 12.13 | 17 | 4 | 46.5 | 64 |
| 6 | 15.83 | 7 | 6 | 17.11 | 13 | 6 | 57.79 | 74 |
| 8 | 22.20 | 6 | 8 | 20.28 | 13 | 8 | 49.2 | 76 |
| 10 | 31.37 | 4 | 10 | 27.29 | 11 | 10 | 60.49 | 73 |

All three polymeric surfactants have the same hydrolyzable maleic anhydride head group which will form an ester bond with the hydrophilic paperboard surface. They do, however, have different hydrophobic tail groups. ASA has an alpha olefin tail group, while MAH/BMA and MAH/LMA have an alkyl ester tail groups. The alkyl ester tail groups are slightly hydrophilic because they consist of an ester function which can also interact via hydrogen bonds with the paperboard [4]. The structures, type of bonding interaction with paperboard and alkyl chain lengths of the three surfactants are given in Table 5.3.

**Table 5.3: Structures, type of bonding interaction with cellulose and the alkyl chain lengths of ASA, MAH/BMA and MAH/LMA**

| **Compound** | **Bonding interaction** | **R = alkyl chain length** |
|---|---|---|
| MAH/BMA 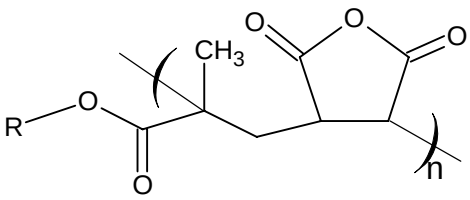 | Ester | C4 |
| MAH/LMA 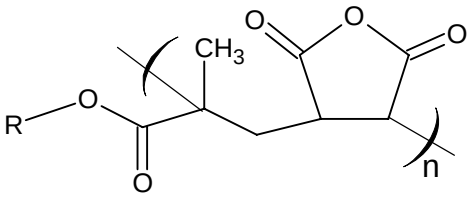 | Ester | C12 |
| ASA 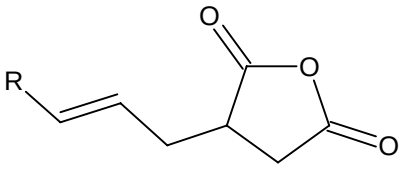 | Ester | C18-24 |

The amount of surfactant adsorbed by the uncoated paperboard is graphically illustrated in Figure 5.1.

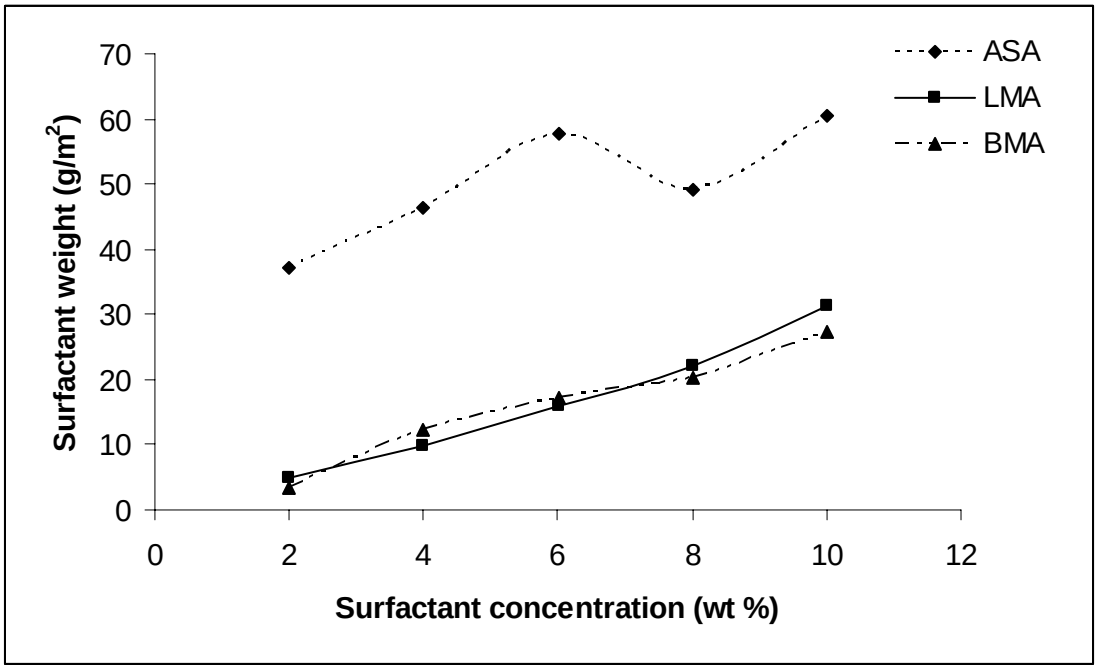


**Figure 5.1: Amount of surfactant adsorbed by uncoated paperboard.**

The amount of surfactant adsorbed by the paperboard is of the order: ASA>MAH/LMA>MAH/BMA. This adsorption tendency appears contrary to what is found in literature [1]. This phenomenon can be ascribed to the ASA binding to starch and fiber, creating a larger surface for adsorption as suppose to MAH/BMA and MAH/LMA (*see Figure 3.7*).

The fluctuations in the graphs are due to defects in the recycled paperboard such as holes in the fibers and wide pore throats [5]. These defects can be seen in the SEM image of uncoated paperboard (*see Figure 3.5, Chapter 3*). The SEM images of MAH/BMA and MAH/LMA are given in Figures 5.2 and 5.3 respectively. These images show the paperboard surface covered with the respective surfactants. Pinholes are still visible on the surface of the surfactant coated paperboard. The polymers do, however, cover the paperboard surface better in comparison with ASA (*see SEM image of ASA in Figure 3.7, Chapter 3*). The pinholes and especially the pore throats are less visible in the SEM images of paperboard coated with these surfactants than that coated with ASA.

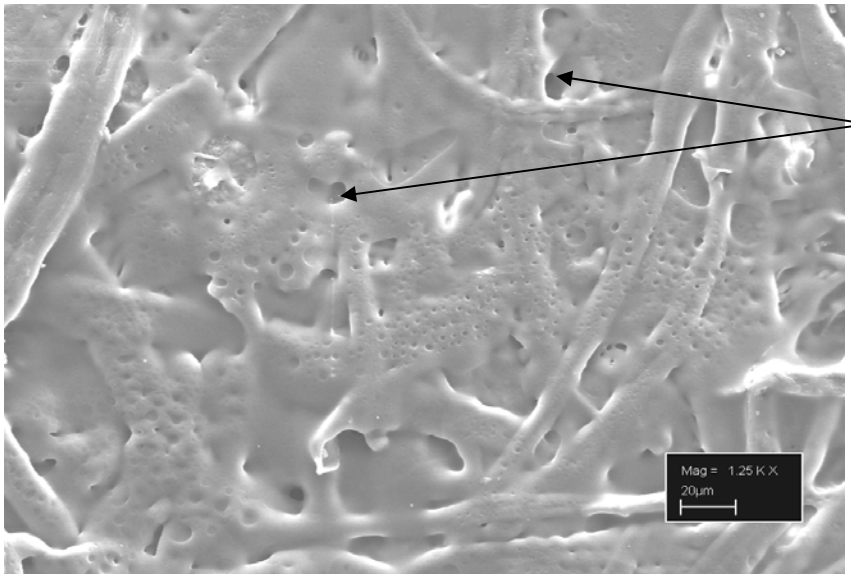


**Figure 5.2: SEM image of 10% MAH/BMA coated paperboard (Magnification = 1.25K X 20µm).**

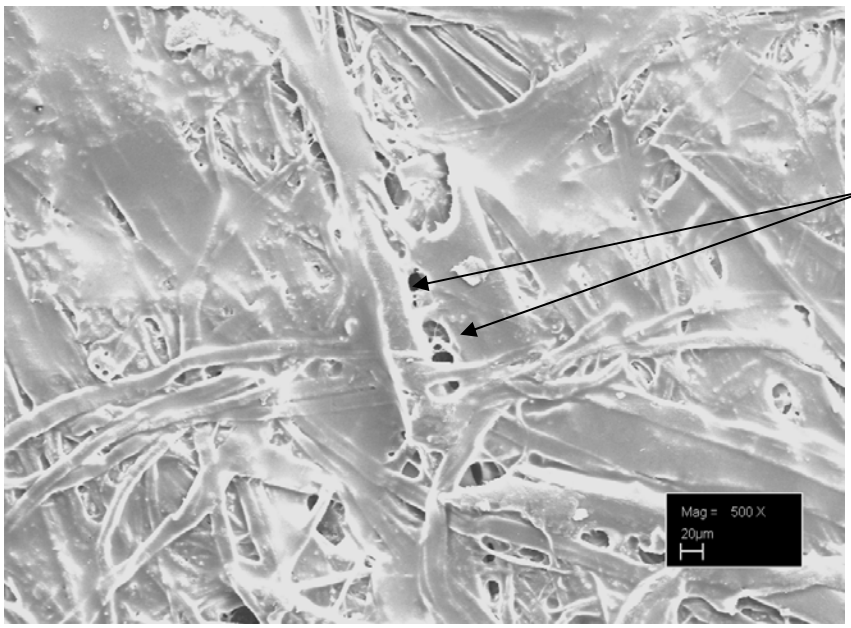


**Figure 5.3: SEM image of 10% MAH/LMA coated paperboard (Magnification = 500 X 20µm).**

The hydrophobicity and sizing efficiency of the surfactants were determined by measurement of the amount of water absorbed by each surfactant coated paperboard.

This was done with the use of the Cobb test and contact angle measurements. The amount of water absorbed, given as Cobb values, by each surfactant is graphically illustrated in Figure 5.4.

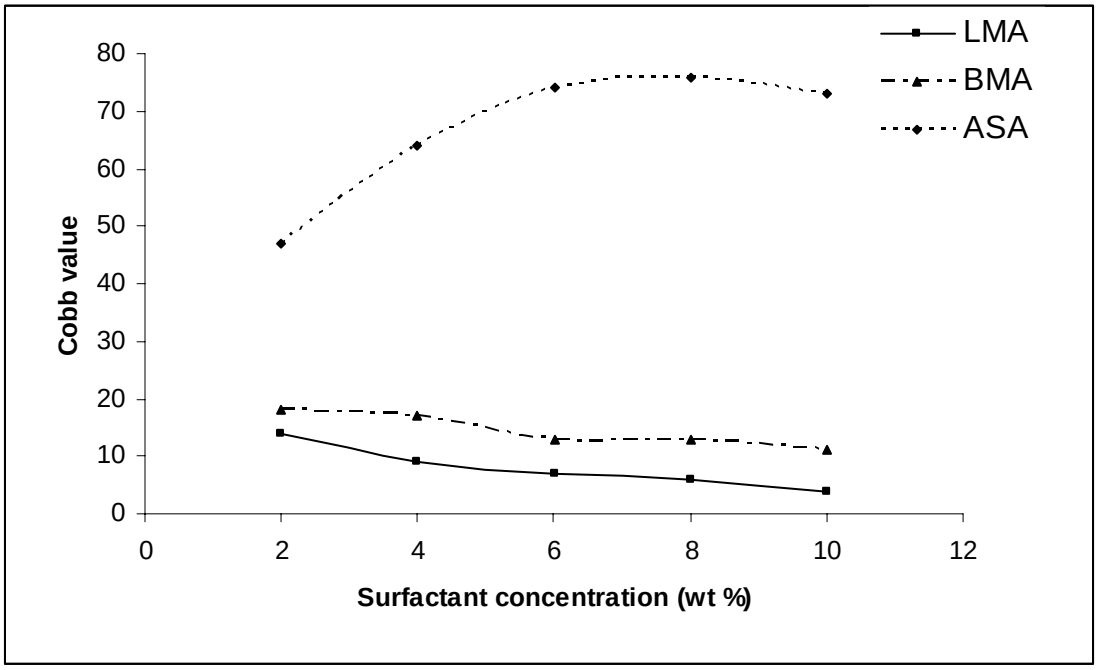


**Figure 5.4: Amount of water absorbed by surfactant coated paperboard.**

The hydrophobicities of the three surfactants were compared and it was found that MAH/LMA absorbed the least amount of water and ASA the most water. This result can be ascribed to the irreversible adsorption of polymers, which can be explained by the slow dynamics in polymer systems [1,2]. The polymer chain is grounded on the surface by its own inertia and, in order for it to desorb from the surface, all polymer segments that are attached to the surface must detach at approximately the same time. There is, however, a high probability that other segments will adsorb before the whole polymer desorbs [1]. The better contention is that ester bonds are formed, chemically binding the size to the fiber surface.

The contact angle measurements of ASA, MAH/BMA and MAH/LMA are tabulated in the Table 5.4 and graphically illustrated in Figure 5.5. There are a lot of variations in the contact angles of all three surfactants and their contact angles also do not correlate well with their Cobb values. This can be ascribed to the roughness and

geometry of the paper surface, which can give misleading contact angle measurements [1].

**Table 5.4: Contact angles of ASA, MAH/BMA and MAH/LMA**

| ASA in starch | | MAH/BMA in acetone | | MAH/LMA in THF | |
|---|---|---|---|---|---|
| Conc. (wt %) | Contact angle ($^0$) | Conc. (wt %) | Contact angle ($^0$) | Conc. (wt %) | Contact angle ($^0$) |
| 2 | 98.0 | 2 | 87.0 | 2 | 112.7 |
| 4 | 87.9 | 4 | 97.3 | 4 | 118.1 |
| 6 | 89.0 | 6 | 94.1 | 6 | 115.2 |
| 8 | 83.9 | 8 | 102.0 | 8 | 104.9 |
| 10 | 90.7 | 10 | 102.3 | 10 | 104.5 |

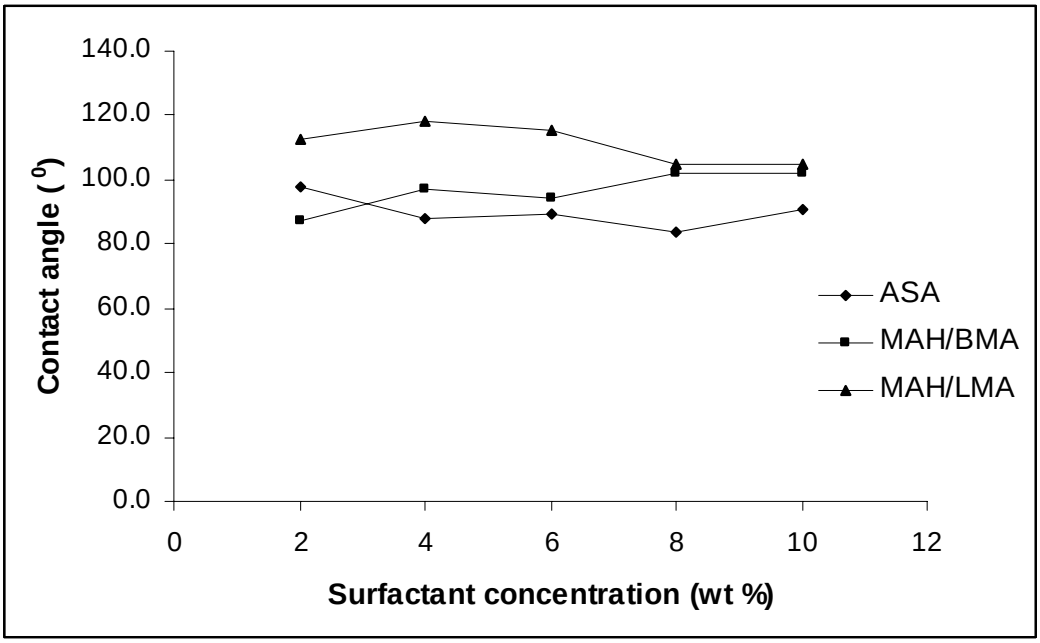


**Figure 5.5: Contact angles of ASA, MAH/BMA and MAH/LMA.**

## 5.4. Conclusions

The conclusions reached from these results are:

- There is a significant difference between the extent to which the three surfactants are adsorbed even though they consist of the same hydrophilic head group. This can be seen in Figure 5.1, where ASA is by far the most adsorbed compared to MAH/BMA and MAH/LMA.

- The irreversible adsorption phenomenon and chemical bonding of polymer systems is the factor determining the sizing efficiency of the three surfactants. This explains why MAH/LMA and MAH/BMA are more hydrophobic than ASA even though ASA has a longer alkyl tail group. The ASA can have less chemical attachments than polymeric MAH/BMA and MAH/LMA.

The main and final conclusion reached is that the two synthesized surfactants, MAH/BMA and MAH/LMA, exhibited the best performances in terms of sizing recycled paperboard compared to the currently used sizing agent, ASA. A technique needs to be developed however to apply them in emulsion form.

## 5.5. References

(1) Holmberg, K.; Jonsson, B.; Kronberg, B.; Lindman, B. *Surfactants and Polymers in Aqueous Solution*, In*: Surfactants and Polymers in Aqueous Solution*, 2nd ed.; John Wiley & Sons: West Sussex, 2003; p 545.

(2) Tadros, T.F.; Vandamme, A.; Levecke, B.; Booten, K.; Stevens, C.V. *Advances in Colloid and Interface Science* **2004**, 207-226.

(3) Lin, E.K.; Pochan, D.J.; Wu, W-i.; Satija, S.K. *Mat. Res. Soc. Symp.* **2000**, *629*, FF2.10.11-FF12.10.16.

(4) Ham, G.E. *Copolymerization*; Interscience: Kansas, 1964; Vol. XVII.

(5) Ghassemzadeh, J.; Sahimi, M. *Chemical Engineering Science* **2004**, *59*, 2265-2280.

# CHAPTER 6

# CONCLUSIONS AND RECOMMENDATIONS

## 6.1. Conclusions

The original proposal of this thesis resulted from the massive challenge the paper industry faces in terms of achieving optimum sizing performance and cost efficiency when using recycled paper.

In Chapter 3 it was found that the sizing agent, ASA, currently used by the paper industry has the best sizing efficiency compared to SDS and SE. A SEM image revealed defects such as fiber pinholes and wide pore throats on the surface of uncoated, recycled paperboard. The surface coverage of recycled paperboard by the three respective surfactants was also shown by their respective SEM images. The results of this chapter led to the focus of synthesizing copolymers with the same surfactant head group as ASA.

In Chapter 4 two copolymers, MAH/BMA and MAH/LMA were successfully synthesized via free radical copolymerization. Quantitative $^{13}C$ NMR analysis was used in determining the co-monomer incorporation in the isolated copolymers formed in the bench-scale experiments. This showed that random copolymers were synthesized and not alternating copolymers (as was expected). In situ $^{1}H$ NMR spectroscopy was used to study the kinetics of the two copolymer system. It was found that the technique was too insensitive in studying dissimilar monomers. This originated from the fact that the study failed to give accurate quantitative data for the monomer incorporation in the respective copolymer systems. The study nonetheless gave a clear picture of the reactivity of MAH towards BMA and LMA.

In Chapter 5 the sizing efficiency of ASA, MAH/BMA and MAH/LMA were compared and it was found that the latter two exhibited the best performances in terms

of sizing recycled paperboard compared to the currently used sizing agent, ASA. The irreversible adsorption and chemical attachment phenomenon of polymer systems was the factor determining the sizing efficiency of the three surfactants. This explained why MAH/LMA and MAH/BMA was more hydrophobic than ASA even though ASA had a longer alkyl tail group.

## 6.2. Recommendations

The major disadvantage of using solution copolymerization is the difficulty in removing and handling large quantities of solvent [1]. Emulsion copolymerization on the other hand would hydrolyze the MAH because water is the main ingredient in this type of copolymerization [2]. Recommendations in terms of synthesis and application would thus be to use solution copolymerization and afterwards emulsify the copolymers in order to eliminate the hydrolysis of MAH during synthesis.

A further recommendation would be to use controlled radical polymerization (CPR) such as reversible addition fragmentation chain transfer polymerization (RAFT) to produce copolymers with narrow molar mass distributions in order to better control the structural characteristics of these copolymers [3,4].

## 6.3. References

(1) Kaufman, H.S.; Falcetta, J.J. *Introduction to Polymer Science and Technology: An SPE Textbook*; John Wiley & Sons: New York, 1977.

(2) Lovell, P.A.; El-Aasser, M.S. *Emulsion Polymerization and Emulsion Polymers*; Wiley & Sons: New York, 1997.

(3) Davies, M.C.; Dawkins, J.V.; Hourston, D.J. *Polymer* **2005**, *46*, 1739-1753.

(4) Chernikova, E.; Terpugova, P.; Bui, C.; Charleux, B. *Polymer* **2003**, *44*, 4101-4107.